INCORPORATING VOLTAGE SECURITY INTO THE PLANNING, OPERATION AND MONITORING OF RESTRUCTURED ELECTRIC ENERGY MARKETS

A Dissertation

by

NIRMAL-KUMAR NAIR

Submitted to the Office of Graduate Studies of
Texas A&M University
in partial fulfillment of the requirements for the degree of

DOCTOR OF PHILOSOPHY

December 2004

Major Subject: Electrical Engineering

INCORPORATING VOLTAGE SECURITY INTO THE PLANNING, OPERATION AND MONITORING OF RESTRUCTURED ELECTRIC ENERGY MARKETS

A Dissertation

by

NIRMAL-KUMAR NAIR

Submitted to Texas A&M University
in partial fulfillment of the requirements
for the degree of

DOCTOR OF PHILOSOPHY

Approved as to style and content by:

Garng Huang (Chair of Committee)	
Chanan Singh (Member)	Aniruddha Datta (Member)
Vivek Sarin (Member)	Chanan Singh (Head of Department)

December 2004

Major Subject: Electrical Engineering

ABSTRACT

Incorporating Voltage Security into the Planning, Operation and
Monitoring of Restructured Electric Energy Markets. (December 2004)
Nirmal-Kumar Nair, B.E., Maharaja Sayajirao University;
M.E., Indian Institute of Science
Chair of Advisory Committee: Dr. Garng Huang

As open access market principles are applied to power systems, significant changes are happening in their planning, operation and control. In the emerging marketplace, systems are operating under higher loading conditions as markets focus greater attention to operating costs than stability and security margins. Since operating stability is a basic requirement for any power system, there is need for newer tools to ensure stability and security margins being strictly enforced in the competitive marketplace. This dissertation investigates issues associated with incorporating voltage security into the unbundled operating environment of electricity markets. It includes addressing voltage security in the monitoring, operational and planning horizons of restructured power system.

This dissertation presents a new decomposition procedure to estimate voltage security usage by transactions. The procedure follows physical law and uses an index that can be monitored knowing the state of the system. The expression derived is based on composite market coordination models that have both PoolCo and OpCo transactions, in a shared stressed transmission grid. Our procedure is able to equitably distinguish the impacts of individual transactions on voltage stability, at load buses, in a simple and fast manner.

This dissertation formulates a new voltage stability constrained optimal power flow (VSCOPF) using a simple voltage security index. In modern planning, composite power system reliability analysis that encompasses both adequacy and security issues is being developed. We have illustrated the applicability of our VSCOPF into composite reliability analysis.

This dissertation also delves into the various applications of voltage security index. Increasingly, FACT devices are being used in restructured markets to mitigate a variety of operational problems. Their control effects on voltage security would be demonstrated using our VSCOPF procedure. Further, this dissertation investigates the application of steady state voltage stability index to detect potential dynamic voltage collapse.

Finally, this dissertation examines developments in representation, standardization, communication and exchange of power system data. Power system data is the key input to all analytical engines for system operation, monitoring and control. Data exchange and dissemination could impact voltage security evaluation and therefore needs to be critically examined.

To My Family and Friends

ACKNOWLEDGMENTS

I would like to express my sincere gratitude to my graduate studies advisor, Dr. Garng Huang, and the members of my graduate studies committee Dr. Chanan Singh, Dr. Anirudhha Datta and Dr. Vivek Sarin. In particular, Dr. Huang's advice, guidance and support throughout the course of my graduate studies are above and beyond appreciation. Thanks to his broad engineering insights and regular guidance, the research in this dissertation attempts to be practical and concurrent with recent developments. Moreover, his understanding and patience are indispensable to the completion of this work.

I also would like to thank Prof. Robert Nevels, Ms. Nancy Reichart and Ms. Tammy Carda for their help throughout my graduate study at Texas A&M University.

Acknowledgement is extended to ABB Network Management Ltd. for providing an internship opportunity during summer of 2001 and 2002, and to Dr. Buntha Pek for his wonderful supervision. Special thanks are extended to Dr. Mani, Director of the Network Applications group of ABB, for selecting me as an intern and for his support.

I would like to mention the encouragement from all my colleagues and friends, in particular, Yishan Li and Cansin Evrenosoglu.

Finally, I would like to thank my family for their unfailing love and constant support in all my endeavors. Most of all, I am grateful to my dearest wife, Viji, for without her support and understanding this work would not have been complete.

My research was funded in part by the PSERC consortium and a Texas Advanced Technology program grant.

To all the people who have made this work possible, I once again say, Thank You!

TABLE OF CONTENTS

CHAPTER Page

CHAPTER Page

Page

LIST OF FIGURES

FIGURE Page

LIST OF TABLES

TABLE Page

NOMENCLATURE

AGC:	Automatic Generation Control
AMR:	Automatic Meter Reading
AS:	Ancillary Services
ATC:	Available Transmission Capacity
BC/BCM:	Bilateral Contract/Bilateral Contract Market
CIM:	Common Information Model
CCAPI:	Control Center Application Program Interface
DISCO:	Distribution Company
DMS:	Distribution Management Systems
EMS:	Energy Management Systems
EMSAPI:	Energy Management Systems Application Program Interface
ERCOT:	Electric Reliability Council of Texas
FACTS:	Flexible AC Transmission Systems
GAPP:	General Agreement on Parallel Paths
GENCO:	Generation Company
IED:	Intelligent Electronic Devices
ISO:	Independent System Operator
NERC:	North American Electric Reliability Council
OASIS:	Open access Same-time Information System
POD/POR:	Point of delivery/Point of Receipt
PTP:	Point-To-Point
PX/TX:	Power Exchange/Transaction
RDF:	Resource Description Framework
RTO:	Regional Transmission Organization
RTU:	Remote Terminal Units
SC:	Scheduling Coordinator
SCADA:	Supervisory Control and Data Acquisition
SE:	State Estimator

SVC:	Static Voltage Capacitors
TCSC:	Thyristor Controlled Series Capacitors
TOA:	Transmission Open Access
TRANSCO:	Transmission Company
TP:	Transmission Provider
UML:	Unified Modeling Language
XML:	Extensible Markup Language
WAN:	Wide Area Network
WML:	Wireless Markup Language
WSCC:	Western System Coordinating Council

CHAPTER I

INTRODUCTION

A. Electric Market Paradigms Following Deregulation

Electric utility industry around the globe is in the process of deregulation and restructuring. Unbundling of generation, transmission and distribution services and ensuring a non-discriminatory equal access high voltage transmission grid forms the basis of this concept. The major economic objective of this process is to introduce more competitive forces into power markets [1][2][3], while maintaining non-discriminatory access to the transmission networks, called as Transmission Open Access (TOA) amongst the suppliers and consumers of electric power. The implementation of the TOA facilitates the formation of a multiple-segments power market [4]. Main segments of a power market include standard energy trading markets, ancillary services (AS) markets, transmission capacity markets, real-time balancing market and so on [5]. Although the physical layouts and technical constraints are similar for all power systems, the adopted market structures may be different from each other. To summarize, two principal market coordination models under current practice are PoolCo and OpCo [6][1][2].

The PoolCo market coordination model depend on a central and auction-based power exchange (PX) system, which appears as either of the spot market (an hour-ahead) like U.K Pool, or the forward market (a day- ahead) like the previous Cal PX. The PoolCo model is advocated by some policy-makers, such as U.S. Federal Energy Regulatory Commission (FERC). It is asserted that competition in wholesale electricity markets is the best way to protect the public interest and ensure that electricity consumers pay the lowest price possible for reliable services [7].

The journal model is *IEEE Transactions on Power Systems*.

On the other hand the OpCo model is established on long-term bilateral energy contracts. Usually a bilateral contract is called bilateral transaction (TX), which is defined as "the right to inject a certain amount of power at node i and to remove it at another node j at a specified price p_{ij}" [8]. This model has been characterized as the best way to achieve free market competition through providing the customers "direct access" to a supplier of choice. As a hedging instrument against the risk of energy prices, recently, bilateral TXs with the OpCo model are rapidly growing in some major energy markets throughout the United States, like ERCOT. As a result, a hybrid market structure that combines advantages of both models is on the horizon now.

As a consequence of unbundling, generation-based AS commodities are separated from the standard energy market. Usual commodities of AS market include AGC, spinning reserve, supplemental operating reserve, energy imbalance, loss replacement, reactive power support and blackout start et al. Real time balancing market is conducted by an independent entity like the ISO to secure energy balance. The ISO is also responsible for ensuring the operating security constraints of the entire market in a real-time environment.

B. Some Security Issues Following Deregulation

All economic transaction models concentrate heavily on real power, MW, since it costs money to produce. From a control perspective the requirement to maintain frequency very closely, if not exactly, to scheduled frequency ensures that all entities participate effectively to maintain the real power balance. It is easier to evolve tools to trace responsibility of individual transactions towards MW flows and losses [9][10][11]. On the other hand, reactive power is a total different story. For examples, reactance is spread all over the system and it is very difficult to exactly trace in real-time, reactive consumption (inductive) and generation (capacitive) of the various components and relate it with voltage security. There is also this notion that reactance is a property contributed by all the power system components and reactive energy does not cost

money to produce. However, it is to be noted that in lightly or highly stressed condition of power system operation reactive flows do constrain the generation, flow and consumption of MW power, which affects the economics [12]. Further, the required voltage magnitude, maintained by generator and load buses by controlling reactive injections or consumptions, is also specified over a band which adds to the complication of tracing exact responsibility during highly stressed transmission operation.

Thus, from viewpoint of security and reliability studies we still operate on the basis of regulated structures by delegating voltage support and reactive power management as Ancillary Services (AS). However, in the marketplace of today's electricity operation it is necessary to come up with an approximate, if not exact, indicator that shows responsibility of the various entities during potential insecurities quickly [13]. This research necessity brings to the fore the following topics that needs attention. These objectives are spread over operational, monitoring, planning and control horizons of deregulated market structures but all of them are linked to system security. Such as

1. Voltage Stability, Voltage Collapse or Voltage Security

Voltage stability covers a wide range of phenomena over varying time frames [14]. Voltage stability has often been viewed as a steady-state "viability" problem suitable for static (power flow) analysis. The ability to transfer reactive power from production sources to consumption sinks during steady operating conditions is a major aspect of voltage stability. In this dissertation we focus on longer-term framework. We have used the term voltage security instead of voltage stability. This is because the term voltage stability is usually associated with a collapse point beyond which system power system operation is not feasible. However, voltage security implies an operating region between the current operating state and the instability point. Two power flow based methods called as P-V curves and V-Q curves, are commonly used to get an approximate steady-state loadability limit in electric utilities [14]. Continuation methods give accurate

loadability limit and location. However, all these methods implicitly use repeated power flow computation that is inherently time consuming [15][16][17][18].

In the last couple of years, the blackouts that have been witnessed in US and Europe mostly contribute voltage collapse as one of their prime reason. Implicitly, it seems to indicate security taking a back-seat in comparison with economic consideration. It also is due to lack of faster analytical tools and indicators, to entity like ISO, that quickly show up operational security threats and potential emerging instabilities.

Thus, voltage security needs to be readdressed in the planning, operational and monitoring phases of modern power system deregulated operations. These indicators for security needs to be quickly computed and would act as supplement to the already existing slower and accurate analytical tools for voltage stability analysis [13][19].

2. Composite Power System Reliability Analysis

Traditionally, power system reliability analysis used for planning studies has focused on adequacy of supply. In the vertically integrated operation generation capacity based reliability indices were sufficient measures. However, in the market operation the transmission segment, in other words security, must also be incorporated into the reliability analysis. Evaluating both adequacy and long-term security in planning is called as composite power system reliability [20]. There is a need to include voltage security into the composite reliability analysis of emerging electricity market planning [21][22]. However, care should be taken that the proposed procedures do not account for large computational burden to the already computation intensive reliability evaluation algorithms.

3. Impacts of FACTS on Voltage Security

Many Flexible AC Transmission System (FACTS) devices, like TCSC, are finding increased applications in power system networks [23][24]. As de-regulation evolves the

need to evaluate the impacts of these control devices on transactions would become even greater [25][26]. Traditionally, TCSC is being used in power delivery as a series compensator in lines designed to control power flow, to increase transient stability, to reduce power oscillations and to dampen sub-synchronous resonances. However, the use of TCSC invariably should impact load curtailment during congestion due to redistribution of flows and loop flow/parallel flow due to network topology changes. Hence, apart from the traditional use of these devices their impact on issues associated with voltage security [24] [27] and parallel flows [26] that finally affect economics need to be investigated and understood.

4. Exchange and Dissemination of Data in Deregulated Electric Markets

Deregulation demands seamless flow of relevant data amongst the power system entities, both to ensure reliable operation and maintain competitive electricity markets [28][29]. The existing datapath in the restructured electrical systems involves numerous physical and analytical components employing various communication technologies. There is a need to review the standardization efforts pertaining to EMS and modeling of power system data using CIM [30][31][32]. Further, evolving communication and information architecture needs to be carefully looked into from viewpoint of security of operational data [32][33]. Voltage security evaluation procedures rely on power system data and therefore there is a need to address emerging information architecture issues.

C. Objectives and Organization of This Dissertation

The main research contribution reported in this dissertation is in proposing methods and procedures to incorporate voltage security feature into the power system operation and reliability assessment for emerging electricity markets. The organization of this dissertation is given below.

Chapter II presents a decomposition procedure to estimate impacts of power transactions on voltage stability. The expressions have been derived reflecting the

physical laws and composite market structures that have both PoolCo and OpCo co-ordination models. If load curtailment is used as a corrective strategy to mitigate potential voltage insecurity, our proposed estimation procedure is shown to equitably account the total curtailed amount amongst participating transactions.

Chapter III proposes a new formulation to include voltage stability constraints into the conventional OPF problem used for satisfying system adequacy ie. VSCOPF.

Chapter IV discusses the different applications of using voltage security index. FACT devices are being increasingly used in modern electric network for a variety of operational purposes. The procedure to quantify loop flow impacts of TCSC on transactions is illustrated. The voltage security impact of TCSC is studied by incorporating it in VSCOPF procedure. Further the chapter discusses the applicability of voltage stability index to detect dynamic voltage collapse.

Chapter V addresses the procedures and discusses the results of using VSCOPF into the composite power system reliability analysis. Composite reliability analysis which includes both generation and transmission components to address adequacy and security, is being increasingly used in long-term planning studies for electricity markets.

Chapter VI reviews the various developments concerning power system data standards, communication issues and emerging information systems. These changes would impact voltage security evaluation tools used in practical EMS systems. A new way to speed up EMS data exchange is presented and concerns around the emerging electric market information infrastructure raised.

Finally, Chapter VII is a summary of the dissertation and reviews the contributions of this research. It also suggests the future directions for research based on this dissertation.

All the chapters between II and IV include various testing results or case studies based on WSCC 9-bus system, network parameters of which are given in Appendix A. The generation and load data are sometimes modified to better demonstrate the proposed methods, which are illustrated in relevant chapters. Other simple 3-bus system is chosen, whose details are provided wherever used, to illustrate the proposed concepts.

CHAPTER II

ESTIMATING VOLTAGE SECURITY USAGE IN DEREGULATED MARKETS

This chapter presents a new method to estimate the usage of steady state voltage stability margin by transactions in the deregulated energy markets. This procedure has been developed for the composite market model that consists of both the pool market and bilateral transactions. The approach readily reflects underlying physical laws. The proposed method for decomposition is simple, fast and confirms with singularity of load flow jacobian during voltage collapse.

A. Introduction

Restructuring of the electrical power industry, motivated by the need to induce competition and efficiency, has led to the need for developing viable technical procedures addressing system operation, system security and commercial arrangements all together. The transmission provider assumes the obligation to optimally transfer the power [34] as per the economic agreements except under an emergency situation. There is a need to evolve methods to account for responsibility, amongst the participating power transactions, during an emergency or potential security violation situation. The ISO is responsible for monitoring system operation and ensuring system security and therefore must act whenever security is threatened, and such action must be technically sound and commercially equitable. An equitable scheme for rescheduling pool generation and adjusting contract transactions using transient energy margin concept has been suggested for dynamic security enhancement against transient instability [35]. In another work [36], new market structures are proposed wherein bilateral contracts can submit curtailment bid. In this new scheme, pool and bilateral participants can exercise various curtailment options during security situations.

Voltage security is a major feature that needs to be monitored and incorporated into the context of a power market framework. Voltage stability covers a wide range of phenomena over varying time-frames [14]. Transient voltage stability is associated with time frames from zero to about ten seconds, usually accompanying a fault. The dynamics of load components and generators affect this phenomenon. Then there is the time frame of several minutes associated with terms like “mid-term” stability and “post-transient” stability wherein operator intervention is still not possible. This phenomenon is usually associated with large loads and a sudden large disturbance. Then there is this scenario, usually called as “steady-state voltage stability”, which is usually associated over a longer time period, wherein preventive and corrective operator actions could be taken. In this dissertation, we focus on this type of voltage security issue. Voltage stability problems may not occur frequently, but their impacts when they happen can be enormous. The blackout of the eastern US grid in 2003 shows how widespread such a security disturbance can travel. Continuation method determines the collapse point accurately and identifies the critical bus but is time consuming for large systems [15][16][18]. There is need for potential on-line tools and methods to be evolved that can help in visualizing the onset of instability, identify the contributors of instability [13] and thereby recommend remedial actions to mitigate potential voltage security problems. These functionalities need to be performed in real-time by operating personnel like a system operator and hence the method must be easy to visualize and effective in its implementation. Voltage security of power systems is dependent on sufficient local availability of reactive resources. There are reported works estimating pricing strategies for voltage security [37] and reactive power [38] but to date reactive spot pricing does not exist in practice. These and other reported works do not directly address the issue of evaluating impacts by individual transactions on overall voltage security. Thus, all these works and existing analytical tools developed for voltage stability have the following limitations:

- They are time-consuming to compute.
- Very difficult to implement them for on-line applications.

- Impacts of individual transactions in electric markets not quantifiable.

To address these requirements there is a need to develop supplementary tools and techniques for voltage security analysis.

B. Voltage Stability Indicator

There are several voltage stability indicators that have been reported using different measures like reactive power loss, P-V sensitivities, Q-V sensitivities etc [14]. However, since our main objective is to come up with a simple indicator that has the potential to be implemented in real-time and is in conformance with physical laws of voltage collapse we have chosen the L indicator [39][40]. The formulation and details of this indicator are provided herewith in following sub-sections.

1. Voltage Collapse Point Using Two Bus Model

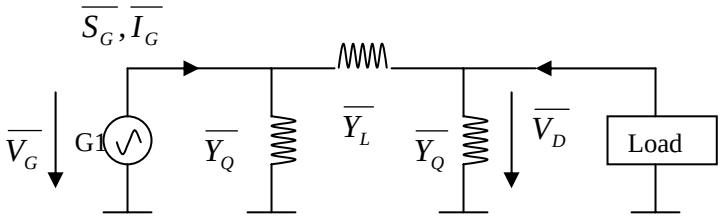

Fig.1. Single Generator and Single Load

As shown in Fig. 1, one simple system is conceived where there is a load bus and a generator bus. We are interested in their voltage behavior.

$$\overline{I_D} = \overline{V_D}\,\overline{Y_Q} + (\overline{V_D} - \overline{V_G})\overline{Y_L} = \frac{\overline{S}^{*}_{D}}{\overline{V_D}} \tag{2.1}$$

$$\overline{S}^{*}_{D} = V_D{}^2\overline{Y_Q} + V_D{}^2\overline{Y_L} - \overline{V}^{*}_{D}\,\overline{V_G}\,\overline{Y_L} = V_D{}^2\overline{Y_{11}} + \overline{V_0}\,\overline{V_D}\,\overline{Y_{11}} \tag{2.2}$$

Here $\overline{Y_{11}} = \overline{Y_Q} + \overline{Y_L}$ *and* $\overline{V_0} = -\frac{\overline{Y_L}}{\overline{Y_L} + \overline{Y_Q}}\overline{V_G}$ (2.3)

Since voltage at load bus is to be observed, we would like to find solution of $\left|\overline{V_D}\right|$ from the expression given in equation (2.2). Please note that in the equations that follow we represent the magnitude of $\overline{V_D}$ as V_D

Let $\frac{\overline{S}_D^*}{\overline{Y_{11}}} = a + jb$. Then (2.2) is expressed as follows:

$$\frac{\overline{S}_D^*}{\overline{Y_{11}}} = a + jb = {V_D}^2 + \overline{V_0}\,\overline{V}_D^* = {V_D}^2 + V_0 V_D \cos(\delta_0 - \delta_D) + jV_0 V_D \sin(\delta_0 - \delta_D) \quad (2.4)$$

$$\cos\delta = \cos(\delta_0 - \delta_D) = \frac{a - {V_D}^2}{V_0 V_D} \quad (2.5)$$

$$\sin\delta = \sin(\delta_0 - \delta_D) = \frac{b}{V_0 V_D} \quad (2.6)$$

$(2.5)^2 + (2.6)^2$, We will get

$${V_0}^2 {V_D}^2 = (a - {V_D}^2)^2 + b^2 = a^2 - 2a{V_D}^2 + {V_D}^4 + b^2 \quad (2.7)$$

Solving this equation, we get:

$$V_D = \sqrt{\frac{{V_0}^2}{2} + a \pm \sqrt{\frac{{V_0}^4}{4} + a{V_0}^2 - b^2}} = \sqrt{\frac{S_D}{Y_{11}}(r \pm \sqrt{r^2 - 1})} \quad (2.8)$$

Because $\frac{\overline{S}_D^*}{\overline{Y_{11}}} = a + jb$, hence $a = \frac{S_D}{Y_{11}}\cos(\phi_{S_D} + \phi_{Y_{11}}),\ b = -\frac{S_D}{Y_{11}}\sin(\phi_{S_D} + \phi_{Y_{11}})$.

Then

$$V_D = \sqrt{\frac{{V_0}^2}{2} + a \pm \sqrt{(\frac{{V_0}^2}{2} + a)^2 - (a^2 + b^2)}}$$

$$= \sqrt{\frac{V_0^{\,2}}{2} + \frac{S_D}{Y_{11}}\cos(\phi_{S_D} + \phi_{Y_{11}}) \pm \sqrt{\left(\frac{V_0^{\,2}}{2} + \frac{S_D}{Y_{11}}\cos(\phi_{S_D} + \phi_{Y_{11}})\right)^2 - \frac{S^2{}_D}{Y^2{}_{11}}}}$$

$$= \sqrt{\frac{S_D}{Y_{11}}(r \pm \sqrt{r^2 - 1})} \tag{2.9}$$

Here r is defined as $r = \frac{V_0^{\,2} Y_{11}}{2S_D} + \cos(\phi_{S_D} + \phi_{Y_{11}})$ (2.10)

2. Formulating Stability Indicator

Based on discussions from the previous section we can now define a voltage stability indicator. We observe that when $\sqrt{\frac{V_0^{\,4}}{4} + aV_0^{\,2} - b^2} = 0$, the voltage at load bus will collapse. Since, $\overline{V_0} = -\frac{\overline{Y_L}}{\overline{Y_L} + \overline{Y_Q}}\overline{V_G}$, it can be specified and supported by generator. Hence when $\frac{V_0^{\,4}}{4} + aV_0^{\,2} - b^2 \geq 0$, the voltage at load bus will be sustained but when $\frac{V_0^{\,4}}{4} + aV_0^{\,2} - b^2 < 0$, the voltage cannot be sustained, that is to say, the threshold of the voltage collapse is expressed by $a = \frac{b^2}{V_0^{\,2}} - \frac{V_0^{\,2}}{4}$. Taking $\frac{\overline{S}_D}{\overline{Y}_{11}} = a + jb$, we can deduce the active power P_D and reactive power Q_D of $\overline{S_D}$ ($\overline{S_D} = P_D + jQ_D$) to be expressed as follows:

$$P_D = \mathrm{Re}(\overline{Y_{11}}(a + jb)), Q_D = \mathrm{Im}(\overline{Y_{11}}(a + jb)).$$

If we draw a curve in $\overline{S_D}$ complex plane, the borderline of this curve represents the voltage collapse at load node. Then we can represent an indicator to reflect the proximity to this borderline. From equation (2.9), we see that when the voltage collapses, $r = 1$, $\frac{S_1}{V_D^{\,2} Y_{11}} = 1$. From the equation of (2.2), we can get:

$$\frac{\overline{S_1}^*}{V_D{}^2\overline{Y_{11}}} = 1 + \frac{\overline{V_0}}{\overline{V_D}} \tag{2.11}$$

So, we define an indicator L for voltage collapse as:

$$L \overset{\Delta}{=} \left| 1 + \frac{\overline{V_0}}{\overline{V_D}} \right| = \left| \frac{\overline{S_1}^*}{V_D{}^2\overline{Y_{11}}} \right| \tag{2.12}$$

When the load is zero ($\overline{S_1} = 0$) then L=0, if the voltage of bus 1 collapses then L=1. Thus the voltage stability indicator varies between 0(no collapse) to 1(voltage collapse).

3. Conforming Validity of Indicator

This discussion is to prove for the voltage stability indicator conforming to singularity of load flow jacobian that is associated with steady state voltage collapse. Considering from the viewpoint of Jacobian matrix singularity, the following statement is true: “if the voltage at load bus collapse, the Jacobian matrix will be singular, that is to say, the determinant of the matrix will equal to zero.”

From equation (2.5) and (2.6), we can list the power flow equations for the two-bus system as follows:

$$f(V_D, \delta) = V_0 V_D \cos\delta + V_D{}^2 = a \tag{2.5a}$$

$$g(V_D, \delta) = V_0 V_D \sin\delta = b \tag{2.6a}$$

So, the corresponding Jacobian Matrix would be as follows:

$$J = \begin{bmatrix} 2V_D + V_0\cos\delta & -V_D V_0 \sin\delta \\ V_0 \sin\delta & V_D V_0 \cos\delta \end{bmatrix} \tag{2.13}$$

When the determinant of Matrix J equals to zero, the voltage at load bus will collapse:

$$\det(J) = 2V_D{}^2 V_0 \cos\delta + V_D V_0{}^2 = 0 \Rightarrow \frac{V_D \cos\delta}{V_0} = \mathrm{Re}\left\{\frac{\overline{V_D}}{\overline{V_0}}\right\} = -\frac{1}{2}$$

Expressing $\frac{\overline{V_D}}{\overline{V_0}} = -\frac{1}{2} + jb$, where b is a real number, we get:

$$\left|1 + \frac{\overline{V_0}}{\overline{V_D}}\right| = \left|1 + \frac{1}{-\frac{1}{2} + jb}\right| = \left|\frac{\frac{1}{2} + jb}{-\frac{1}{2} + jb}\right| = 1 \qquad (2.14)$$

Actually, when we divide equation (2.2) by the term $V_D{}^2 \overline{Y_{11}}$, we get:

$$\frac{\overset{*}{S}_1}{V_D{}^2 \overline{Y_{11}}} = 1 + \frac{\overline{V_0}}{\overline{V_D}} \qquad (2.15)$$

From above analysis, we understand that the indicator of voltage stability conforms to the singularity of the load flow jacobian matrix.

4. Index Expression for Multi-bus System

The N bus transmission system can be represented using a hybrid representation, by the following set of equations:

$$\begin{bmatrix}\overline{V_L} \\ \overline{I_G}\end{bmatrix} = H\begin{bmatrix}\overline{I_L} \\ \overline{V_G}\end{bmatrix} = \begin{bmatrix}Z_{LL} & F_{LG} \\ K_{GL} & Y_{GG}\end{bmatrix}\begin{bmatrix}\overline{I_L} \\ \overline{V_G}\end{bmatrix}$$

Here suffix L and G denotes load and generator buses respectively.

When we consider the voltage at load node j, we know that

$$\overline{V_j} = \sum_{i \in L} \overline{Z_{ji}}\,\overline{I_i} + \sum_{i \in G} \overline{F_{ji}}\,\overline{V_i} \qquad (2.16)$$

Carrying out the following transformations:

$\overline{V_j} - \sum_{i \in G} \overline{F_{ji}}\,\overline{V_i} = \sum_{i \in L} \overline{Z_{ji}}\,\overline{I_i}$, Multiplying $\overset{*}{V}_j$ at the both sides of the equation:

$$V_j^{\,2} + \overline{V_{0j}}\,\overset{*}{V}_j = \overset{*}{V}_j \sum_{j\in L} \overline{Z_{ji}} \cdot \overline{I_j}\,, \text{ Here } \overline{V_{0j}} = -\sum_{i\in G} \overline{F_{ji}}\,\overline{V_i}$$

$$= \overset{*}{V}_j (\overline{Z_{jj}} \cdot \overline{I_j} + (\sum_{\substack{i\in L \\ i\neq j}} \overline{Z_{ji}}\,\frac{\overset{*}{S}_i}{\overset{*}{V}_i}))$$

$$= \overset{*}{V}_j \cdot \overline{I_j} \cdot \overline{Z_{jj}} + \overline{Z_{jj}} (\sum_{\substack{i\in L \\ i\neq j}} \frac{\overline{Z_{ji}}}{\overline{Z_{jj}}}\,\frac{\overset{*}{S}_i}{\overset{*}{V}_i})\overset{*}{V}_j$$

$$= \overset{*}{S}_j \cdot \overline{Z_{jj}} + \overline{Z_{jj}} (\sum_{\substack{i\in L \\ i\neq j}} \frac{\overline{Z_{ji}}}{\overline{Z_{jj}}}\,\frac{\overset{*}{S}_i}{\overset{*}{V}_i})\overset{*}{V}_j \quad \text{Let } \overline{Y_{jj+}} = \frac{1}{\overline{Z_{jj}}}\text{, Then:}$$

$$= \frac{\overset{*}{S}_j}{\overline{Y_{jj+}}} + \frac{1}{\overline{Y_{jj+}}} (\sum_{\substack{i\in L \\ i\neq j}} \frac{\overline{Z_{ji}}}{\overline{Z_{jj}}}\,\frac{\overset{*}{S}_i}{\overset{*}{V}_i})\overset{*}{V}_j$$

$$= \frac{\overset{*}{S}_j}{\overline{Y_{jj+}}} + \frac{\overset{*}{S}_{jcorr}}{\overline{Y_{jj+}}}\text{, In which } \overline{S_{jcorr}} = (\sum_{\substack{i\in L \\ i\neq j}} \frac{\overset{*}{Z}_{ji}}{\overset{*}{Z}_{jj}}\,\frac{\overline{S_i}}{\overline{V_i}})\overline{V_j}$$

So, equation (2.16) can be converted to the following expression.

$$V_j^{\,2} + \overline{V_{0j}}\,\overset{*}{V}_j = \frac{\overset{*}{S}_{j+}}{\overline{Y_{jj+}}}$$

Here, the term $\overline{V_{0j}} = -\sum_{i\in G} \overline{F_{ji}}\,\overline{V_i}$ can be regarded as an equivalent generator comprising the contribution from all generators, like the $\overline{V_0}$ for the two bus case and further $\overline{Y_{jj+}} = \frac{1}{\overline{Z_{jj}}}$ $\overline{S_{j+}} = \overline{S_j} + \overline{S_{jcorr}}$ $\overline{S_{jcorr}} = (\sum_{\substack{i\in L \\ i\neq j}} \frac{\overset{*}{Z}_{ji}}{\overset{*}{Z}_{jj}}\,\frac{\overline{S_i}}{\overline{V_i}})\overline{V_j}$.

The $\overline{S_{jcorr}}$ expression is representative of contributions of the other loads at the node j.

Extending the same logic used for 2-bus system towards a N-bus system, we can express the voltage stability indicator as shown by equation (2.17).

$$L_j = \left| 1 + \frac{\overline{V_{0j}}}{\overline{V_j}} \right| = \left| \frac{\overset{*}{S}_{j+}}{\overline{Y_{jj+}} \left| V_j \right|^2} \right| \tag{2.17}$$

Thus, we get an indicator to show the proximity of a system away from voltage collapse. When a load bus j approaches a steady state voltage collapse situation, the index L_j approaches the numerical value 1.0. Hence for a system wide voltage stability assessment, the index evaluated at any of the buses must be less than unity. Typically, for practical systems it is between 0.3-0.4 [12]

C. AC Flow-Based Unbundling Techniques

Some original proposals for accurate allocations of transmission system use or unbundling have been reported recently in the literature. In particular, Galinana et al [41] present a novel integration scheme to allocate transmission loss for the simultaneous transactions. Kirschen et al [9] developed flow-tracing techniques, which introduce a basic assumption of proportionality. However, the objective of flow-tracing approaches is to allocate transmission system use for bidding generators (or loads), not for bilateral TXs. Zobian et al [10] and Huang et al [11] present the decomposition techniques to calculate major and interacting components of various power flow quantities associated with a bilateral TX. The general basis for recasting AC power flow equations to include economic transactions is discussed herewith.

Physically, the route of electricity for active and reactive power flows in the network strictly follow Kirchoff's Laws. The conventional coupled AC power flow equations, which governs the flows is represented by the following:

$$\begin{cases} (P_{Gi} - P_{Di}) - V_i \sum_{j \in i} (g_{ij} \cos \theta_{ij} + b_{ij} \sin \theta_{ij}) = 0 \\ (Q_{Gi} - Q_{Di}) - V_i \sum_{j \in i} (g_{ij} \sin \theta_{ij} - b_{ij} \cos \theta_{ij}) = 0 \end{cases} \tag{2.18}$$

$i = 1,2...,n \ \ (i \neq s)$, s being the slack bus.

Here, P_{Gi}, Q_{Gi} are active and reactive power generations at bus i, P_{Di}, Q_{Di} are active and reactive power loads at bus i, $V_i \angle \theta_i$ is the voltage magnitude and angle of bus i, $\theta_{ij} = \theta_i - \theta_j$, $y_{ij} = g_{ij} + jb_{ij}$ is the branch admittance between nodes i and j.

For deregulated power markets there are reported works, based on DC power flow, to decompose impacts of transactions [42]. But these methods neglect the effect of reactive power flow distribution. To consider the impacts of reactive flows it is necessary to rationally decompose coupled AC power flow expression (2.18). Let us understand the general basis behind formulation of AC flow based decomposition methods.

The solution (V, θ) for power flow equations (2.18) would fully describe the state of the power system. The nodal voltage, system admittance and current injection at a node can be expressed by $Ve^{j\theta} = [Y_{bus}]^{-1}\overline{I_{bus}}$. From the Kirchoff's Laws, nodal power injections P_i and Q_i can be expressed in terms of real and imaginary current components as shown below.

$$P_i = \mathrm{Re}[V_i e^{j\theta_i} \times (\overline{I_i^*})] = V_i \cos\theta_i \, \mathrm{Re}(\overline{I_i}) + V_i \sin\theta_i \, \mathrm{Im}(\overline{I_i})$$

$$Q_i = \mathrm{Im}[V_i e^{j\theta_i} \times (\overline{I_i^*})] = V_i \sin\theta_i \, \mathrm{Im}(I_i) - V_i \cos\theta_i \, \mathrm{Re}(I_i) \qquad (2.19)$$

Rearranging, (2.19) to express real and imaginary part of $\overline{I_i}$

$$\mathrm{Re}(\overline{I_i}) = \frac{(P_i \cos\theta_i + Q_i \sin\theta_i)}{V_i}$$

$$\mathrm{Im}(\overline{I_i}) = \frac{(P_i \sin\theta_i - Q_i \cos\theta_i)}{V_i} \qquad (2.20)$$

Let us assume that the transaction amount P_k and Q_k, associated with transaction k of the N_T transactions, has δ_{ki} and γ_{ki} fractions of real and reactive power respectively associated with bus i. Then (2.19), (2.20) can be rewritten as (2.21), (2.22) to reflect the market transactions.

$$P_i = \sum_{k=1}^{N_T} \delta_{ki} P_k = V_i \cos\theta_i \left(\sum_{k=1}^{N_T} \mathrm{Re}(\overline{I_{ki}}) \right) + V_i \sin\theta_i \left(\sum_{k=1}^{N_T} \mathrm{Im}(\overline{I_{ki}}) \right)$$

$$Q_i = \sum_{k=1}^{N_T} \gamma_{ki} Q_k = V_i \sin\theta_i \left(\sum_{k=1}^{N_T} \mathrm{Im}(\overline{I_{ki}}) \right) - V_i \cos\theta_i \left(\sum_{k=1}^{N_T} \mathrm{Re}(\overline{I_{ki}}) \right) \quad (2.21)$$

$$\mathrm{Re}(\overline{I_i}) = \sum_{k=1}^{N_T} \mathrm{Re}(\overline{I_{ki}}) = \frac{\left(\left[\sum_{k=1}^{N_T} \delta_{ki} P_k \right] \cos\theta_i + \left[\sum_{k=1}^{N_T} \gamma_{ki} Q_k \right] \sin\theta_i \right)}{V_i} \quad (2.22)$$

Once the real part of current associated with a transaction is calculated, its impact on system performance measures like transmission loss and loop flow could be estimated. In the commercial power markets, transactions are specified in terms of real power traded without typically specifying reactive power. The integrated reactive power balance and procurement of reactive support in the market would be done by some independent entity like ISO. Knowing just δ_{ki} but not γ_{ki} would mean that (2.22) cannot be evaluated exactly. The uncontrollable reactive elements like line charging, load power factors, line inductance and controllable operations like generator field excitation, transformer tap changing, switching capacitors, Flexible AC transmission (FACT) device operation all impact reactive injection at a bus. All these real-time reactive injection changes complicate the exact determination of γ_{ki} for real-power transactions in power market operation. Thus, to reflect the commercial market practice, strategies could be formulated to rationally compute nodal transaction current injections based on just real power traded and system operating state. In this paper we shall use the method given in [11] which has been used for equitable transmission loss allocation. In that work, the real component of current associated with real power injection, for a transaction k, at bus i, is given by (2.23) which is an approximation of (2.21). It was formulated on the basis of having a common Q market coordinated by ISO, which picks up the approximation errors.

$$\delta_{ki} P_k \approx V_i \cos\theta_i \, \mathrm{Re}(\overline{I_{ki}}) \quad (2.23)$$

We shall now use AC flow decomposition along with the voltage stability index, reviewed in section B, to estimate voltage security usage by transactions. The detailed

derivation of the procedure is given in the next section. Even though our proposed procedure uses (2.23), to reflect the current market practices, it can also be derived on the basis of (2.22) provided γ_{ki} for all transactions is known.

D. Estimating Voltage Security Usage and Its Application

In this section, we shall develop a procedure to estimate the voltage security usage by transactions. It exploits physical properties of the circuit and economic contexts of the TX to decompose AC power flows in a competitive power market. The L index which can be computed from state quantities and measurable parameters would be used for indicating voltage security. We shall further use these estimates to formulate an equitable load curtailment allocation policy in electricity markets.

1. A Decomposition Algorithm

a. Assumptions

Before we begin with the formulation of the decomposition method based on the approximation listed in the previous section, we first introduce some economic contexts and involved assumptions.

(1) An energy market consists of individual energy scheduling coordinators, who are entitled to arrange MW exchange schedules. These schedules could be pool type (PX) and also bilateral transactions (TX).

(2) A SC may not maintain its own reactive power balance. Instead, a market entity Q within the central and ISO-dependent reactive power scheduling is responsible for the reactive power support. The ISO is also responsible for ensuring the overall security and reliability requirements for the system.

b. Procedures for Decomposition

We shall derive the decomposition algorithm on a general power system with N buses. Since the composite model of electric power market is chosen, we assume only two types of market players in the system: PX appears as a central power exchange market dealing with the Poolco model market entity; TX represents the N_T bilateral transactions which represents the long term energy contract between generators and loads. Let us assume that the operating state of the system is known either from a State Estimator, based on measurements from Supervisory Control and Data Acquisition (SCADA), or from a valid load flow solution. Thus, the voltage V and angle θ for all the nodes in the system is known. Further the injections by the generators and the load demand is also known for the whole system. The following three steps, based on the approximation given in the previous section and the economic context listed as assumptions in this section, describes the proposed estimation of voltage security usage by transactions.

Step 1: Decompose nodal current vector for PX and TXs, from

$$\left[\overline{I_{bus}}\right]_{N*1} = [\overline{Y_{bus}}]_{N*N} \times \left[\overline{E_{bus}}\right]_{N*1} \text{where} \qquad \left[\overline{E_{bus}}\right] = \begin{bmatrix} V_1 e^{j\theta_i} \\ . \\ V_n e^{j\theta_i} \end{bmatrix}$$

The decomposition equations for the currents based on the transactions could be expressed as follows.

$$\left[I_{PX}\right]_{N*1} = \begin{bmatrix} . \\ \dfrac{P_{G,i}^{PX} - P_{D,i}^{PX}}{V_i \cos\theta_i} \\ . \\ . \\ \dfrac{P_{G,n}^{PX} - P_{D,n}^{PX}}{V_n \cos\theta_n} \end{bmatrix} \qquad \left[I_{TX}^{(j)}\right]_{N*1} = \begin{bmatrix} 0 \\ \dfrac{P_{G,m}^{TX^{(j)}}}{V_m \cos\theta_m} \\ 0 \\ \dfrac{-P_{D,k}^{TX^{(j)}}}{V_k \cos\theta_k} \\ 0 \end{bmatrix} \qquad j = 1,\ldots,N_T$$

$$\left[\overline{I_Q}\right]_{N*1} = \left[\overline{I_{bus}}\right]_{N*1} - \left[I_{PX}\right]_{N*1} - \sum_{j=1}^{N_T} \left[I_{TX}^{(j)}\right]_{N*1} \qquad (2.24)$$

Here, $P_{G,*}^{SC_k}, P_{D,*}^{SC_k}$ are the active power generation and load at bus i, in association with PX or TX. There are N_T bilateral transactions in TX market between source and sink buses represented as m and k respectively.

Please note that (2.24) is based on the flow decomposition used in [11]. However, any other AC flow decomposition could be used to evaluate the real currents associated with the transaction.

Step 2: Evaluate decomposed nodal voltage components

$$\begin{aligned}
\left[\overline{E_{TX}}^{(j)}\right]_{N*1} &= [\overline{Y_{bus}}]_{N*N}^{-1} \times [I_{TX}^{(j)}]_{N*1} \quad j = 1,....,N_T \\
\left[\overline{E_{PX}}\right]_{N*1} &= [\overline{Y_{bus}}]_{N*N}^{-1} \times [I_{PX}]_{N*1} \\
\left[\overline{E_{Q}}\right]_{N*1} &= [\overline{Y_{bus}}]_{N*N}^{-1} \times [\overline{I_{Q}}]_{N*1}
\end{aligned} \tag{2.25}$$

All the above are vectors of length N, corresponding to the N bus system.

The relationship between the bus voltages and these decomposed components of voltage is given by

$$\left[\overline{E_{bus}}\right]_{N*1} = \sum_{j=1}^{N_T} \left[\overline{E_{TX}}^{(j)}\right]_{N*1} + \left[\overline{E_{PX}}\right]_{N*1} + \left[\overline{E_{Q}}\right]_{N*1} \tag{2.26}$$

The $\overline{E_Q}$ component in (2.25) is representative of the common Q market. All PV buses need to maintain set-point voltages and voltage at PQ buses is controlled, locally, using tap-changing transformers or capacitors such that the power factor is within acceptable limit. Hence, the reactive injection and absorption of these devices impact the Q market. On the other hand, the $\overline{E_{PX}}$ and $\overline{E_{TX}}$ components of (2.25) is got from the real current injection associated with the transaction and the connectivity of the network $\overline{Y_{bus}}$. It is observed that there is a large increase in overall reactive line losses, demonstrated in illustrative example, when the system state approaches voltage insecurity. A major increase in real and reactive losses occurs for lines connected to the potentially voltage

insecure bus. The real current injection associated with the transactions that use those lines is responsible for the losses.

Step 3: Evaluating index L based on the decomposed voltage components.

The complex power delivered at the load buses can be represented, based on the market transactions, as follows.

$$\left[\overline{S_{PX}}\right]_{N*1}=\begin{bmatrix}-P_{d_1}-jQ_{d_1}\\ .\\ -P_{d_n}-jQ_{d_n}\end{bmatrix}_{N*1}\quad \left[\overline{S_{TX}^{(j)}}\right]_{N*1}=\begin{bmatrix}0\\ .\\ -P_{d_k}^{(j)}-jQ_{d_k}^{(j)}\\ 0\end{bmatrix}_{N*1}\qquad j=1,....,N_T \tag{2.27}$$

The index L associated with PX transaction, at load bus k, could be expressed as:

$$L_k^{PX}=\left|\frac{\overset{*}{S}_{(PX)_{k+}}}{\overline{Y_{kk+}}\quad \left|\overline{V_{PX_k}}\right|^2}\right| \tag{2.28}$$

Here $\overline{S_{(PX)_{k+}}}=\overline{S_{PX_k}}+\overline{S_{(PX)_{kcorr}}}$,

$$\overline{S_{(PX)_{kcorr}}}=\left(\sum_{\substack{i\in L\\ i\neq k}}\frac{\overset{*}{Z}_{ki}}{\overset{*}{Z}_{kk}}\frac{\overline{S_{PX_i}}}{\overline{V_{PX_i}}}\right)\overline{V_{PX_k}}\quad,\qquad \overline{Y_{kk+}}=\frac{1}{\overline{Z_{kk}}}\qquad \overline{V_{PX_k}}=\overline{E_{PX_k}}+\overline{E_{Q_k}}$$

Now the index expression associated with PX and adding bilateral transaction one after another, could be got by reflecting the appropriate changes in the $\overline{S_{(PX)_{k+}}}$ and $\overline{V_{PX_k}}$ terms of (2.28). In general for N_T bilateral transactions the index evaluated at the k load bus can be represented by,

$$L_k^{PX+\sum_{m=1}^{j}TX^{(m)}}=\left|\frac{\overset{*}{S}_{(PX+\sum_{m=1}^{j}TX^{(m)})_{k+}}}{\overline{Y_{kk+}}\quad \left|\overline{V_{(PX+\sum_{m=1}^{j}TX^{(m)})_k}}\right|^2}\right|\qquad j=1,....,N_T \tag{2.29}$$

Where $\overline{S_{(PX+\sum_{m=1}^{j}TX^{(m)})_{k+}}}=\overline{S_{PX_k}}+\sum_{m=1}^{j}\left(\overline{S_{TX_k^{(m)}}}\right)+\overline{S_{(PX+\sum_{m=1}^{j}TX^{(m)})_{kcorr}}}$

$$\overline{S}_{(PX+\sum_{m=1}^{j} TX^{(m)})_{kcorr}} = \left(\sum_{\substack{i \in L \\ i \neq k}} \frac{\overline{Z}^{*}_{ki}}{\overline{Z}^{*}_{kk}} \frac{\left(\overline{S_{PX_i}} + \sum_{m=1}^{j} \overline{S_{TX_i^{(m)}}} \right)}{\overline{V}_{(PX+\sum_{m=1}^{j} TX^{(m)})_i}} \right) * \overline{V}_{(PX+\sum_{m=1}^{j} TX^{(m)})_k}$$

$$\overline{V}_{(PX+\sum_{m=1}^{j} TX^{(m)})_k} = \overline{E_{PX_k}} + \overline{E_{Q_k}} + \sum_{m=1}^{j} \overline{E_{TX_k}}^{(m)}$$

For example, to evaluate the index considering the transaction $TX^{(1)}$ and PX together, at k load bus would be given by:

$$L_k^{PX+TX^{(1)}} = \left| \frac{\overline{S}^{*}_{(PX+TX^{(1)})_{k+}}}{\overline{Y_{kk+}} \quad \overline{\left| V_{(PX+TX^{(1)})_k} \right|^2}} \right|,$$

The change in value of index for load buses when a transaction is considered, represent the contribution of that transaction to voltage security margin utilization. The contribution of $TX^{(j)}$ at bus k towards utilization of voltage security can be generally represented by (2.30).

$$\Delta L_k^{TX^{(j)}} = L_k^{PX+\sum_{i=1}^{j} TX^{(i)}} - L_k^{PX+\sum_{i=1}^{j-1} TX^{(i)}} \qquad j = 1,...., N_T \tag{2.30}$$

If there are two bilateral transactions, i.e $N_T = 2$, the contribution of the transactions $TX^{(1)}$ and $TX^{(2)}$ would be given as shown in (2.31).

$$\Delta L_k^{TX^{(1)}} = L_k^{PX+TX^{(1)}} - L_k^{PX}$$

$$\Delta L_k^{TX^{(2)}} = L_k^{PX+TX^{(1)}+TX^{(2)}} - L_k^{PX+TX^{(1)}} \tag{2.31}$$

Power flow equations being non-linear and index being not linear over complete range until voltage collapse, the sequence of transactions can affect the change of index associated with individual transaction. Hence, the decomposition scheme proposed in this work is just an estimate of the impacts for transactions on voltage security.

2. Load Curtailment Policy Based on Estimation

For secure operation of the system following a contingency the N-1 contingency rule is generally used. This means that the system should operate within limits, following the most severe contingency that is identified around that operating scenario. If the system after a contingency is operating close to voltage instability it would reflect in the index at that bus being large and close to one according to our procedure. The change in index value for load buses when a transaction is considered, represent the contribution of that transaction to voltage security margin utilization as derived in section V.

When the system is observed to have reached near a voltage insecure operation corrective actions needs to be taken. The short-term control actions could include options like switching SVC and capacitors as controllable reactive sources, blocking tap-changing, generator excitation control, generation re-dispatch [12] and load curtailment. The priority of action would depend on availability of the various control options with the utility. The most disruptive control i.e load curtailment [43][44] would invariably be the last option.

In the restructured electric system operation it is highly desirable that if load curtailment is the option chosen by the ISO, to alleviate potential voltage collapse, then curtailment amount be allocated over the participating transactions in an equitable manner. This would ensure that economics of market is tied with control actions during situations of emergency. The voltage security usage procedure derived in the previous section could be used to formulate a fair curtailment allocation policy amongst transactions.

Let the amount of curtailment evaluated at load bus k be P_{DC_k}. The bus k where curtailment is to be effected could be easily got from the index value. One way to estimate an approximate value for P_{DC_k} is to define a threshold value of index $L_{threshold}$ and ensure that all indices be less than this. If curtailment is to be effected at bus k, then

P_{DC_k} can be estimated from equation (2) by substituting $L_k^{PX+\sum TX} = L_{threshold}$ and $\left|\overline{V_K}\right| =$ 0.9. The choice of $L_{threshold}$ depends on the system. Typically, for practical systems it is between 0.3-0.4 [12]. In the current work, we reduce the load at bus k such that the voltage at that bus is 0.9 p.u. Once P_{DC_k} is found then an equitable way of allocating this amongst the participating transactions at that load bus can be given by the equation (2.32).

$$P_{DC_k} = P_{DC_k}^{PX} + \sum_{i \in S} P_{DC_k}^{TX(i)} \qquad P_{DC_k}^{PX} = P_{DC_k} * \left[\frac{L_k^{PX}}{L_k^{PX} + \sum_{i \in S} \Delta L_k^{TX(i)}} \right]$$

$$P_{DC_k}^{TX(j)} = P_{DC_k} * \left[\frac{\Delta L_k^{TX(j)}}{L_k^{PX} + \sum_{i \in S} \Delta L_k^{TX(i)}} \right] \qquad (2.32)$$

$P_{DC_k}^{PX}$ and $P_{DC_k}^{TX(j)}$ represents the amount of curtailment that needs to be accounted by PX and $TX(j)$ respectively. In the equation the term S found in the limit of the summation term represents the set of all participating bilateral transactions at the load bus k where curtailment is to be effected.

Within the scope of this dissertation the generator participating in the transaction, that is to be curtailed, is assumed to reduce its real power output by the curtailed amount. In reality, other operational and commercial issues like generator rescheduling, responsiveness, down-ramp rate, curtailment bids etc. needs to be considered to picture the full curtailment policy. The reference [14] discusses algorithm to form effective control pairs during curtailment situations. In our case we take the generator at bus m, participating in the bilateral transaction $TX(j)$ with load bus k, to reduce its output power by the amount $P_{GC_m}^{TX(j)}$ shown by equation (2.33).

$$P_{GC_m}^{TX(j)} = P_{DC_k} * \left[\frac{\Delta L_k^{TX(j)}}{L_k^{PX} + \sum_{i \in S} \Delta L_k^{TX(i)}} \right] \tag{2.33}$$

3. An Illustrative Example

We apply decomposition procedure on the simplified WSCC 9 bus system. This test system is usually used to demonstrate analysis dealing with voltage stability studies. The parameters of the system are such that the operation tends to get constrained by voltage stability rather then by thermal limits. The line parameters for the test system are shown in Appendix A. The generator at Bus 1 is taken to be the slack bus. To demonstrate the method in this simulation, the voltage V and angle θ for all the nodes in the system is got by running a power flow.

Let us demonstrate the procedures proposed in the previous sections for the transaction scenario shown in Fig. 2. Let us assume that the market participants are a PX, which can be considered as base case, and two point to point transactions TX as shown in Fig. 1. The power transactions [G1, G2, G3]→[D1, D2, D3] represent the PX spot market. The two simultaneous point-to-point bilateral transmission services in the system are $TX^{(1)}$: G4→D4 of 44 M W and $TX^{(2)}$: G5→D5 for 50 MW Thus generator at Bus 2 is involved with both these bilateral transactions and also with supplying the load of 125 + j 50 MVA to bus 9, in pool with generators at buses 1 and 3.

The voltage security usage index is computed for normal operation with all lines operational and a contingency of the loss of the transmission line # 6 between buses 4 and 9. The choice of 44 MW for transaction $TX^{(1)}$ is chosen such that for a contingency of loss of line 6, between buses 4 and 9, the load bus 9 reaches at the verge of steady state voltage instability. If $TX^{(1)}$ had been even 46 MW then the power flow solution fails to converge following loss of line 6. The results obtained after application of the security decomposition procedure are tabulated in Table 1. The term ALL in the table

indicates the entry corresponding to all the power transactions, pool and all bilateral, at that time.

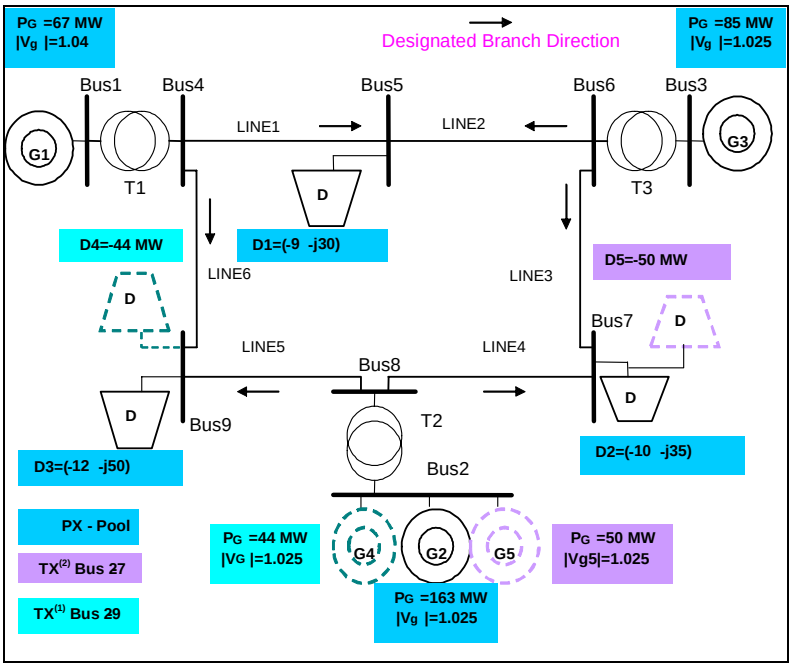

Fig.2. Case with Generator at Bus 2 Involved in Two Bilateral Transactions

For normally stressed condition, i.e before contingency in Table 1, the largest index values is only around 0.2049 at bus 9. This corresponds to normal operation of system wherein voltage at all buses is around 1.0 p.u. and line losses comparably small. The procedure brings out the change in the index being largest at the load bus where transaction takes place. For example, following $TX^{(1)}$ i.e a firm power transaction of 44 MW between generator at Bus 2 and load at Bus 9, the index at Bus 9 changes from 0.1582 to 0.1970. Similarly, following $TX^{(2)}$, a transaction of 50 MW between generator Bus 2 and load Bus 7, the index at Bus 7 changes from 0.1157 to 0.1970. This is consistent with the fact that loads that are local to bus impact its voltage security the most.

Table 1. Estimated Voltage Security Usage Before and After Contingency

	Before Line 6 outage			*After Line 6 outage*		
Bus→	5	7	9	5	7	9
PX	0.1304	0.1095	0.1582	0.1028	0.1559	0.6328
PX+ $TX^{(1)}$	0.1414	0.1157	0.1970	0.1105	0.1873	0.8676
ALL	0.1479	0.1496	0.2049	0.1172	0.2298	0.9548

Table 2. Decomposition Components Before Contingency

Bus ->	*5*	*7*	*9*
I_{PX_k}	-0.8933 /0	-0.9964 /0	-1.2744 /0
$I_{TX_k}^{(1)}$	0	0	-0.4486 /0
$I_{TX_k}^{(2)}$	0	-0.4982 /0	0
$\overline{E_{PX_k}}$	0.0673/1.7715	0.1443 /1.5106	0.0579 /1.8014
$\overline{E_{TX_k}^{(1)}}$	0.0179 /1.6895	0.0459 /1.4815	0.0060 /-2.794
$\overline{E_{TX_k}^{(2)}}$	0.0207 /1.5639	0.0052 /1.9851	0.0296 /1.5356
$\overline{E_{Q_k}}$	1.0326 /-0.1631	1.0059 /-0.1659	1.0055 /-0.1607
$\overline{E_{bus_k}}$	1.0055 /-0.0629	1.0032 /0.0283	0.9778 /-0.0789

It is seen that following contingency, overall index value at bus 9 is 0.9548 which indicates voltage insecure operation. This observation is also got from power flow solution where the voltage magnitude at bus 9 is 0.666 p.u. The transactions PX and $TX^{(1)}$ accounts for index usage about 0.8676 i.e sum of L_9^{PX} and $\Delta L_9^{TX^{(1)}}$, which is reasonable because they are directly involved at load bus 9. The other load bus indices are well below unity indicating no voltage insecurity.

Tables 2 and 3 detail the decomposition components obtained before and after contingency using the method. The magnitudes are in p.u. while angles are in radians for the tables. No meaningful information about transaction impacts on voltage security is directly got by comparing the $\overline{E_{TX}}$ components. The decomposed real current injections I_{PX_k} and $I^{(1)}_{TX_k}$ at bus 9, associated with PX and TX$^{(1)}$, has increased after contingency because of bus 9 reduced voltage. This obviously would lead to increased losses associated with lines feeding the load bus 9.

Table 3. Decomposition Components After Contingency

Bus ->	*5*	*7*	*9*
I_{PX_k}	-0.8811 /0	-1.0312 /0	-1.5667 /0
$I^{(1)}_{TX_k}$	0	0	-0.5515 /0
$I^{(2)}_{TX_k}$	0	-0.5156 /0	0
$\overline{E_{PX_k}}$	0.4090 /1.5496	0.3392 /1.5684	0.1099 /2.0388
$\overline{E_{TX_k}^{(1)}}$	0.1261 /1.5346	0.1112 /1.5573	0.0237 /2.4030
$\overline{E_{TX_k}^{(2)}}$	0.0127 /1.6811	0.0112 /1.7038	0.0488 /1.5047
$\overline{E_{Q_k}}$	1.2016 /-0.5981	1.1376 /-0.6195	0.8152 /-0.7069
$\overline{E_{bus_k}}$	1.0131 /-0.1278	0.9481 /-0.2116	0.6660 /-0.5831

An observation of increased real and reactive losses, especially in the lines near the voltage insecure bus, has been used to monitor and detect voltage instability[15]. Table 4 shows the losses associated with the lines before and after contingency. It can be seen that active and reactive losses associated with LINE 5, between buses 8 and 9 has a large increase following contingency. Transactions PX and TX$^{(1)}$ which uses this line is

responsible for this loss and thereby impending voltage collapse, which concurs with the conclusion got from observing index change.

Table 4. Real and Reactive Line Losses From Power Flow Analysis

Buses	*Loss before Contingency*		*Loss after Contingency*	
From -To	*P (MW)*	*Q(MVAR)*	*P (MW)*	*Q(MVAR)*
4-5	0.128	0.69	1.365	7.39
5-6	1.592	6.94	0.001	0.01
6-7	0.099	0.83	1.208	10.24
7-8	1.445	12.24	0.470	3.98
8-9	4.875	24.53	21.951	110.44
9-4	0.421	3.58	-	-
TOTAL	8.560	96.79	24.996	197.16

Table 5. Results Estimation of Table 1 After Changing Sequence of Transactions

	Before Line 6 outage			*After Line 6 outage*		
Bus→	5	7	9	5	7	9
PX	0.1304	0.1095	0.1582	0.1028	0.1559	0.6328
PX+ $TX^{(2)}$	0.1370	0.1437	0.1659	0.1094	0.1956	0.6996
ALL	0.1479	0.1496	0.2049	0.1172	0.2298	0.9548

To see the impact of sequence assignment of bilateral transaction in the voltage security decomposition, results are computed taking $TX^{(2)}$ before $TX^{(1)}$ as shown in Table 5, using equation (14). $TX^{(1)}$ accounts for index at bus 9 to change from 0.6328 to 0.8676 i.e. $\Delta L_k^{TX\ (1)} = 0.2348$ referring to Table 1 while it accounts for 0.2552 from

Table 5. Thus, the sequence of the transactions does affect the change of index associated with individual transaction.

To prevent total voltage collapse one of the corrective action, in current scenario, is to curtail load at bus 9. In the first step, the total amount of load curtailment should be such the voltage magnitude at load bus 9 must be around the minimum acceptable, generally 0.9 p.u. One can then estimate the amount of load curtailments for the participating transactions PX and $TX^{(1)}$ at load bus 9 as shown in Table 1. using equation (15). In our case PX load at bus 9 has reactive load of 50 MVAR. A policy of either curtailing or not curtailing reactive load could be followed. Both policies give different real MW load curtailment requirements to achieve acceptable voltage magnitude of 0.9 p.u. The voltage security allocation following both these policies is shown in Table 6. In the current simulation the generator participating in the bilateral transaction that is to be curtailed is assumed to reduce its real power output by the curtailed amount using (16).

Table 6. Index Estimation With Line 6 Outage Following Curtailment

Curtail →	*$TX^{(1)}$ by 25.44 MW*			*$TX^{(1)}$ by 14.614 MW*		
	PX by 68.56 MW			*PX by 39.39 + j 15.75 MVA*		
Bus →	5	7	9	5	7	9
PX	0.0993	0.1153	0.2414	0.1004	0.1233	0.2901
PX+ $TX^{(1)}$	0.1006	0.1222	0.2848	0.1024	0.1349	0.3661
ALL	0.1059	0.1574	0.3030	0.1078	0.1708	0.3888

As per results tabulated in Table 1, PX and $TX^{(1)}$ can be curtailed by the proportion of L_k^{PX} : $\Delta L_k^{TX^{(1)}}$ i.e 0.6328: 0.2348 to factor the contribution of these transactions. If only real power in MW is curtailed for PX, then the final allocation for PX and $TX^{(1)}$ is 56.4394 and 18.5606 MW following curtailment of 68.56 and 25.44 MW respectively. However, if curtailment of PX should follow constant power factor then final allocation

for PX and $TX^{(1)}$ is 85.6141 + j 34.246 MVA and 29.3859 MW following curtailment amounts of 39.99 + j 15.75 MVA and 14.614 MW respectively. In both cases the voltage magnitude at load bus 9 is close to 0.9 p.u. One thing to notice is that when MVAR load is curtailed then less real MW load needs to be curtailed overall. This is because voltage insecurity is closely linked with reactive power transfer across lines. The above illustration emphasizes the point that the voltage security decomposition method could be used to estimate curtailment amounts amongst participating transactions during voltage insecurities.

4. Implementing on Practical Systems

From the proposed methodology and demonstration on generic system discussed in the previous sections, following could be deduced for a large system of buses having load buses and participating transactions:

- The number of entries in the decomposition table, similar to Table 1, would have entries for every operating state. Evaluating these entries could be done in one shot, using (2.28) and (2.29), after the transaction decomposition components have been evaluated from the operating state.
- However, it should be noted that the current sub-matrix of equation (2.16) should be readily available to evaluate the indices. This means that the topology processor in EMS must be robust and reliable. An error in either the topology evaluation or the system state might lead to erroneous voltage security assessment.
- The algebraic computational complexity of the procedure is not of much concern since only matrix multiplication and algebraic evaluations are involved for our procedure. These issues have been well understood and taken care of in modern EMS software. The computational complexity is not large since the operations involve only matrix multiplication and arithmetic operations.

• From a monitoring perspective only when the load index value jumps a threshold, say 0.3, need the operator be cautious of potential voltage insecurity. Hence out of all the entries the operator needs to look out for any entry in the last row, corresponding to all transactions, crossing that threshold for further action.

Fig. 3 shows how the proposed method can be integrated into existing Energy Management System (EMS) environment. In the figure this estimation tool is shown to be triggered either by a Dispatcher Load Flow (DLF) or a State Estimator (SE) application of the EMS. When it is triggered by the State Estimator the indices reflect the current usage of the security margins by the transactions. Additionally, the Contingency Analysis (CA) application package of EMS could also trigger the proposed estimation tool. Thus, the modularity of the proposed method would help it work seamlessly with existing application suites of any commercial EMS.

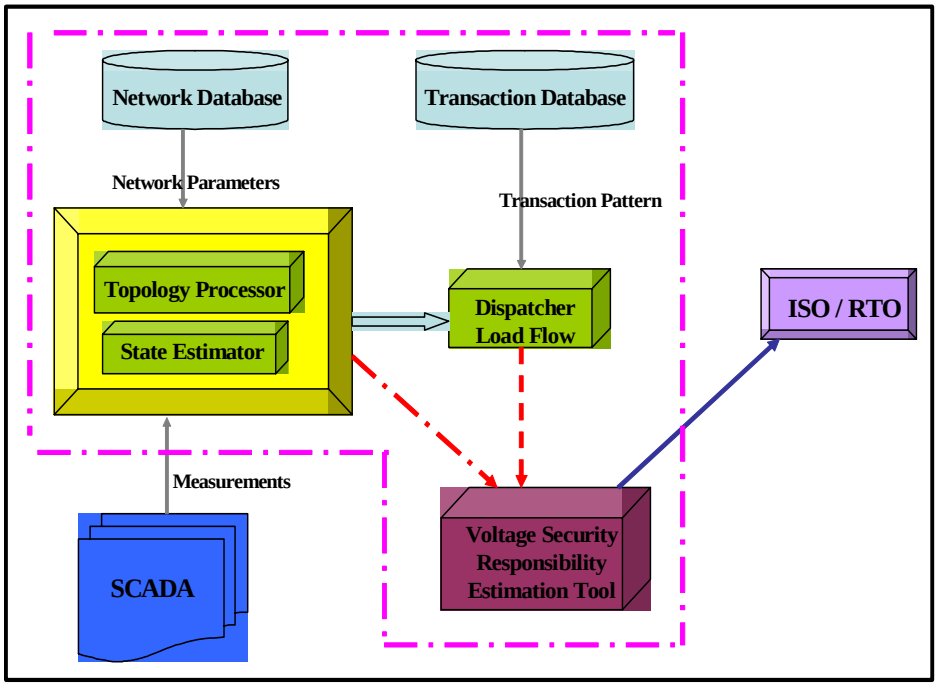

Fig.3. Integrating the Voltage Security Application Into Existing EMS

E. Summary

This chapter describes our work related to voltage security in the monitoring and operational horizon, which is summarized below.

First, we address the need for evolving newer quicker methods to monitor voltage security in the context of deregulated markets.

Second, we review the derivation and validity of a simple voltage stability indicator which can be used to quickly estimate the overall voltage security of the system.

Third, we present the derivation of a new estimation procedure to understand the impacts of transactions on overall voltage security. The expression for using this procedure for equitable load curtailment allocation policy is also discussed. The strength of our approach is demonstrated through an example.

In closing this chapter, we would like to point out that the procedure outlined in this chapter supplements to other existing voltage security tools and should not be viewed as a replacement. However the speed in evaluation, potential as a monitoring tool, simplicity and expressiveness of our proposed method are advantages over existing methods.

CHAPTER III

VOLTAGE STABILITY CONSTRAINED OPTIMAL POWER FLOW (VSCOPF) FORMULATION

In this chapter we discuss the formulation of an OPF problem that is security constrained by voltage stability. In the introduction section, we review the details of existing algorithm used to solve our proposed OPF problem.

A. Introduction

A power flow can have any number of operating limit violations. When such conditions occur, the violations can be alleviated by appropriate or various corrective actions. The analytical process of evolving this procedure is known as Optimal Power Flow (OPF) [45]. The Newton based approach to OPF was proposed in [46]. In [47] the authors formulated the OPF extension to take into effect the contingencies that occur in power systems. The procedure to address singularity of Jacobian matrix, in an OPF formulation, is demonstrated by relaxing some inequalities or through load shedding [48].

In the vertically integrated utility, OPF was used to dispatch generating units economically such that demand constraint and the generating unit capacity limits are obeyed [49]. In deregulated market operations, OPF has found increasing applications in market pricing issues and reliability studies [50]. In the operational horizon, OPF is being increasingly used to ensure secure operation. The current practice is to use the constraints based on the operating limits imposed by bus voltages, branch flows, power transfers over interfaces, etc. Controls may include generator, real power phase shifter angle, load curtailment or all the three. The objective of the corrective action algorithm is to observe all constraints while minimizing the weighted sum of the control movement. The reported work [51] attempts to formulate the incorporation of the transient angle stability, into an OPF routine, as an additional constraint. In this chapter, we discuss the details of our proposed inclusion of voltage security as a constraint to OPF.

1. Constrained Optimization Problem

The General Optimization (GP) problem is represented as follows:

$$\min_{x \in \Re^n} imize \quad f(x)$$

Subject to

$$\begin{aligned} G_i(x) &= 0 \quad i = 1,....m_e \\ G_i(x) &\le 0 \quad i = m_e + 1,....m \\ x_l &\le x \le x_u \end{aligned} \tag{3.1}$$

where x is the vector of design parameters $x \in \Re^n$, f(x) is the objective function that returns a scalar value ($f(x) : \Re^n \to \Re$), and the vector function G(x) returns the values of the equality and inequality constraints evaluated at x ($G(x) : \Re^n \to \Re^m$).

In solving the complete constrained optimization problem, the general aim is to transform the problem into an easier sub-problem that can then be solved and used as the basis of an iterative process. Two basic classes of approaches to the solution phase have been typically deployed:

- A characteristic of a large class of early methods is the translation of the constrained problem to a basic unconstrained problem by using a penalty function for constraints that are near or beyond the constraint boundary. In this way the constrained problem is solved using a sequence of parameterized unconstrained optimizations, which in the limit (of the sequence) converge to the constrained problem. These methods are now considered relatively inefficient.
- The newer and efficient methods have focus on the solution of the Kuhn-Tucker (KT) equations. The KT equations are necessary conditions for optimality for a constrained optimization problem. If the problem is a so-called convex programming problem, that is, and , are convex functions, then the KT equations are both necessary and sufficient for a global solution point.

The Kuhn-Tucker equations for this GP is given by the following expression

$$\nabla f(x^*) + \sum_{i=1}^{m} \lambda_i^* . \nabla G_i(x^*) = 0$$
$$\lambda_i^* . G_i(x^*) = 0, \qquad i = 1,..., m_e$$
$$\lambda_i^* \geq 0, \qquad i = m_e + 1,....m \tag{3.2}$$

The expression of (3.2) describes a canceling of the gradients between the objective function and the active constraints at the solution point. For the gradients to be canceled, Lagrange multipliers ($\lambda_i, \quad i = 1,..., m$) are necessary to balance the deviations in magnitude of the objective function and constraint gradients. Because only active constraints are included in this canceling operation, constraints that are not active must not be included in this operation.

The solution of the KT equations forms the basis to many nonlinear programming algorithms. These algorithms attempt to compute the Lagrange multipliers directly. Constrained quasi-Newton methods guarantee super-linear convergence by accumulating second order information regarding the KT equations using a quasi-Newton updating procedure. These methods are commonly referred to as Sequential Quadratic Programming (SQP) methods, since a QP sub-problem is solved at each major iteration (also known as Iterative Quadratic Programming, Recursive Quadratic Programming, and Constrained Variable Metric methods).

2. Sequential Quadratic Programming (SQP)

SQP methods represent the state of the art in nonlinear programming methods. The method allows you to closely mimic Newton's method for constrained optimization just as is done for unconstrained optimization. At major iterations, an approximation is made of the Hessian of the Lagrangian function using a quasi-Newton updating method. This is then used to generate a QP sub-problem whose solution is used to form a search direction for a line search procedure.

For the GP problem, the principal idea is the formulation of a QP sub-problem based on a quadratic approximation of the Lagrangian function.

$$L(x,\lambda) = f(x) + \sum_{i=1}^{m} \lambda_i g_i(x) \tag{3.3}$$

Here we simplify GP, by assuming that bound constraints have been expressed as inequality constraints. We obtain the QP sub-problem by linearizing the nonlinear constraints. A general QP sub-problem is of the form

$$\begin{aligned} &\min_{d \in \Re^n} imize \frac{1}{2} d^T H_k d + \nabla f(x_k)^T d \\ &\nabla g_i(x_k)^T d + g_i(x_k) = 0, \qquad i = 1,...,m_e \\ &\nabla g_i(x_k)^T d + g_i(x_k) \le 0, \qquad i = m_e + 1,...,m \end{aligned} \tag{3.4}$$

This sub-problem is solved using any QP algorithm. The solution is used to form the new iterate

$$x_{k+1} = x_k + \alpha_k d_k$$

The step length α_k is determined by an appropriate line search procedure so that a sufficient decrease in a merit function is obtained. The matrix H_k is a positive definite approximation of the Hessian matrix of the Lagrangian function. It can be updated using any of the quasi-newton methods.

A nonlinearly constrained problem can often be solved in fewer iterations than an unconstrained problem using SQP. One of the reasons for this is that, because of limits on the feasible area, the optimizer can make informed decisions regarding directions of search and step length.

3. Implementing SQP

Based on the above fundamentals the basic steps for implementation of the SQP is divided into three main steps which are

- Updating of the Hessian Matrix of the Lagrangian function
- Quadratic Programming Problem Solution
- Line Search and Merit Function Calculation

a. Updating the Hessian Matrix

At each major iteration a positive definite quasi-Newton approximation of the Hessian of the Lagrangian function, H, is calculated using the BFGS method, where is an estimate of the Lagrange multipliers.

$$H_{k+1} = H_k + \frac{q_k q_k^T}{q_k^T s_k} - \frac{H_k^T H_K}{s_k^T H_k s_k} \text{ where}$$
$$s_k = x_{k+1} - x_k$$
$$q_k = \nabla f(x_{k+1}) + \sum_{i=1}^{n} \lambda_i . \nabla g_i(x_{k+1}) - \left(\nabla f(x_k) + \sum_{i=1}^{n} \lambda_i \nabla g_i(x_k) \right) \qquad (3.5)$$

b. Quadratic Programming (QP) Solution

At each major iteration of the SQP method, a QP problem of the following form is solved, where A_i refers to the ith row of the m-by-n matrix A

$$\begin{aligned} &\min_{d \in \Re^n} imize\, q(d) = \frac{1}{2} d^T H\ d + c^T d \\ &A_i d = b_i, \quad i = 1,..., m_e \\ &A_i d \le b_i, \quad i = m_e + 1,..., m \end{aligned} \qquad (3.6)$$

The solution procedure involves two phases. The first phase involves the calculation of a feasible point (if one exists). The second phase involves the generation of an iterative sequence of feasible points that converge to the solution. In this method an active set, $\overline{A_k}$ is maintained that is an estimate of the active constraints (i.e., those that are on the constraint boundaries) at the solution point. Virtually all QP algorithms are active set methods.

$\overline{A_k}$ is updated at each iteration k, and this is used to form a basis for a search direction $\hat{d}_k$ Equality constraints always remain in the active set $\overline{A_k}$ .The notation for the variable $\hat{d}_k$ is used here to distinguish it from d_k in the major iterations of the SQP method. The

search direction $\hat{d}_k$ is calculated and minimizes the objective function while remaining on any active constraint boundaries. The feasible subspace for $\hat{d}_k$ is formed from a basis Z_k whose columns are orthogonal to the estimate of the active set Thus a search direction, which is formed from a linear summation of any combination of the columns of is guaranteed to remain on the boundaries of the active constraints.

Once Z_k, is found, a new search direction $\hat{d}_k$, is sought that minimizes $q(d)$, where $\hat{d}_k$ is the null space of active constraints. That is, $\hat{d}_k$ is a linear combination of the columns of $Z_k.\hat{d_k} = Z_k\rho$ for some vector ρ. Then if we view the quadratic as a function $\hat{d}_k$ by substituting for $\hat{d}_k$, we have

$$q(p) = \frac{1}{2} p^T Z_k^T H Z_k p + c^T Z_k p \tag{3.7}$$

Differentiating this with respect to ρ yields

$$\nabla q(p) = Z_k^T H Z_k p + Z_k{}^T c \tag{3.8}$$

$\nabla q(p)$ is referred to as as the projected gradient of the quadratic function because it is the gradient projected in the subspace defined by Z_k. The term $Z_k^T H Z_k$ is called as the projected Hessian. Since the Hessian is positive in the SQP implementation the minimum of $q(p)$ in the space defined by Z_k, is given by $\nabla q(p) = 0$.

Hence a step is taken of the following form,

$$x_{k+1} = x_k + \alpha_k \hat{d}_k$$
$$\text{where } \hat{d}_k = Z_k^T p. \tag{3.9}$$

At each iteration, because of the quadratic nature of the objective function, there are only two choices of step length α. A step of unity along $\hat{d}_k$ is the exact step to the minimum of the function restricted to the null space of $\overline{A_k}$. If such a step can be taken,

without violation of the constraints, then this is the solution to QP. Otherwise, the step along $\hat{d}_k$ to the nearest constraint is less than unity and a new constraint is included in the active set at the next iteration. The distance to the constraint boundaries in any direction $\hat{d}_k$ is given by

$$\alpha = \min_i \left\{ \frac{-(A_i x_k - b_i)}{A_i \hat{d}_k} \right\} \qquad (i = 1,...,m) \tag{3.10}$$

which is defined for constraints not in the active set, and where the direction $\hat{d}_k$ is towards the constraint boundary, i.e., $A_i \hat{d}_k > 0, i = 1,...,m$

When n independent constraints are included in the active set, without location of the minimum, Lagrange multipliers λ_k ,are calculated that satisfy the nonsingular set of linear equations.

$$\overline{A_k}^T \lambda_k = c$$

If all the elements of λ_k are positive x_k is the optimal solution of QP. However, if any component of λ_k is negative, and the component does not correspond to an equality constraint, then the corresponding element is deleted from the active set and a new iterate is sought.

c. Line Search and Merit Functions

The solution to the QP sub-problem produces a vector d_k which is used to form the new iterate given by,

$$x_{k+1} = x_k + \alpha_k d_k \tag{3.11}$$

The step length parameter α_k is determined in order to produce a sufficient decrease in a merit function. One such merit function based on a penalty parameter is given as follows:

$$r_i = (r_{k+1})_i = \max_i \left\{ \lambda_i, \frac{1}{2}((r_k)_i + \lambda_i) \right\}, i = 1,..., m \tag{3.12}$$

This allows positive contribution from constraints that are inactive in the QP solution but were recently active. In this implementation, the penalty parameter r_i is initially set to

$$r_i = \frac{|\nabla f(x)|}{|\nabla g_i(x)|}, \tag{3.13}$$

Here $|\ |$ represent the Euclidean norm. This ensures larger contributions to the penalty parameter from constraints with smaller gradients, which would be the case for active constraints at the solution point.

4. Algorithm used in this dissertation

The *fmincon* function of MATLAB [52] has been used to solve the constrained optimization problem of our dissertation. This function is available in the Optimization Toolbox kit of MATLAB. We have used the medium scale optimization algorithm option of the *fmincon* function for our simulations.

fmincon uses a Sequential Quadratic Programming (SQP) method. In this method, a Quadratic Programming (QP) subproblem is solved at each iteration.

B. Formulation of Voltage Stability Constrained OPF (VSCOPF)

The voltage stability index L, which was discussed in Chapter II, could be estimated from the results of power flow. This indicator has a value that ranges between zero (no load) through unity (voltage collapse) for the load buses. Hence, we propose to use this indicator as an additional constraint to the OPF formulation.

1. OPF with Load-Curtailment as Objective

The conventional system-wide OPF objective of minimizing overall generation cost [49] ceases to be relevant in power markets. Other objective functions like minimizing real power losses, minimizing overall control movements etc., are being used when OPF is used in operational horizon. From view-point of planning studies, like in composite reliability analysis the objective usually used is minimizing load curtailment. We use load curtailment as the objective to propose our VSCOPF algorithm.

The objective function for minimizing load curtailment, can be expressed as follows for a n-bus system.

$$\min \sum_{i=1}^{n} Load\_Curtailment_i$$

$$\text{For all buses from } i = 1,2....,n \tag{3.14}$$

$$\text{Here, } \quad Load\_Curtailment_i = P_{lireq} - P_{li}$$

Where P_{lireq} is the initial load expectation at bus i and P_{li} is the actual load demand, finally possible to be met within the constraint specified.

Having decided on the objective for this optimization problem, we now have to include the other physical algebraic equations and control limits as constraints. For a stable operating condition the power flow equations need to be satisfied and can be represented by the following set of equations.

$$P_{gi} - P_{li} - \sum_{j=1}^{n} |V_i||V_j|(G_{ij}\cos\delta_{ij} + B_{ij}\sin\delta_{ij}) = 0 \qquad Q_{gi} - Q_{li} - \sum_{j=1}^{n} |V_i||V_j|(G_{ij}\sin\delta_{ij} - B_{ij}\cos\delta_{ij}) = 0 \tag{3.15}$$

The minimum and maximum limits on generators active and reactive power output is given by,

$$P_{gi\,min} \le P_{gi} \le P_{gi\,max}$$
$$Q_{gi\,\min} \le Q_{gi} \le Q_{gi\,\max} \tag{3.16}$$

The transmission line constraints, to account for thermal loading limits can be generally specified for line between buses i and j as follows:

$$P_{ij}^2 + Q_{ij}^2 \le S_{ij\max}^2 \tag{3.17}$$

The load shedding philosophy can be simplified if we assume that shedding, is carried out in equal proportion of active and reactive power. In other words, the power-factor of all the loads remains the same as the initial value. This can be represented as shown below:

$$P_{li} / P_{lireq} = Q_{li} / Q_{lireq}$$

$$0 \le P_{li} \le P_{lireq} \quad \text{and} \quad 0 \le Q_{li} \le Q_{lireq} \tag{3.18}$$

2. Including Voltage Security Constraints

Now let us include constraint expression to include voltage security into our OPF formulation. Traditionally, we include voltage magnitude as a constraint which corresponds to the narrow band of acceptable magnitudes to be maintained at buses. Thus, for all buses i, we include the following voltage magnitude constraints,

$$|V_i|_{min} \le |V_i| \le |V_i|_{max} \tag{3.19}$$

It has been generally accepted that voltage magnitude alone does not give a good indicator of voltage instability. Hence, we shall supplement the voltage security constraint by adding the L index constraint. For all the load buses (PQ) and buses where there are no loads and generators i, use the following additional constraint, based on local index evaluation,

$$L_i \le L_{crit} \tag{3.20}$$

3. Complete Proposed VSCOPF Formulation

We summarize the expressions discussed in the previous sub-sections here.

Objective: $min \sum_{i=1}^{n} load\_curtail_i$

S.T.

$$P_{gi} - P_{li} - \sum_{j=1}^{n} |V_i||V_j|(G_{ij} cos\delta_{ij} + B_{ij} sin\delta_{ij}) = 0$$

$$Q_{gi} - Q_{li} - \sum_{j=1}^{n} |V_i||V_j|(G_{ij} sin\delta_{ij} - B_{ij} cos\delta_{ij}) = 0$$

$$P_{li} / P_{lireq} = Q_{li} / Q_{lireq}$$

$$0 \le P_{li} \le P_{lireq}$$

$$0 \le Q_{li} \le Q_{lireq}$$

$$|V_i|_{min} \le |V_i| \le |V_i|_{max}$$

$$P_{gi\,min} \le P_{gi} \le P_{gi\,max}$$

$$Q_{gi\,\min} \le Q_{gi} \le Q_{gi\,\max}$$

$$P_{ij}^2 + Q_{ij}^2 \le S_{ij\,\max}^2$$

$$L_i \le L_{crit}$$

Here,

$$load\_curtail_i = P_{lireq} - P_{li} \tag{3.21}$$

Further,

P_{lireq} : real load demand at bus i P_{li} : actual real load supply at bus i

n : total number of load flow buses in the system P_{gi} : real power generation at bus i

Q_{gi} : reactive power generation at bus i Q_{lireq} : reactive load demand at bus i

Q_{li} : actual reactive load supply at bus i $|V_i|$: voltage magnitude at bus i

$|V_j|$: voltage magnitude at bus j

G_{ij}, B_{ij} : real/reactive part of the ijth element of the bus admittance matrix

δ_{ij} : angle difference between the voltage phasor at bus i and bus j

$P_{gi\,\min,} P_{gi\,\max}$: minimum/maximum real power generation at generation bus i

$Q_{gi\,\min,} Q_{gi\,\max}$: minimum/maximum reactive power generation at generation bus i

$|V_i|_{min}, |V_i|_{max}$: minimum/maximum voltage magnitude at bus i

P_{ij}, Q_{ij} : real /reactive power flow through transmission line ij

$S_{ij\,\max}$: maximum apparent power flow allowable through the ijth line

L_i is the index L evaluated at the i th bus other than the generation buses

L_{crit} is the threshold value of the index acceptable for the system

4. Illustrative Example

The WSCC 9 bus system is taken as a sample system to illustrate the VSCOPF algorithm proposed in the previous sub-section. The network detail for this example is shown in Appendix A.

Before running the OPF the loadings at the load buses were as follows

Bus 5: 150 + j 120 MVA
Bus 7: 100 + j 35 MVA
Bus 9: 125 + j 50 MVA

Table 7 gives result of OPF formulation based on proposed algorithm for the above case. It is observed that there is no load curtailment on Bus 7 and Bus 9. Only Bus 5 has load curtailment.

Table 7. Load Curtailment for Different Security Thresholds

L_{crit}	*Load curtailment (Bus 5)*
0.1	90.57 + j72.45
0.2	36.45 + j291.6
0.25	26.51 + j 21.21

Note that all the PV buses are held at voltage equaling 1.0 p.u. Without the constraint of voltage stability index imposed on the load buses, the load curtailment value got at bus 5 after running OPF was found to be 26.51 + j 21.21.

We observe the following from the simulations and their results:

- For the above case if we choose any value of L_{crit} just above 0.21, the voltage stability index constraint does not seem to effect the OPF for our load pattern and system chosen. This is because of the fact that the constraint V_{min} is already violated and hence held constant at the violated bus. Hence, thereafter the algorithm stops from searching a solution based on the voltage stability index constraint criterion.

- Choice of a low value of L_{crit} increases the load curtailment to be carried out. Hence, the above OPF algorithm encompasses the security based feature of voltage stability in the calculation of load curtailment.
- If the allowable V_{min} for Bus 5 was kept 0.8 p.u, the load curtailment got by the incorporation of the stability margin criterion, for L_{crit} of 0.3, was found out to be more than that calculated without using it. This brings out the fact that the index takes care of voltage stability, even if the voltage magnitude constraint is relaxed.

C. Summary

The focus of this chapter is formulating a procedure to incorporate steady state voltage stability into the optimal power flow. We shall refer to our proposed procedure as VSCOPF in later chapters. For reliability studies VSCOPF procedure can take care of the voltage security feature along with adequacy issues of real MW power.

Our VSCOPF procedure can be extended to incorporate FACT devices like TCSC, as discussed in Chapter IV, wherein the algorithm blends effectively to the steady state characteristic of these devices. Moreover, application of VSCOPF to composite reliability analysis has been detailed in Chapter V.

CHAPTER IV

APPLICATIONS OF VOLTAGE SECURITY INDEX

This chapter reports new applications of using voltage security index. Firstly we examine the use of index to address security impact due to operation of FACT devices. A methodology to quantify loop flow impacts of using TCSC in deregulated market operations is illustrated. Understanding that TCSC affect flow patterns and thereby the security situation, the VSCOPF algorithm of Chapter III would be extended to incorporate TCSC control. Secondly, this chapter discusses our investigations into using voltage security index to monitor dynamic voltage stability. For modeling the dynamics of the system, before evaluating the system state and thereafter computing the index, an advanced time domain simulation package EUROSTAG is used. The results of our investigations are illustrated and discussed.

A. FACT Devices

Many Flexible AC Transmission System (FACTS) devices, like Thyristor Controlled Series Capacitor (TCSC) and Static Var Compensator (SVC), are finding increased applications in power system networks. As de-regulation evolves the need to evaluate the impacts of these control devices on transactions would become even greater. TCSC is being used in power delivery as a series compensator in lines designed to control power flow, to increase transient stability, to reduce power oscillations and to dampen sub-synchronous resonances. The use of TCSC invariably results in redistribution of power flow and its various impacts have been explored in different works [25][26][34]. Since the network topology changes, the parallel flow patterns would also change. In this work we like to demonstrate a procedural routine to study the impacts of TCSC operation on the estimation of parallel flow/loop flow for transactions in the deregulated markets.

In highly stressed system, TCSC operation can reduce the amount of load curtailment, which will in turn reduce the cost associated with load curtailment. In this chapter we propose extending VSCOPF algorithm to include FACT devices operation [27]. We shall demonstrate the use of TCSC impacts using VSCOPF. These ideas can be extended to other FACT devices, like SVC.

B. Steady State Modeling of FACT Devices

1. TCSC

TCSC is a series compensation component. With the firing control of the thyristors, it can change its apparent reactance smoothly and rapidly. There are many papers on the models of TCSC, including the steady state model [53][54] and the dynamic one [55][56]. The steady state model used in our investigations is shown in Fig.4 [57].

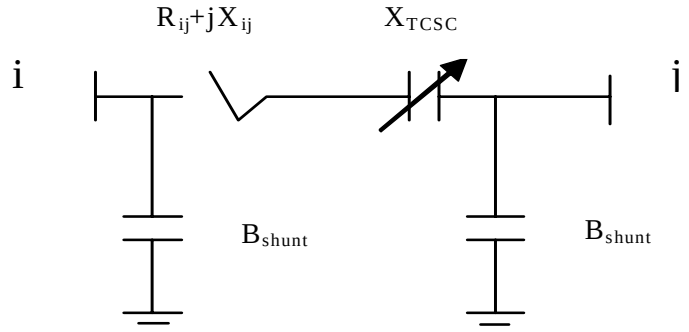

Fig 4. Steady State Model for TCSC

Where, i and j are the end buses of the transmission line; X_{ij} is the reactance of the line; R_{ij} is the resistance of the line.In this model, we treat TCSC as a capacitor/inductor whose reactance can vary between –0.5 and 0.5 times of the reactance of the branch.

2. SVC

SVC is a shunt compensation component. When it is installed in the transmission line, it can be treated as a PV bus with the generation of real power as 0. The model is shown in Fig.5 [57]. In the figure i, j are the end buses of the branch.

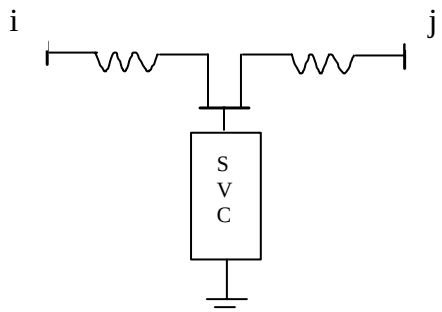

Fig 5. Steady State Model for SVC

C. Impact of FACT Devices on Loop Flow

1. Illustration

The test system used is the simplified WSCC nine-bus configuration having three generator buses. For the trading scenario, we assume a central Pool market and two point-to-point transmission services PTP-1 and PTP-2 in the system. The network diagram including preferred schedules is shown in Fig. 6. The network parameters are given in Appendix A.

The Pool market has three generators G1, G2 and G3 to supplying centrally to three loads D1, D2 and D3, where G2 is designated to pick up the loss shares of the Pool.

PTP-1 supplies 100MW firm power of G4 to D4. The contract path is LINE 6 from Bus 4 to Bus 9.

PTP-2 supplies 100MW firm power of G5 to D5. The contract path is LINE 2 from Bus 6 to Bus 5.

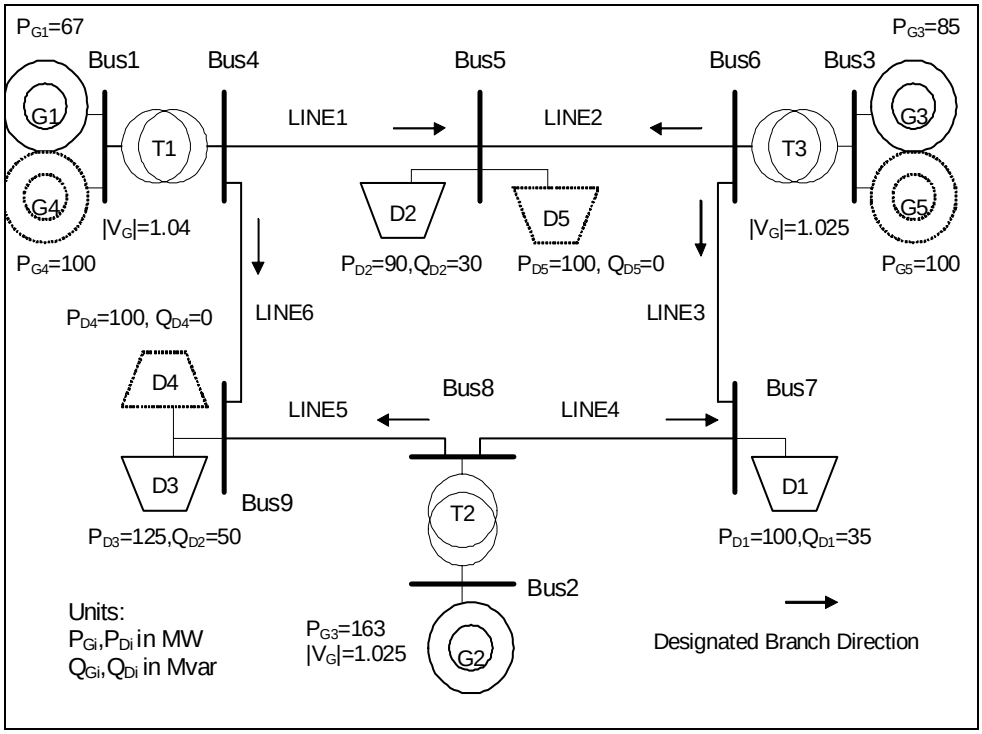

Fig 6. Transaction Schedule to Demonstrate Loop Flow

A system-wide reactive power scheduling function is assumed. We assume that the Pool and the two PTP transactions are treated as simultaneous transmission services. Each of them is required to follow the preferred energy schedule plus associated loss share through its own generation. Bus-1 is designated as the reference bus for angle. We use the Transaction Based Power Flow (TBPF) for loss and flow allocation [11]. The details of the algorithm is shown in Appendix B. The TBPF takes five adjustment iterations to converge (0.0001 MW) to an operating equilibrium, where each market player takes care of the contractual loads and associated loss shares alone.

Table 8. Parallel Loop Flow Components from TBPF

Branch	*Loop flow components without TCSC (MW)*			*Loop flow components with TCSC (MW)*		
	PTP-1	PTP-2	Total	PTP-1	PTP-2	Total
LINE 1	6.0825	27.459	67.299	8.0003	16.317	50.527
LINE 2	-11.329	**78.747***	126.30	-12.708	**88.321***	143.776
LINE 3	12.729	26.347	60.347	13.8568	15.749	42.436
LINE 4	-14.663	-27.192	39.939	-16.201	-16.17	57.818
LINE 5	14.1971	27.164	128.60	15.620	16.353	111.418
LINE 6	**85.344***	-25.187	99.74	**84.113***	-15.505	116.392

The TCSC is incorporated in LINE 2. Let us assume that it operates at -0.5 times the nominal value of its impedance. The nominal value of LINE 2 reactance is 0.17 p.u. Thus when TCSC is operative the impedance of LINE 2 is 0.085 p.u. Tables 8 through 10 presents the results that focuses on loop flows components resulting from PTP-1 and PTP-2. These tables contain information regarding the impacts of TCSC on the flows and its consequences. Table 8 shows the decomposed real flow components across each transmission line for both PTP transaction and the total line flows, both with and without TCSC. Table 9 shows the decomposed real loss components for each PTP transaction and the total real loss, branch-wise, with and without TCSC. The * represents losses across the contract paths. Table 10 depicts the interactions of all the market entities on active losses as given by TBPF. In Table 10, the diagonal terms are self-induced loss components while the non-diagonal terms are interaction losses between associated market players.

Table 9. Active and Reactive Losses Resulting from Loop Flows with TCSC

Branch	*Decomposed Loss components without TCSC (MW)*			*Decomposed Loss components with TCSC (MW)*		
	PTP-1	PTP-2	Total	PTP-1	PTP-2	Total
LINE 1	0.0946	0.3125	0.8732	0.0820	0.1676	0.5324
LINE 2	- 0.5245	3.7218*	6.3261	- 0.6754	4.7624*	8.0746
LINE 3	0.0923	0.1879	0.4339	0.0680	0.0849	0.2277
LINE 4	- 0.0520	- 0.1027	0.1403	- 0.0778	- 0.0854	0.2793
LINE 5	0.5920	1.0920	5.4981	0.5506	0.5826	4.1007
LINE 6	0.8194*	- 0.2596	1.1909	0.9371*	- 0.2056	1.5175
SUM	1.0218	4.9519	14.4625	0.8845	5.3065	14.7322

Table 10. Interactions of Transactions on Real Losses

	Without TCSC in LINE 2 (MW)				*With TCSC in LINE 2* (MW)			
	POOL	PTP-1	PTP-2	Q	POOL	PTP-1	PTP-2	Q
POOL	5.0716	0.9826	5.6016	-0.4571	5.1014	0.8830	5.7723	-0.4595
PTP-1	0.9826	0.9214	-0.6882	-0.0468	0.8830	0.9167	-0.8415	-0.0529
PTP-2	5.6016	-0.6882	2.5737	-0.0784	5.7723	-0.8415	2.9002	-0.0591
Q	-0.4571	-0.0468	-0.0784	0.5822	-0.4595	-0.0529	-0.0591	0.5715

Table 8 clearly shows that when TCSC is introduced the amount of PTP-2 increases from 78.747 MW to 88.321, a change of 12.16%, through contracted line 2. This is because the generator 3, electrically, is now closer to load at bus 5. It is seen that the loop flow contributions for this PTP-1 decreases by about 11 MW through the parallel path encompassing Lines 3-4-5-6-1. However, the parallel flow components of PTP-1, through Lines 1-2-3-4-5, changes only marginally by about 1 MW because of TCSC. One significant impact on Line 6, because of TCSC operation, is that the flow increases to 116.39 from 99.74 MW causing reduction in its ATC value. This is because of the fact that without TCSC, the loop flow components because of PTP-2 which is -25.187 MW helped in reducing the flow through Line 6. But with TCSC, this negative loop component reduces to -15.505 MW which is responsible for a potential loss of opportunity for Line 2 due to reduced ATC.

The total loss component from Table 9 for PTP-2 in the contract path increases from 4.95 to 5.31 MW, with TCSC, which corresponds to the increased flow across Line 2 due to change in topology. However, PTP-1 has to now account for only 0.8845 MW instead of 1.0218 MW losses because of TCSC operation. This is because of two reasons. Firstly, the loop flow due to PTP-1 in Line 2 gains more negative credit as it relieves the increased loading due to PTP-2 on it. Secondly, Line 5 is less loaded because of decreased loop flow caused by PTP-1, due to TCSC operation, causing less loss associated with PTP-1. Please note that both Lines 2 and 5 are long lines with considerable line resistances. Another impact observed is that the total loss increases from 14.46 to 14.73 MW because of TCSC operation.

The traditional contract path method ignores the loss of loop flows, or only charges resistance losses dissipated in contract path, hence it is unable to reflect actual transmission loss cost. However, Table 9 indicates equitable decomposition of losses due to loop flow to all the transmission lines which could be used for a fair loss costing settlement. It is to be noted that the reactive flows and reactive loss decomposition, for all the transactions, is also got by TBPF. However, within the scope of this work we would limit our discussion to active power only.

Table 10 shows the loss interactions between the various market participants. Note that indicates the contribution of reactive power flows to real power loss. Self-induced loss of each transaction is always positive, while cross terms of loss may be negative. Physically, the negative loss allocation implies that the transaction (in combination with all other transactions) reduces the system loss. This table can be used to evaluate the impact of other transactions on the loss amount of a particular transaction. Table 10 shows that the loss self coefficient of PTP-2 has increased to 2.9002 MW from 2.5737 MW, with TCSC, which seems reasonable because of the increase in flow across its contract path. The other self coefficients are not significantly affected. However, the cross terms have changed, which are reflective of the changes in flow patterns due to TCSC. The loss coefficients associated with is small and moreover it is barely affected by TCSC operation. This indicates that the loss due to reactive power support is small.

However, the reactive flows cannot be ignored and the contribution of reactive power support for transactions must be evaluated in order to evolve responsibility and pricing mechanisms.

2. Remarks

Based on the illustration of the previous sub-section and detailed discussions on the results, the following points are summarized:

- The operation of TCSC does impact the parallel/loop flow patterns. The majority flow, for transactions associated with the line having TCSC, is impacted the most. As a consequence, the parallel flows associated with impacted transactions tend to change. This could potentially lead to decrease of ATC for other distant lines that previously benefited from negative loop flow components through it.
- The values of real loss across the transmission lines also change with TCSC operation. Using the TBPF it was shown that loss values associated with the PoolCo and bilateral transactions is effected because of TCSC operation. The real power loss for a transaction caused because of interactions with other transaction is also observed to change with TCSC operation. The parallel flow pattern change is responsible for these changes.
- We believe that for the same system having similar transaction patterns, the value of TCSC compensation and placement of the device would have different degree of impact on parallel flow and hence its consequences. Based on this work it is evident that for the competitive power market to perform efficiently and equitably, assessment of the impacts of TCSC (if used) control in parallel flows is necessary.

It has generally been understood that using TCSC changes the flow pattern and thereby impact congestion and loop flow. The illustration outlined in our work shows how to decompose the impacts of TCSC towards transactions in deregulated

environment. Since flow patterns are affected by TCSC operation it would impact voltage security situation also. In the next section we show the usage of voltage security index to address voltage security.

D. Incorporating FACTS into Voltage Security

1. Incorporating TCSC into VSCOPF

The formulation for incorporating the TCSC control, into the VSCOPF procedure formulated in Chapter III, is presented herewith [27]. When TCSC is installed in the system, its reactance is added as another control variable into the OPF algorithm.

To simplify the simulations we have kept the load power factor to be constant i.e. we assume that when a certain amount of real load has been shed at one bus, the corresponding reactive load will also be shed.

Objective: $min \sum_{i=1}^{n} load\_curtail_i$

S.T.:

$$P_{gi} - P_{li} - \sum_{j=1}^{n} |V_i||V_j|(G_{ij}\cos\delta_{ij} + B_{ij}\sin\delta_{ij}) = 0 \quad (4.1)$$

$$Q_{gi} - Q_{li} - \sum_{j=1}^{n} |V_i||V_j|(G_{ij}\sin\delta_{ij} - B_{ij}\cos\delta_{ij}) = 0 \quad (4.2)$$

$$P_{li} / P_{lireq} = Q_{li} / Q_{lireq} \quad (4.3)$$

$$0 \le P_{li} \le P_{lireq} \quad (4.4)$$

$$0 \le Q_{li} \le Q_{lireq} \quad (4.5)$$

$$|V_i|_{min} \le |V_i| \le |V_i|_{max} \quad (4.6)$$

$$P_{gi\,min} \le P_{gi} \le P_{gi\,max} \quad (4.7)$$

$$Q_{gi\,\min} \le Q_{gi} \le Q_{gi\,\max} \quad (4.8)$$

$$P_{ij}^2 + Q_{ij}^2 \le S_{ij\,\max}^2 \quad (4.9)$$

$$L_i \le L_{crit} \quad (4.10)$$

$$-0.5X_{mn} \le X_{TCSC} \le 0.5X_{mn} \quad (4.11)$$

All terms in the above formulation are exactly the same as Chapter III formulation of VSCOPF [40]. Only one extra constraint equation (5.11) corresponding to the TCSC device steady state operation is added.

2. Choice of Voltage Security Threshold in VSCOPF

The studies were carried out for the WSCC test system. The details of the focus, the simulation set-up conditions and their details are discussed in the following sub-sections.

Table 11. Line Flows, Voltage and Margin Indices

Quantity	*(p.u)*	*Quantity*	*(p.u)*
P_{8-9}	0.8719	P_{9-8}	-0.8261
Q_{8-9}	0.1913	Q_{9-8}	-0.0677
S_{8-9}	0.8506	S_{9-8}	0.8288

Load Bus Number	*Index Evaluated*	*Voltage Magnitude (p.u)*	*Voltage angle (deg)*
5	0.1471	0.9727	-4.8816
7	0.1169	0.9873	-1.1337
9	0.1958	0.9458	-6.6039

Before evaluating the effect of TCSC incorporation into the system, let us first demonstrate the choice of the L_{crit} value for the test system. Load bus 5 was supposedly having a load demand of 90+ j 30 MVA, bus 7 a load demand of 100 + j 30 MVA and load bus 9 having demand of 149.67 + j 59.87 MVA.

Table 12. Line Flows, Voltage and Margin Indices When Line 4-9 is DOWN

Quantity	*(p.u)*	*Quantity*	*(p.u)*
P_{8-9}	1.7112	P_{9-8}	-1.4967
Q_{8-9}	1.6202	Q_{9-8}	-0.5409
S_{8-9}	2.3565	S_{9-8}	1.5914

Load Bus Number	*Index Evaluated*	*Voltage Magnitude (p.u)*	*Voltage angle (deg)*
5	0.1192	0.9752	-3.2530
7	0.1947	0.9283	-2.3801
9	=~1.0	0.6147	-24.6472

All the generator buses are taken to be PV buses with scheduled voltage at 1.0 p.u. The system operates, with the following parameters of interest being observed and evaluated, as shown in Table 11. It is observed that the load bus 9 has an index close to 0.2 under normal conditions. Now let us consider the loss of the line 4 - 9. Table 12 gives the results for quantity of interest that are necessary to carry out our further discussion.

The results show that under this contingency situation the load bus 9 is very close to steady state voltage collapse situation. The voltage has dropped to a low 0.6147 p.u and the reactive flows and hence line flow has increased significantly which have traditionally been used for sensitivity based voltage collapse detection. The above simulation brings out the fact that for a security based operating situation for the above test system the normal index at bus 9 has to be kept less than 0.2, for the securely maintain the transaction amounts throughout the system.

3. Evaluating Impacts of TCSC Using VSCOPF

Now let us apply the TCSC included Voltage Stability constrained OPF, to the WSCC 9 bus test system, to study its effect on load curtailment reduction. For the simulations we have used the following voltage magnitude constraints.

$$0.9 \le |V_i| \le 1.1 \qquad \text{for i = 1, 2, 3, 4, 6, 8}$$

$$0.8 \le |V_i| \le 1.1 \qquad \text{for i = 5, 7, 9}$$

Load bus 5 was supposedly having a load demand of 90+ j 30 MVA, bus 7 a load demand of 100 + j 35 MVA and load bus 9 having demand of 125 + j 50 MVA. All the generator buses are taken to be PV buses with scheduled voltage at 1.0 p.u.

Table 13. TCSC Position, Curtailment, Impedance of Line With TCSC

TCSC Placement Position	*Curtailment at Bus 5 with TCSC (p.u)*	*Impedance of line with TCSC (p.u / %)*
No TCSC	0.3592	-
8-9	0.3100	0.153 (-50%)
5-6	0.2081	0.085 (-50%)
4-5	0.2382	0.046 (-50%)
5-6 & 4-5	0.0890	0.085&0.046 (-50%)

To demonstrate the effectiveness of TCSC, let us constrain the load bus 5 with a very strict voltage stability margin of Lcrit=0.1 under normal conditions. The Lcrit for load bus 7 and 9 is taken as 0.3. The result of running the voltage stability constrained OPF for various situations of TCSC placement and number of TCSC is given in Table 13. The strict voltage stability margin index of 0.1 causes load curtailment to be effected at load bus 5. However, the incorporation of TCSC causes lowering of the curtailment value. The impedance of the TCSC in all cases hits the maximum of –50% limit. Placing the TCSC on the longest line near the load bus5 i.e line 5-6 causes the most efficient reduction when only one TCSC is used. Incorporating two TCSC's in lines near bus 5 causes more reduction as the load becomes strongly supported by generators at Bus 1 and Bus 3.

4. Impacts of TCSC During Contingency

Another simulation was carried out to see the impacts of TCSC during contingency situation for different value of stability margin index. The details of the load are the same as presented in sub-section (2). However, the L_{crit} for the load buses 5 and 7 were taken to be 0.3. A contingency of line outage 4-9 was considered. This directly effects the load at bus 9. The results of the simulation without and with TCSC are given in Tables 14 and 15.

Table 14. Results Without TCSC for Line 4-9 Outage

L_{9crit}	*Load curtailment at Bus 9 (p.u)*	*Voltage magnitude Bus 9 (p.u)*
0.3	0.3796	0.9017
0.4	0.1754	0.8514
0.5	0.0255	0.8041

Table 15. Results With TCSC for Line 4-9 Outage

L_{crit} *at Bus 9*	*Voltage Magnitude at Bus 9 (p.u).*	*Impedance of Line 8-9 with TCSC (p.u)*	*Index at Bus 9*
0.3	0.8803	0.0892	0.2999
0.4	0.8421	0.1267	0.3990
0.5	0.8296	0.1368	0.4310

It was observed that there is no curtailment when TCSC is placed in line 8-9 for this case. The curtailment was effected when the simulation was carried out without TCSC as shown in Table 14. In each of the simulation the L_{crit} constraint caused the load curtailment However, as seen from Table 15 by incorporating TCSC, the load curtailment has been avoided even for the strict case of a margin of 0.3. This brings out the fact that TCSC helps in improving the loadability of the system with regards to voltage stability. From a security viewpoint, TCSC helps in maintaining the safety margin for voltage stability margin without compromising on the load.

5. Remarks

Based on the illustration of the previous sub-section and detailed discussions on the results, the following points are summarized:

- The approach to apply the constraint that can take care of incorporating TCSC device operation, into VSCOPF algorithm of Chapter III. It is seen that TCSC control improves line flow distribution. Other FACT devices can be incorporated into the formulation in a similar manner.
- TCSC control is able to reduce load curtailment, if any, because of redistribution of flows. We have seen from simulations that TCSC relaxes the OPF algorithm when it is constrained by the voltage stability margin indicator. Thus by effectively redistributing the reactive flows, the TCSC aids in relieving voltage stability constrained system operation to an extent.
- Since TCSC can reduce load curtailment, the EENS would be reduced thus improving reliability indices in composite system studies. Thus, procedure proposed and illustrated in this Chapter, for incorporating FACT devices, can be applied in evaluating system reliability measures for composite security based system reliability studies of Chapter V.

E. Dynamic Voltage Stability

Traditional methods of voltage stability investigation have relied on static analysis using the conventional power flow model. This analysis has been practically viable because of the view that the voltage collapse is a relatively slow process thus being primarily considered as a small signal phenomenon. The various analytical tools classified under steady state analysis mode have been able to address the otherwise dynamic phenomenon of voltage collapse. Several static analysis approaches like multiple power flow solutions [58], Continuation power flow (CPF) [15], Point of collapse approach (PoC) [16] Sensitivity analysis [59], such as $\Delta Qg/ \Delta Qd$, $\Delta Vd/ \Delta Qd$, $\Delta Qg/ \Delta Vd$, and modal voltage variation et al static indices are derived either from the full or reduced power flow Jacobian matrix or from running repeated power flows. They are computationally intensive which makes it less viable for fast computation during a sequence of discontinuities like generators hitting field current or reactive limits, tap changer limits, switchable shunt capacitor's susceptance limits etc. In a dynamic voltage stability computation regime, considering all these discontinuities into the analysis are necessary. However, a quick computation is necessary to take necessary corrective action in time to save the system from an impending voltage collapse. The static evaluation tools demonstrate sufficient potentials for on-line implementation. Nevertheless, their accuracy and effectiveness on the practical power systems may not be reliable enough, due to the inability to exactly model some dynamic responding elements, like governor, voltage regulator (AVR), under load tap change (ULTC) transformer and inductive motor load etc. [17][18]. It is recognized that dynamics of electrical elements has significant influence on voltage collapse evolution of a power system

The voltage stability indicator used in Chapter III has been developed considering generator voltages as constant both in amplitude and phase. It has been shown to detect the tendency of the system towards a critical situation with a very fast computation

speed. However, there has been no work reported on how this indicator behaves considering the dynamics of the generators, compensators, loads and on-load-tap-changers (OLTC) following a disturbance in the system. The main idea of the present investigation is to map the power system attributes at the operating state following disturbances like step load increase or loss of line into an index by which the dynamic behavior of the power system is identified. The index must be able to track the dynamic voltage collapse as it progresses. We have tried to investigate how the index L could provide meaningful voltage instability information during dynamic disturbances in the system [13][60].

Recently, features and modeling capabilities of commercial transient stability time domain simulation programs, i.e., EMTP, PSS/E, NETOMAC and EUROSTAG et al, have been greatly enhanced to make them suitable for the assessment of various voltage stability problems. In effect, these sophisticated simulation programs have enabled the users or researchers to construct very realistic voltage collapse cases of interest in an off-line environment, thus facilitate them to better understand complex voltage instability phenomena. In our investigations, we utilize EUROSTAG to investigate the voltage stability problems under open access via a small yet actual power system. As a time domain simulation program, EUROSTAG is well equipped for detailed and accurate study of the transients, associated with mid-term and log-term phenomena in large power systems. The program contains a set of standard models: full IEEE library, relay and automation devices and main FACTS components.

F. Using L Index for Detecting Dynamic Voltage Stability

EUROSTAG is a software dedicated to the dynamic simulation of electric power systems and developed by Tractebel Energy Engineering and EDF. It allows to encompass all the electrical phenomena in the range of transient, mid and long term stability. The system as described in the previous section was modeled into EUROSTAG. The description of the generator automatic voltage regulator and the

governor was also included into it dynamic test file setup. Based on the time domain simulation outputs provided by EUROSTAG the index L was evaluated as per the equations given in Chapter II.

The index L has been calculated on the same line as has been discussed for the static voltage stability case. It is however, to be noted that the voltage and the angles at all the load buses are not the same during the dynamic time frame of interest. For simplicity, we have considered all the loads to be voltage and frequency independent. Since the voltage at the generator buses is not held constant during the dynamic situation the index L at each generator bus is evaluated, considering other generator buses as constant PV buses. The method of calculating is similar to the one adopted for load buses. The details and issues related with index computation are given in the following sub-sections.

1. Test System Setup

We shall use the WSCC bus test system that has three generators for our simulations. The network parameters are given in Appendix C. Base Case Loadings are as given:

BUS 5: 50 + j 40 MVA

BUS 7: 100 + j 35 MVA

BUS 9: 125 + j 50 MVA

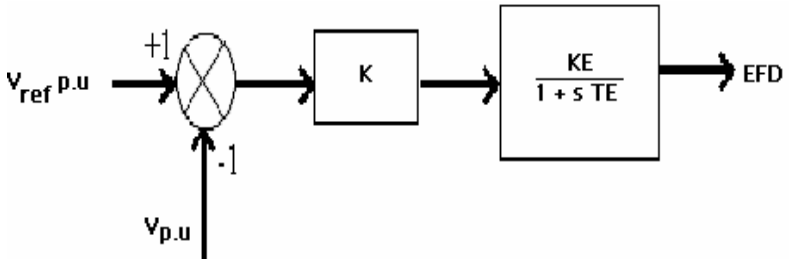

Fig.7. Block Diagram for Voltage Regulator Model

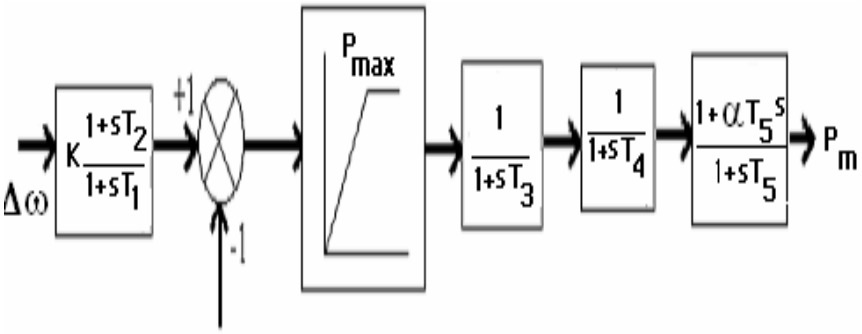

Fig.8. Block Diagram for Governor Model

Dynamic modeling of major elements is as follows. The voltage regulator model and governor model is as shown in Fig.7 and Fig.8. The voltage regulator chain comprises of the exciter and voltage regulator while the governor chain comprises the governor, the boiler and the high and low-pressure turbines. The following models are also provided in the EUROSTAG manual. The parameters for the voltage regulators are K=30, KE=1 and TE=1. While the parameters used for the governor control loop is K=25, T1=4, T2=1, Pmax=1.05, T3=0.1, T4=0.1, T5=10 and α =0.3.

2. Contribution of Other Load Buses Towards Local Bus Index

Let us look at the contributions of other bus loads (Bus 7, Bus 9) on Index L at a local Bus 5 with respect to time. The Table 16 tabulates the observations for a step change of load at bus 5 from 50 + j 40 to 229.69 + 183.7 i MVA initiated at time t=10 units. The index L is given by $L = | Sj^* / (Yjj+ \times |V_5|^2) |$

Where $Yjj+ = 1.6676 - 11.3625$ and $Sj^* = \text{conj}(S_5 + S_7^* + S_9^*)$

Further $S_5 = 2.2969 + i\ 1.837$

Table 16. Evaluation of Index L

Time	S_7*	S_9*	$\lvert V_5 \rvert^2$	*L*
10.001	-0.109 + 0.0103 i	-0.2609 – 0.0319 i	0.3588	0.7887
10.005	-0.1084 + 0.0104 i	-0.26 – 0.0315 i	0.3552	0.7963
10.01	-0.1082 + 0.0106 i	-0.2595 – 0.0309 i	0.3528	0.8014
10.1	-0.1042 + 0.0124 i	-0.2529 –0.0266 i	0.3226	0.8731
10.3	-0.099 + 0.0161 i	-0.2443 –0.0202i	0.2884	0.9717
10.5	-0.1015 + 0.017 i	-0.2499 – 0.0215 i	0.3058	0.9182
15.0	-0.1116 + 0.0139 i	-0.267 – 0.0324 i	0.3844	0.7374
50.0	-0.1113 + 0.0147 i	-0.267 –0.03241 i	0.3832	0.7396

The following observations can be summarized:

- As can be seen from the values of the contributions of different buses, the variations in the real power component is not much. However, the reactive power component swings are perceptible. This is in line with the fact that voltage is related closely with reactive power.
- The index L changes according to the local voltage profile and settles down to a definite value as the voltage settles down.

3. Index Computed at First Voltage Dip Following Change

Simulation was carried out to observe whether the index calculated at the first dip of the voltage at the bus where a step change in load has occurred, can give any information of dynamic stability. It should be noted that in our simulation only governor and AVR models have been included. ULTC have NOT been incorporated.

It was observed that the maximum value of L (when calculated over a time period) occurred at the first trough in the voltage profile. The following Table 17 has been tabulated for a range of step changes and gives the value of index L at the first big dip and the final settling value.

Table 17. Index at First Big Dip and Setting Value

Power (MVA)	*First Negative Peak*	*Steady State (L)*
50 + j 40	-	0.1135
200 + j 160	0.5224	0.4961
210 + j 168	0.5941	0.5548
220 + j 176	0.7002	0.6322
225 + j 180	0.7844	0.6818
229.6 + j 183.68	0.982	0.7396
229.65 + j 183.72	0.9963	0.7396
229.67 + j 183.736	1.0037	0.7396
229.68 + j 183.744	1.0109	0.7396

The following observations can be summarized:

- Looking at the data of the power contributions from other load buses (Bus 7 and 9 in our case) to the index calculated at the referred bus (Bus 5 in our case) it is observed that the active component remains substantial even at higher loads compared with the initial value.
- However, considerable effect is reflected on the reactive power contributions. For example, at a load change from 50 + j40 to 225+j180 at bus 5, the real part of S9* changed from 0.3421 to 0.2626. However the reactive contribution dropped steeply from 0.1106 to 0.0367. This seems to bring out the following two facts:
    - That the voltage at the bus nearing voltage collapse is strongly influenced by the reactive power demand at its bus.
    - The effect of reactive power contributions of other load buses to the index is minimal which seems to support that voltage collapse starts of as a local phenomenon at a particular overloaded voltage bus which is influenced strongly by its local reactive power requirement.
- It is observed that the largest value of the index, which happens to occur at the first trough of the voltage after the load change, approaches 1 as the

dynamic voltage collapse point. The final value of the index L matches with the value which was calculated for the steady state voltage stability case.

4. Index Computed at All Buses

Simulation was carried out to investigate into the profile of the index variations at all load buses and all generator buses during the disturbance for a particular step load change in one load bus.

A load change from 50 + j 40 to 229.6 + j 183.68 was imposed on load bus 5 at time=10sec. The Fig. 9 shows the variations of all the indices with respect to time.

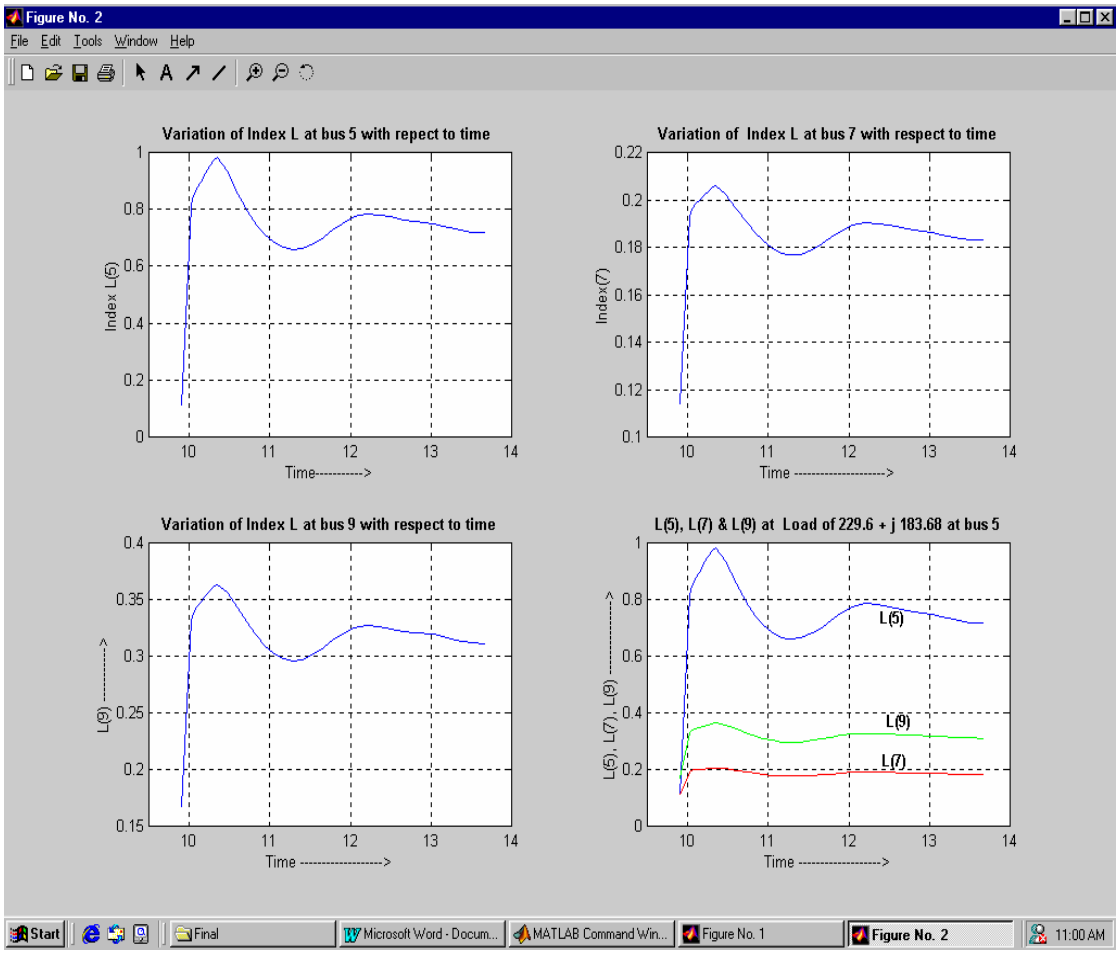

Fig.9. Variations of All Indices w.r.t. Time

Fig. 10 shows the voltage and index variations for all load buses with respect to (w.r.t.) time.

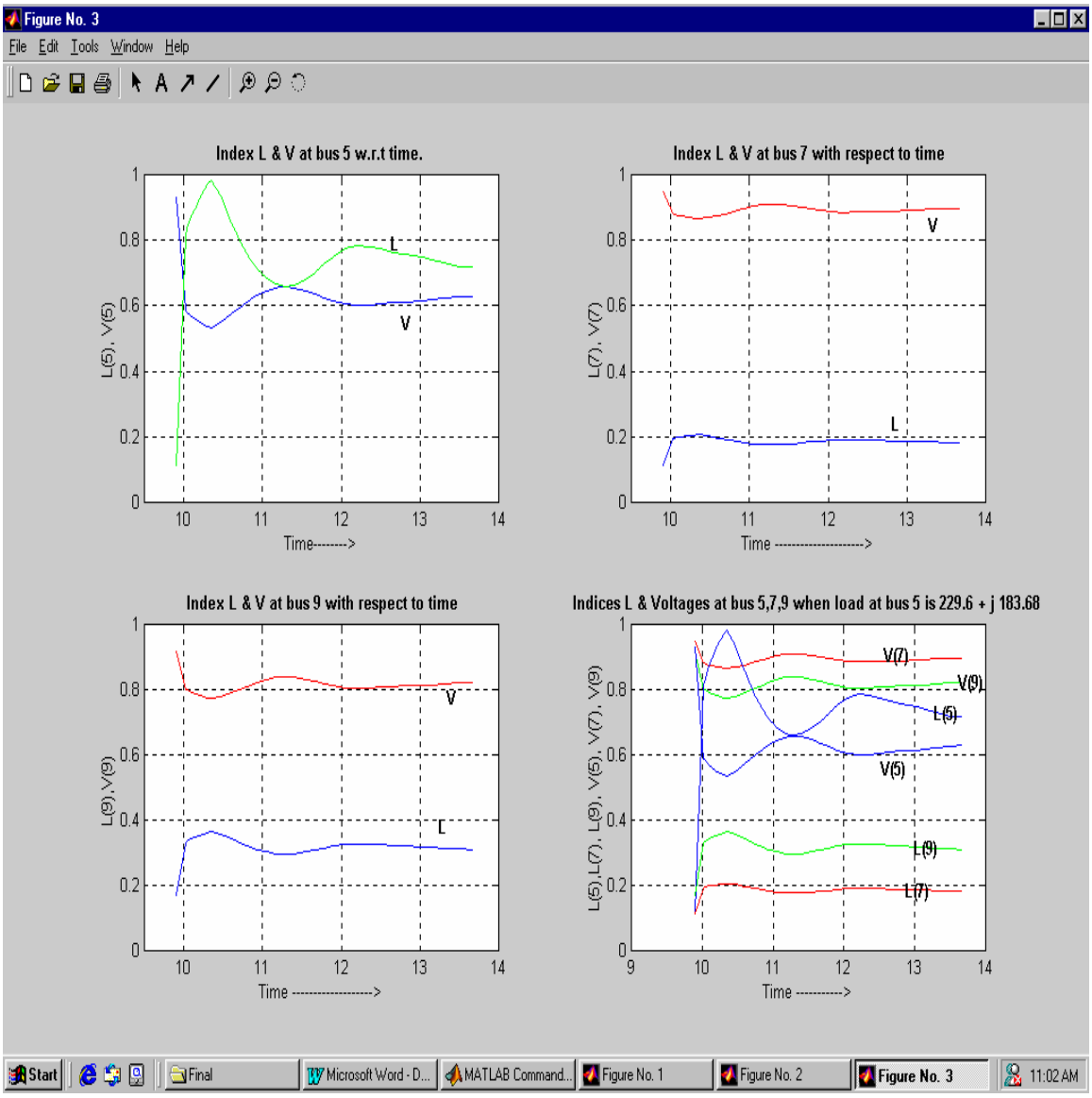

Fig.10. Voltage and Index Variations of All Load Buses w.r.t. Time

Fig. 11 shows the voltage and index variations at Generator bus 2 with respect to time.

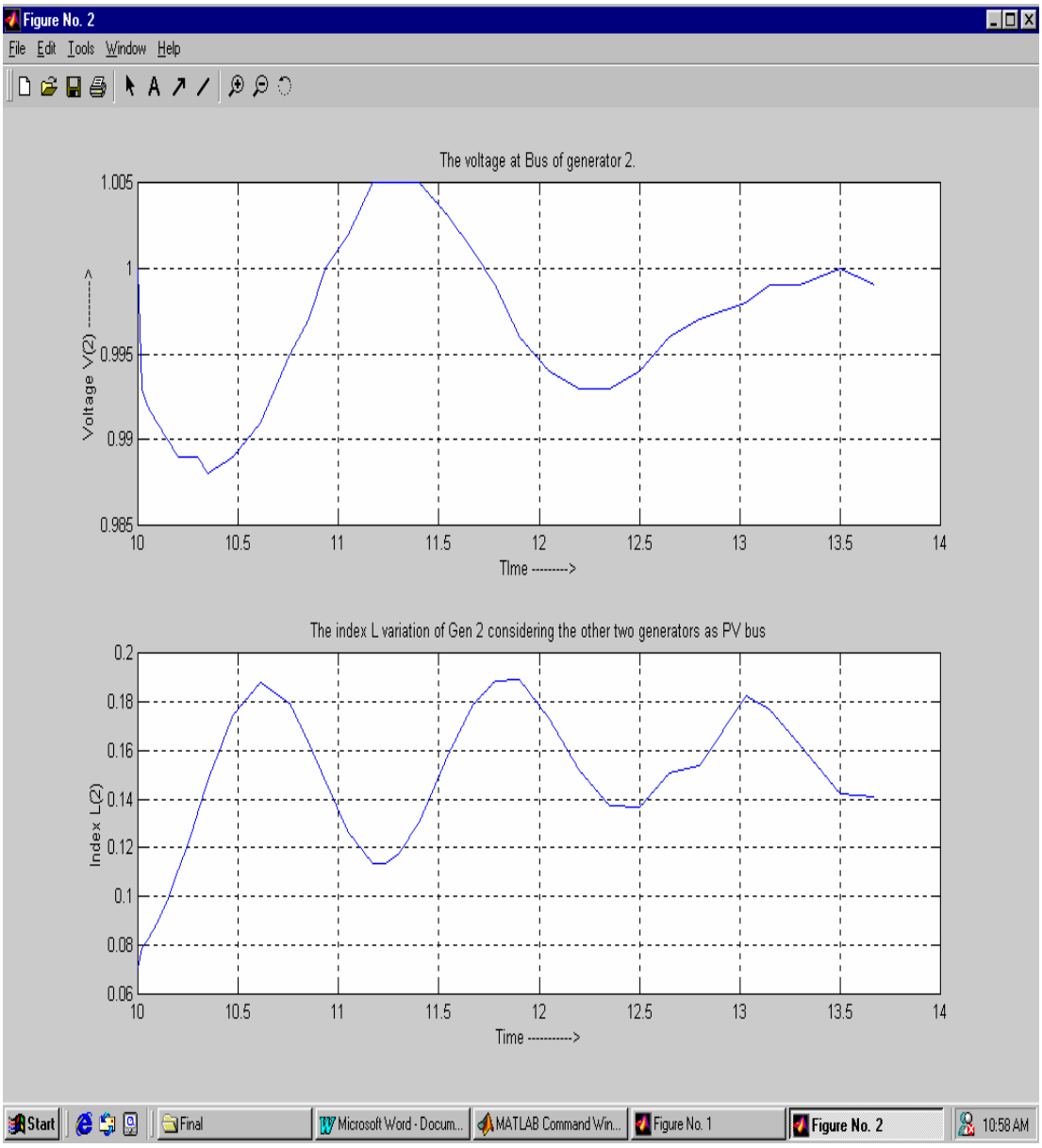

Fig.11. Voltage and Index Variations at Gen. Bus 2 w.r.t Time

The Fig. 12 shows the voltage and index variations at Generator bus 3 with respect to time.

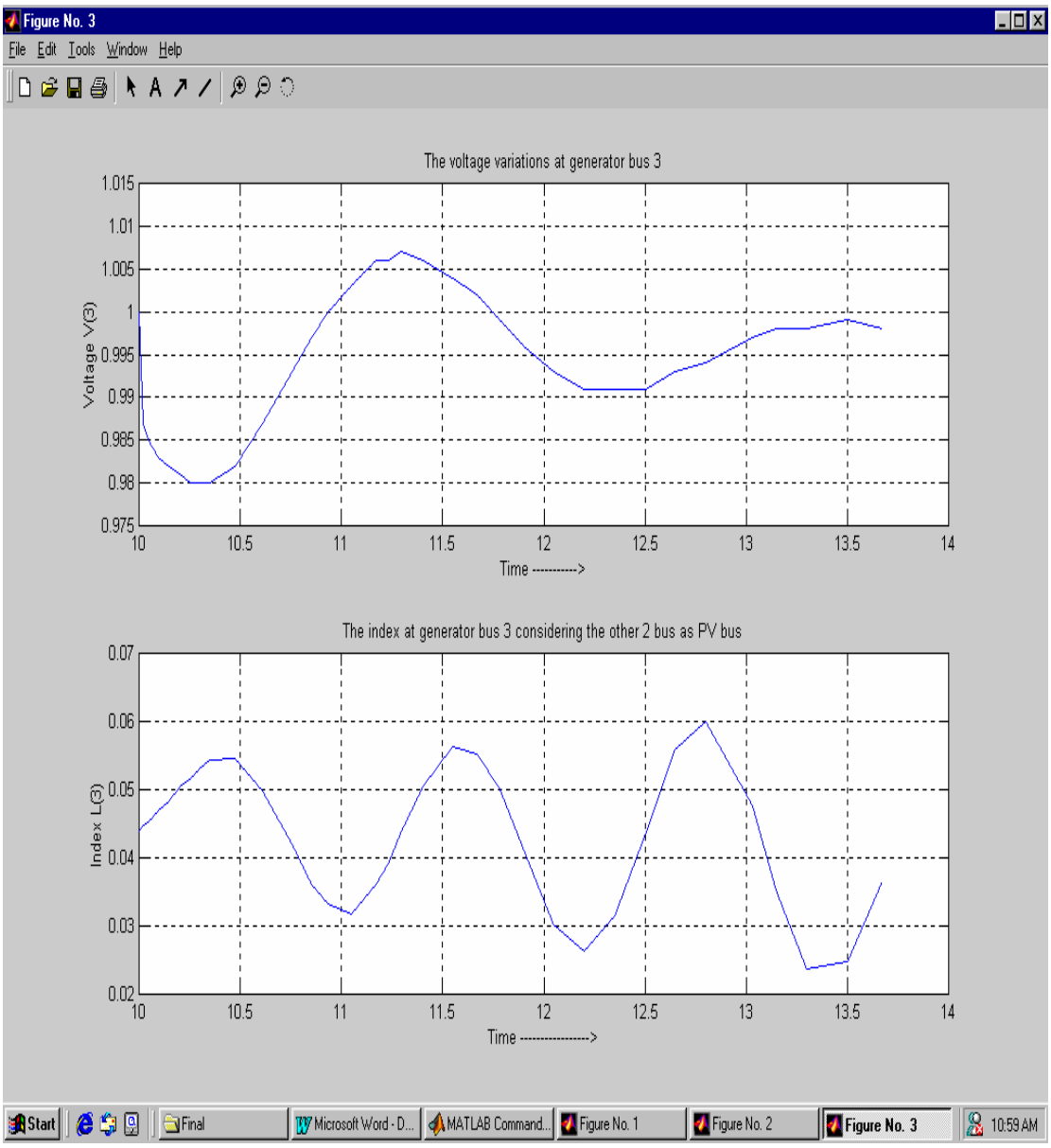

Fig.12. Voltage and Index Variations at Gen. Bus 3 w.r.t Time

The following observations can be summarized:

- The index at generator bus 1 changes to a peak of around 0.1635 from an initial 0.0374. Looking at the position of bus 5 with respect to the generator bus 1, this seems reasonable. The load change affects the nearest generator the most. In this case the line 4-5 impedance is less that line 5-6 impedance. So Load bus 5 is closer to generator 1 than generator 3.
- It is observed that near the dynamic collapse point loading of load bus 5, (229.6 + j 183.68) the index at load bus 9 jumps from 0.1678 to 0.3166 thus decreasing its voltage stability margin. This might be due to the fact that generator 1, which has been affected by load bus 5 loading, is the nearest connected generator to load bus 9. (The impedance of line 4-9 is less than impedance 9-8)
- The index at load bus 7 changes from 0.1138 to around 0.1830 near the collapse point of load bus 5.The differential change in the index value is less than that in case of load bus 9. This might be because of the fact that Load bus 7 is supported by generator 3, which is affected the least because of the disturbance. The L index calculated at generator bus 3 during the disturbance has peaked only to 0.0563 from an initial 0.0438.

G. Behavior of Index During Dynamic Events

In this section the applicability of whether the index L can be used as an early indicator to represent dynamic voltage stability limit is illustrated. The situations investigated are slow change in load, a large step load change and sudden loss of a transmission line.

1. Slow Change in Load

In this simulation setup, the load at bus 5 was increased at the rate of 0.1 + j 0.08 MVA/sec. It was observed that EUROSTAG runs the time domain simulation until the steady state loadability of the system which happens to be about 235 + j 217.11 MVA, after which it stops. Note that in this simulation, we have used constant power factor increase in loading until collapse occurs. Fig.13 shows the result.

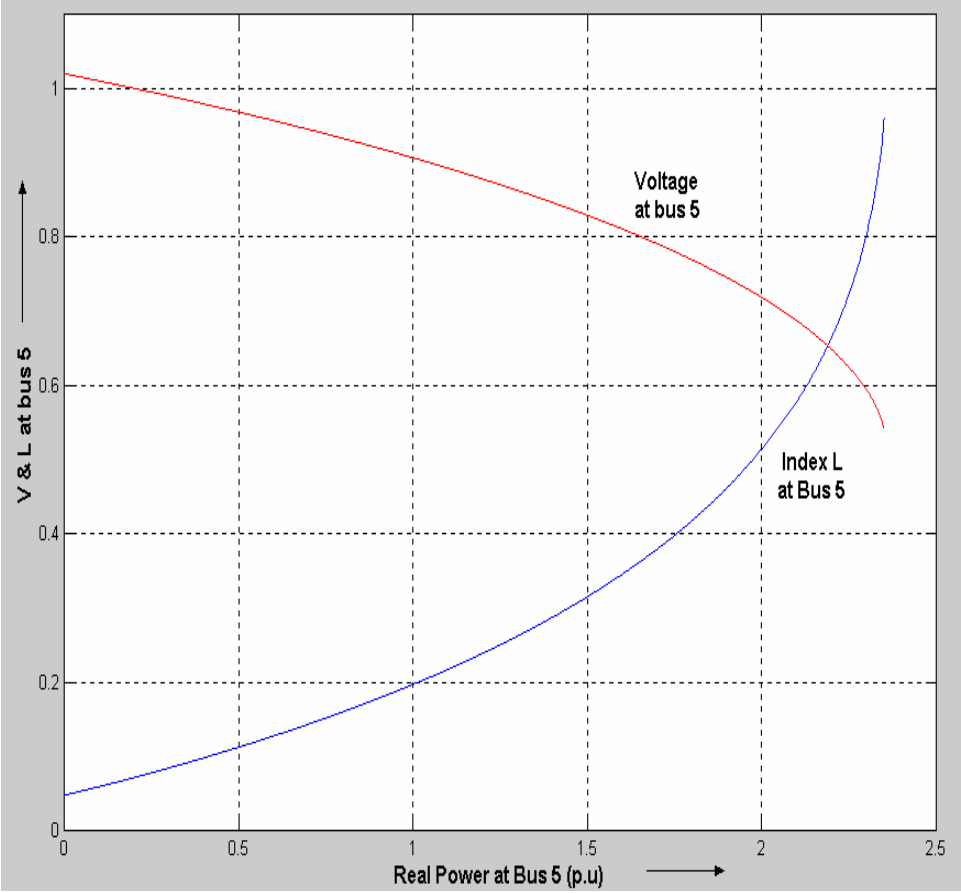

Fig.13. Collapse by Slow Increase in Bus 5 Loading

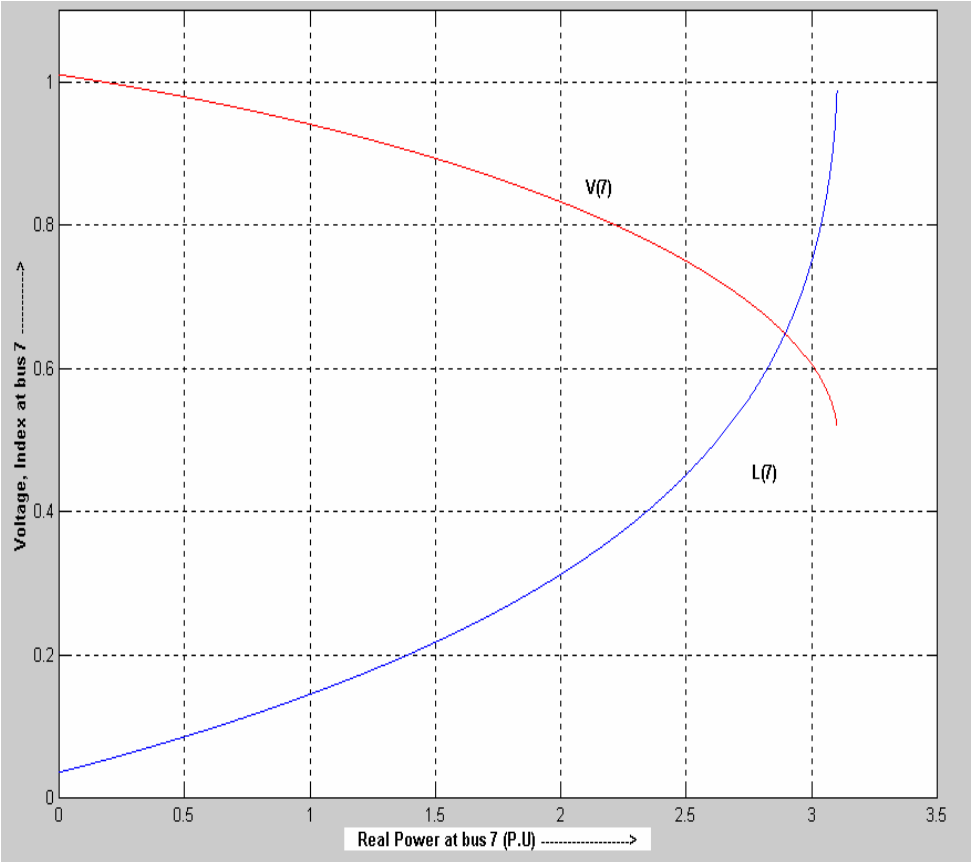

Fig.14. Collapse by Slow Increase in Bus 7 Loading

Fig.14 shows the result for increasing load at bus 7 when the load at bus 5 is 90 + j30 MVA and at bus 9 is 125 + j50 MVA. The collapse occurs when load reaches 310.5 + j 286.86 MVA. Therefore from both the results it can be observed that for slow changes in the loading, the index L gives a pretty accurate picture of the system from viewpoint of voltage stability and it approaches unity towards collapse loading. A practical strategy, to make quick corrective actions, could be realizable if the value of index reaches a set emergency threshold.

2. Step Change in Load

In this simulation setup, the load at Bus 5 is increased in a step from its base value loading of 50 + j 40 MVA at time t=10 seconds. The index, at the first largest dip in the

voltage and at the final settled value of voltage, is computed. The voltages and indices profile, when there occurs a step change at bus 5 from the base load of 50 + j 40 to 229.6 + j183.68 at time 10 seconds, as evaluated using EUROSTAG simulation is as shown in Fig.15.

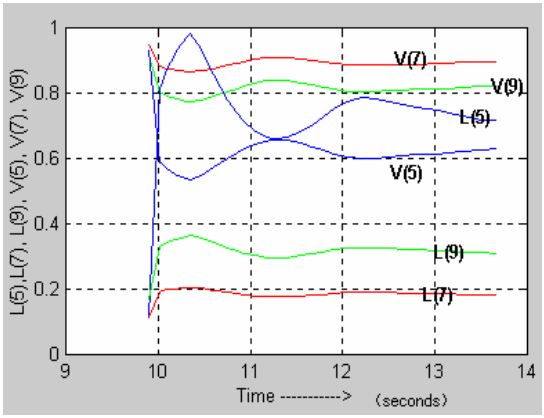

Fig.15. Voltage and Index for Step Change in Bus 5 Load

Table 18 gives the summarized results for various step changes. From Table 18 results it can be seen that the system collapses dynamically when there is a step change from base loading of Bus 5 to about 2.29 + j 1.83 p.u., which is less than the steady state loadability. The index L(5) evaluated at the instant when the first largest dip in voltage occurs is nearing one during the collapse step loading. In other words, the index L is able to predict the dynamic voltage collapse of the system if one were able to evaluate it during these large load changes.

Table 18. Index Evaluated During Step Change at Bus 5

Final Load at Bus 5 (MVA)	*Index at first Voltage dip for Bus 5*	*Index at Bus 5 after disturbance*
50 + j 40	-	0.1135
200 + j 160	0.5224	0.4961
210 + j 168	0.5941	0.5548
220 + j 176	0.7002	0.6322
225 + j 180	0.7844	0.6818
229.6 + j 183.68	0.982	0.7396
229.67 + j 183.736	1.0037	0.7396

EUROSTAG fails to run the simulation if the step change in load is to 229.692 + 183.7536 MVA. The waveform for bus voltage at 5 when this simulation is run is as shown in Fig.16.

The failure of EUROSTAG to run indicates that a voltage collapse has occured at bus 5 and in an actual system a local load voltage collapse spreads to the rest of the system causing potential blackout threats.

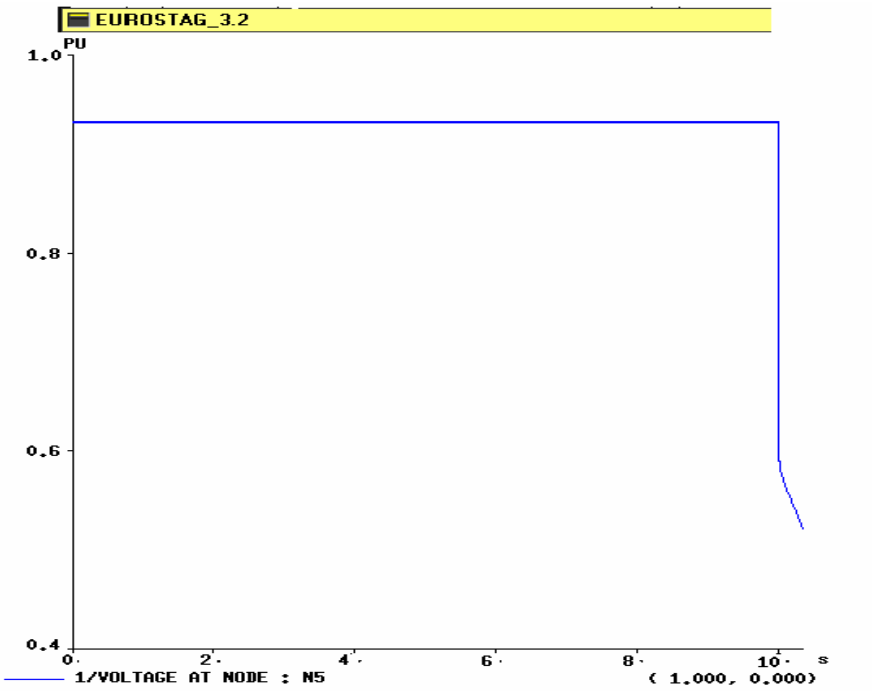

Fig.16. Dynamic Voltage Collapse Due to Step Change in Load

3. Loss of Line

To investigate into the dynamic voltage profile during loss of a transmission line, the loss of line 4-5 supplying to the load bus 5 at time t=10 seconds was simulated. The time domain simulations were run for different loading at load bus 5. The voltage profile when the initial loading was 90 + j72 MVA is as shown in Fig.17.

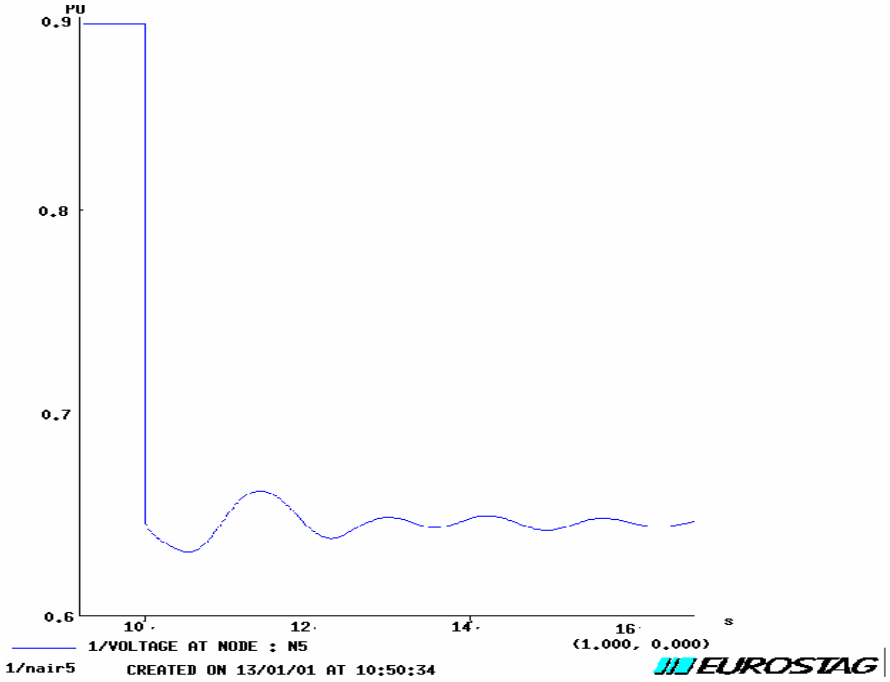

Fig.17. Voltage Profile at Bus 5 Following Line 4-5 Outage

The voltage profile indicates that the system is still voltage stable. However, it was observed that EUROSTAG was not able to run simulation when the initial load at BUS 5 was 94 + j 75.2 MVA, which indicates the dynamic collapse loading for the test system. For the above line contingency, the steady state voltage stability limit works out to be 96.4 + j 89.06 MVA which is higher than the dynamic limit. The indices evaluated for the line 4-5 outage during different loading condition at Bus 5 is as given in Table 19.

Table 19. Index Evaluated During Loss of Line 4-5

Initial Load at Bus 5	*Index at bus 5 before line outage*	*Index at bus 5 at first voltage dip*	*Index at bus 5 after disturbance*
50 + j 40	0.1135	0.2312	0.2300
70 + j56	0.1437	0.3706	0.3666
80 + j 64	0.1602	0.4801	0.4722
90 + j 72	0.1771	0.6787	0.6502
93 + j 74.4	0.1802	0.8093	0.7508
93.97 + j 75.176	0.1823	0.8951	0.7980

It is observed from Table 19 that the index evaluated at the first voltage dip is able to track closely to unity when the disturbance was nearing the dynamic voltage collapse. Thus, the index L is able to indicate in numerical terms the severity from view-point of dynamic voltage collapse for the line contingency disturbance.

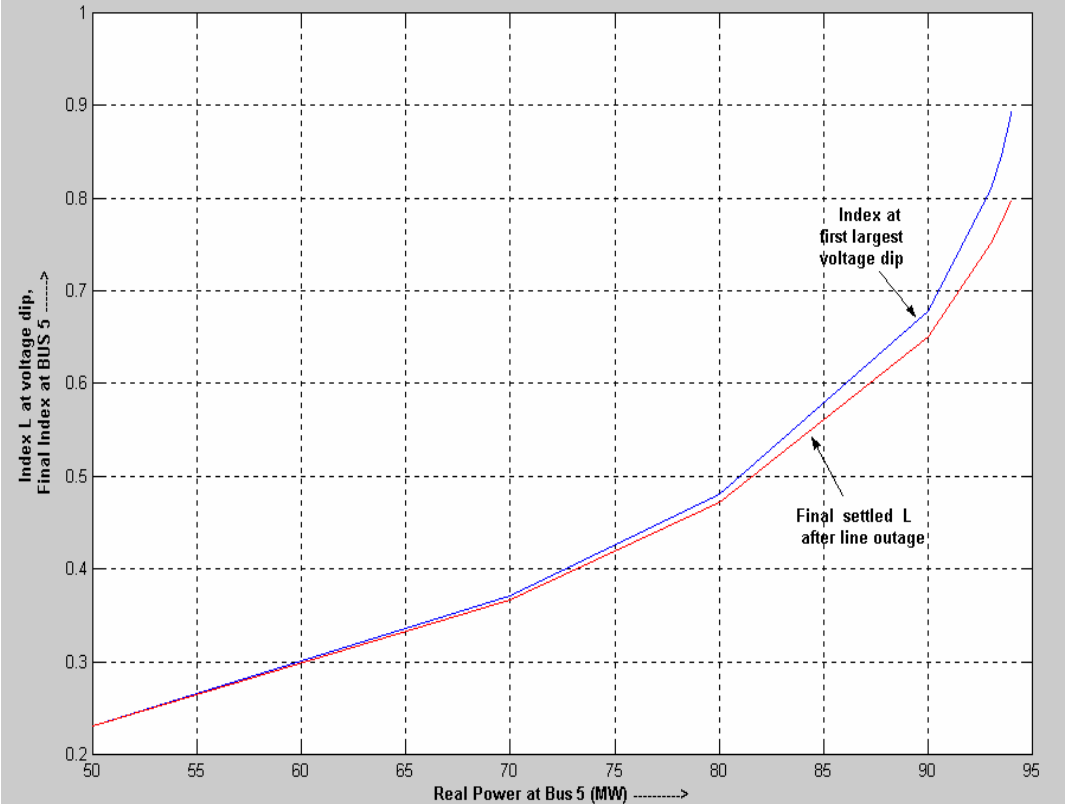

Fig.18. Profile of Index Variations for Result in Table 19

Fig.18. depicts the variations of index, for various Bus 5 loading, as evaluated in Table 19. The top curve shows index evaluated at the first largest voltage dip instant while the bottom curve depicts the index value at instant when the disturbance has died out. The index evaluated at largest dip in voltage is seen to approach approximately unity at collapse loading for Bus 5. Thus as the initial loading on bus 5 increases, during the line outage situation the index computed at the first largest dip in voltage is able to give information as regards to the closeness from a voltage collapse point.

4. Observations

The previous sub-sections discussed applying L index, used as a steady state voltage stability indicator, to detect dynamic instability for a variety of disturbances. We can summarize the observation from the simulations as follows:

- For slow changing load conditions it was observed that the index is able to track the voltage stability condition of the load buses and hence the system effectively. It has been brought about from the results of the simulations that the index approaches very near to unity during a collapse situation. It was also observed that this collapse point coincided with the steady state loadability limit.
- For a sudden step load change scenario, the index computed at the first largest dip in the voltage following the change is able to indicate whether a dynamic voltage collapse is to occur. From the results of the simulations it was also observed that the dynamic voltage collapse loading was less than the steady state loadability point.
- For the loss of line disturbance, the index approximately approached unity when critical initial loading existed. The dynamic loadability, for the contingency considered, was also less than its steady state capability.

H. Conclusions

In this chapter, we demonstrated the use of voltage security index to various operating scenarios. We firstly reviewed the impacts of FACT control devices on power system operational issues. As deregulated market emerges the need to understand and formulate equitable techniques to quantify control impacts of these devices becomes increasingly necessary. We illustrated methods to quantify potential impacts on loop flow due to TCSC operation, in the transaction based environment of electric markets.. We extended the VSCOPF formulation of Chapter III to include TCSC operation

characteristic. We illustrated the impacts of TCSC control and voltage security together on OPF formulation. Other FACT devices can be incorporated using a similar approach. Thus, this part of the chapter discusses the objective related to addressing voltage security from viewpoint of the control horizon in deregulated electric markets.

The investigations discussed in this chapter for prediction of dynamic voltage collapse, based on the L indicator, have shown encouraging results. Further detailed modeling of load dynamics, tap-changing dynamics, over-excitation limiters for generators needs to be incorporated into the EUROSTAG model and the indicator's performance be evaluated for various disturbance scenarios. The advanced time-domain simulations provide a realistic picture about voltage collapse phenomena. Under a major disturbance, dramatic power flow variations lead to rapid rising of reactive losses. As dynamic VAR reserves do not timely compensate the increased reactive loss, the system voltage will have a serious decay. As a consequence, the line charging and shunt capacitor injections decrease dramatically, and further aggravates reactive power imbalance of the system. Subsequently, bus voltage magnitudes continue to drop until a voltage collapse occurs. During the course of our investigation of mapping indicator to dynamic voltage collapse, we have also observed the following findings:

- Rapid rising of reactive losses due to the disturbance is a major factor to trigger a voltage collapse. Reactive power losses are decided by both bus voltage magnitudes and branch currents. Reactive power dominates bus voltage magnitudes while real power contributes to the majority of branch currents. Therefore, both real and reactive power has important impacts on the voltage collapse.
- During voltage decay towards the voltage collapse point, all generators participate in matching reactive power imbalance throughout the entire system. Local generators mainly support reactive power loads, while the rest generators pick up the distributed reactive losses. For serious cases where the system reactive losses surpass the reactive loads, the generators nearby the heavy transmission lines may offer more reactive power support than the generators

within the load center. It demonstrates that voltage control function of the generators is system-wide, not a local nature of reactive power delivery.

- Since steady state analysis methods do not exactly follow dynamics of major electrical components, the solved static voltage stability margin is sometimes too optimistic in comparison to the dynamic simulation result. This potentially imposes major risks on planning and operation of the power systems.

There is a need to investigate and formulate security indicators that can estimate the dynamic voltage stability of the power systems. In electricity markets, associating responsibility to the various participating components towards dynamic voltage security is necessary [61].

CHAPTER V

INCORPORATING VOLTAGE SECURITY INTO PLANNING STUDIES

This chapter presents the enhancement to composite power system reliability analysis by including voltage security. It first reviews the reliability measures, used for planning studies, and methods for computing them. We then demonstrate the use of our VSCOPF procedure to incorporate voltage stability into the composite reliability measures.

A. Introduction

The attempt here is to evaluate composite power system reliability that includes both adequacy and security assessments. The concept of adequacy is generally considered to be the existence of sufficient facilities within the system to satisfy the demand. These facilities include those necessary to generate sufficient energy and the associated transmission capabilities to transfer the energy to the load points. Security, on the other hand, is considered to relate to the ability of the system to respond to disturbances arising within the system during its operation. There have been many methods and techniques to access the adequacy assessment. However, work on the assessment of reliability indices including both adequacy and security is in the research domain [62].

In order to compare the predicted performance of a system with actual operating experience, it is desirable that the predicted indexes and the past performance measures be the same. However, in power system reliability the problem is that the predicted indexes are usually only adequacy based, whereas, the past performance measures (got from operational observations) are reliability (adequacy + security) based. Hence the objective of the present work is challenging.

In the deregulated power systems, reliability evaluation encompassing the system security features has come into focus. Presently research is being carried to evolve methods and procedures to evaluate composite power system reliability indices which incorporate both system adequacy and security issues [62][63][64]. Economic competition, sometimes, results in paying less attention to security features of the overall system. One such security issue is the voltage stability of the system. Several voltage instability incidents have been reported, in the recent past, all over the globe. These are results of operating the system with very less voltage stability margin under normal conditions. Because of the increased demand and the competition induced due to deregulation, congestion management has become one of an important issue. In a deregulated environment, congestion alleviation would mean load curtailment in certain situations. The utilities would definitely prefer to curtail a load as lower as possible during a viability crisis situation. However, from the overall system viewpoint, any policy of load curtailment has definitely to incorporate voltage stability margin considerations [22]. Incorporating the security constraints into the normal operation of a power system would definitely lead to a more reliable system operation. Thus, in the emerging deregulation market control actions have to incorporate security features to maintain an acceptable level of system reliability [22][63].

B. Composite Power System Reliability

1. Introduction

The probabilistic methods for evaluating composite power system reliability are

- Direct Analytical Method
- Monte-Carlo Simulation Method
- Hybrid Method

In the direct analytical method, the complete enumeration of all possible system states is first done. The state transition diagram for these state are drawn. For small

systems such a technique can be adopted. But for larger system contingency ranking methods are adopted where some credible contingencies are taken into consideration.

Monte-Carlo simulation method is a much popular and tested method for large systems. Basically, in this method the time history of the system is evolved based on the available reliability data of the components like failure and repair rates. Evaluations of the indices are then carried out.

We shall demonstrate both the methods for a simple illustrative case. This would basically bring out the features of both methods and also help in ascertaining the veracity of the reliability indices evaluated.

2. Reliability Measures by Analytical Method

Expression for reliability measures like Expected Energy Not Served (EENS), Mean Up Time (MUT), Mean Down Time (MDT) and frequency can be derived analytically, if the complete state space of the system is known. To demonstrate the derivation of the expressions let us consider the three bus system shown in Fig. 19. This would basically bring out the features of both methods and also help in ascertaining the veracity of the reliability indices evaluated.

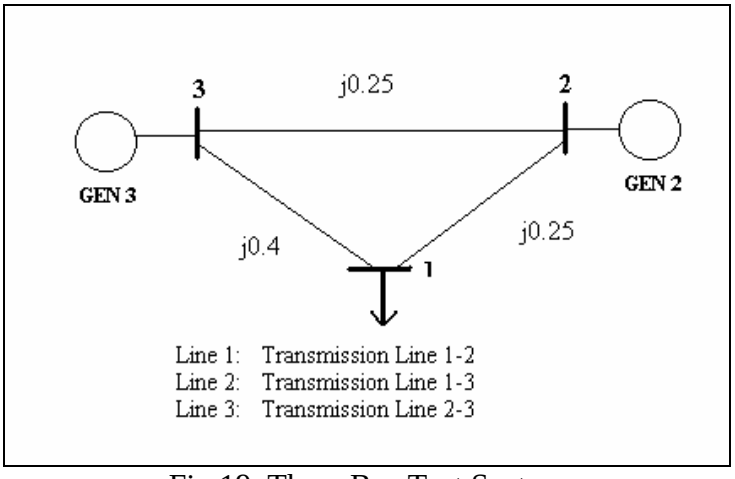

Fig.19. Three Bus Test System

Let the set X+ = {States without load curtailment}, and X- = {States with load curtailment}

Further for the system there are a total of five components namely two generators and three lines. If each of these components are modeled having either UP or DOWN state, then there are a possible of 25 states i.e 32 possible states. Let us assume that states 1 and 6 have no curtailment and all other states have some curtailment amount. Thus,

$X^+ = \{ 1, 6\}$ $X^- = \{ 2,3,4,5,7,8,\ldots\ldots,32\}$

Simplifying the 32 states to a equivalent 3 state model, we get Fig. 20.

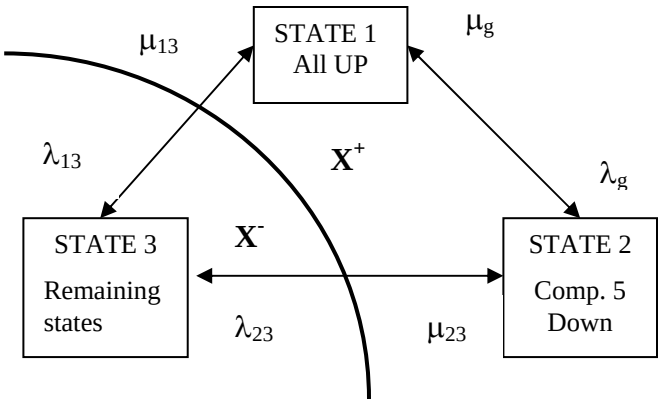

Fig. 20. Equivalent Three State Model

The transition rates of this 3-state model can be evaluated using the frequency balance approach which states that the transition rate $\lambda_{XY} = \frac{\text{Frequency } (X \to Y)}{P_X}$.

Thus for our three state equivalent model, the expressions would be:

λ_{eq} = (Frequency of transition from success to failure) /Probability of success

μ_{eq} = (Frequency of transition from failure to success) /Probability of Failure

For Fig. 20, the transition rates can be given by the following expressions:

$$\lambda_{13} = \frac{P_1(\lambda_g + \lambda_g + \lambda_l + \lambda_l)}{P_1} = 2\lambda_g + 2\lambda_l$$
$$\lambda_{23} = \frac{P_6(\lambda_g + \lambda_g + \lambda_l + \lambda_l)}{P_6} = 2\lambda_g + 2\lambda_l$$
$$\mu_{13} = \frac{P_1(\lambda_g + \lambda_g + \lambda_l + \lambda_l)}{1 - P_1 - P_6} = \frac{P_1(2\lambda_g + 2\lambda_l)}{1 - P_1 - P_6} \quad (5.1)$$
$$\mu_{23} = \frac{P_6(\lambda_g + \lambda_g + \lambda_l + \lambda_l)}{1 - P_1 - P_6} = \frac{P_6(2\lambda_g + 2\lambda_l)}{1 - P_1 - P_6}$$

Where,

$$P_1 = \frac{\mu_l^3 \mu_g^2}{(\lambda_l + \mu_l)^3 (\lambda_g + \mu_g)^3}$$
$$P_6 = \frac{\lambda_l \mu_l^2 \mu_g^2}{(\lambda_l + \mu_l)^3 (\lambda_g + \mu_g)^3}$$

The Mean UP Time (MUT) is given by the following expression

$$MUT = \frac{\sum_{i \in X^+} P_i}{\sum_{i \in X^+} P_i \sum_{j \in X^-} \lambda_{ij}} = \frac{\sum_{i \in X^+} P_i}{\sum_{i \in X^-} P_i \sum_{j \in X^+} \mu_{ij}} \quad (5.2)$$

Mean DOWN Time (MDT) is given by the following expression

$$MDT = \frac{\sum_{i \in X^-} P_i}{\sum_{i \in X^+} P_i \sum_{j \in X^-} \lambda_{ij}} = \frac{\sum_{i \in X^-} P_i}{\sum_{i \in X^-} P_i \sum_{j \in X^+} \mu_{ij}} \quad (5.3)$$

Frequency is given by,

$$\text{Frequency} = \frac{1}{MUT + MDT} \quad (5.4)$$

We also know the load curtailment at all the states evaluated based on the OPF routine with and without the voltage stability margin criteria. The EENS would then be given by the following expression

$$EENS = 8760 * \left[\sum_{i=1}^{32} P_i * Curtailed \quad load(i) \right] hours \tag{5.5}$$

3. Reliability Measures by Monte Carlo Simulation

Some of the typical characteristics of using Monte Carlo simulation method while evaluating composite reliability analysis are listed below:

- Since Monte Carlo Simulation is kind of random sampling, each time we calculate the reliability index the results are somewhat different. So we calculate the reliability index several times and then take average of them to be the final measure.
- When using Monte Carlo Simulation to calculate the reliability index, many identical states are calculated repeatedly which will greatly increase the calculation time. In order to avoid this, we memorize all the states we have already calculated and compare the new state encountered with all the calculated ones. This would help avoding repetition of state evaluation.
- When the contingency make the whole system disconnected, run OPF for all the disconnected parts and sum up all individual load curtailment amounts to get the total system load curtailment.

The flowchart of the Monte-Carlo simulation method used for solving the above sample case is shown in Fig. 21. The next event approach is used here to create the time sequence of the events. A program is developed in MATLAB to solve the above case and the DOWN TIME and EENS were evaluated for both case situations by considering and not considering the voltage stability margin criteria. The results for the simulation are given in the next section.

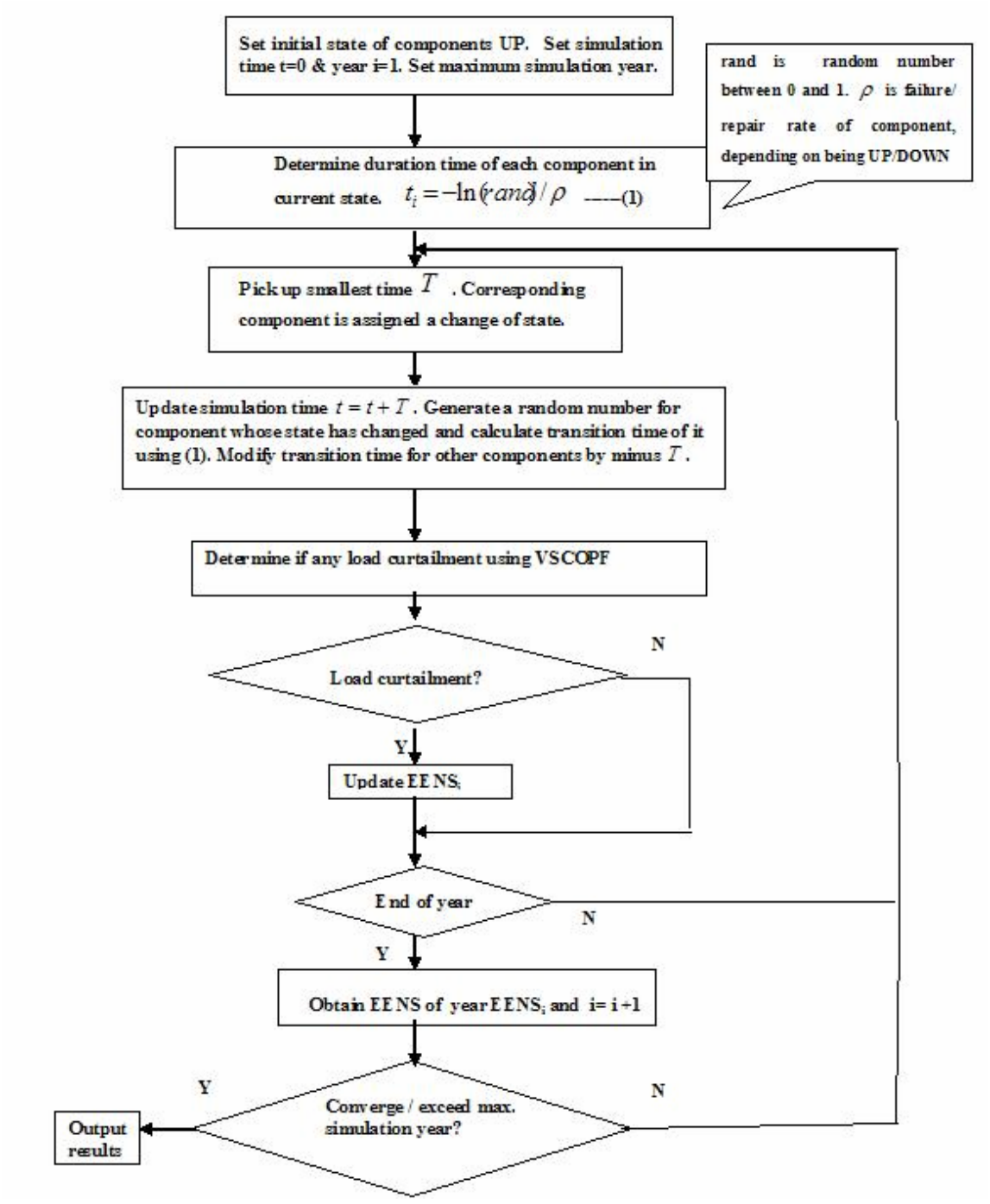

Fig. 21. Next Event Based Monte-Carlo Simulation for Composite Reliability

4. An Illustrative Example

Let us now illustrate the application of voltage security into composite reliability analysis using both analytical and simulation methods discussed in the previous sections. We shall use the test system of Fig. 4 to demonstrate the impacts. The following parameters are chosen for the system:

MVA limits of Line 1 and Line 2 = 2.5 p.u

MVA Limit of Line 3 = 1.5 p.u

Load at Bus 3: 1.4 + j 0.5:

L_{crit} is 0.3 in this simulation

Two different rates of failure rates for components are chosen for demonstration and comparison purposes. They are as follows:

Case I: $\lambda_l = 1$ /year $\mu_l = 1095$ /year
$\lambda_g = 1$ /year $\mu_g = 365$ /year
Case II: $\lambda_l = 10$ /year $\mu_l = 1095$ /year
$\lambda_g = 36.5$ /year $\mu_g = 365$ /year

All the generator buses are taken to be PV buses with scheduled voltage at 1.0 p.u. The maximum and minimum acceptable voltage magnitude at the load bus 3 is taken to be 1.1 and 0.8 p.u. The L_{crit} limit is taken to be 0.3. By changing the value of L_{crit} we can change the voltage stability margin. A larger value indicates lower stability margin.

The VSCOPF algorithm that was discussed in Chapter III was applied for each possible state while carrying out the analytical method of reliability analysis. The state space of all the contingencies, resulting in a load curtailment, for the test system is enlisted in Table 20. For the remaining possible contingencies there happens to be a total loss of the load demand i.e 1.4 p.u. The curtailment value evaluated with and without the voltage stability margin criteria, in the OPF load curtailment formulation as discussed in this paper, are both shown in Table 20. It is to be noted that the curtailment value shown in the table represents the amount of real power curtailment. The load

curtailment policy described in our algorithm sheds the same proportion of the reactive load and the active load

Table 20. Load Curtailment Values for Contingencies

State	*Contingency (Outage Components)*	*Probability of states for Case II*	*Probability of states for Case I*	*Curtailment without L (p.u)*	*Curtailment with L<=0.3 constraint(p.u)*
1	No outage	0.804211266	0.99182317	0.0000	0.0000
2	Line 3	0.00734439	0.00090577459	0.0000	0.0000
3	Gen 2	0.08042112	0.00271732	0.1675	0.1675
4	Gen 3	0.08042112	0.00271732	0.0403	0.0505
5	Line 2	0.00734439	0.00090577459	0.2407	0.5252
6	Line 1	0.00734439	0.00090577459	0.5954	0.8532
7	Gen 2, Line 2	0.000734439	0.00000248157	0.7563	0.7592
8	Gen 3, Line 2	0.000734439	0.00000248157	0.2407	0.5252
9	Gen 3, Line 3	0.000734439	0.00000248157	0.2407	0.2407
10	Lines 2 and 3	0.000067072	0.00000082719	0.2407	0.5252
11	Lines 1 and 3	0.000067072	0.00000082719	0.5954	0.8532
12	Gen 2, Line 1	0.000734439	0.00000248157	0.5954	0.8532
13	Gen 2, Line 3	0.000734439	0.00000248157	0.5954	0.5954
14	Gen 3, Line 1	0.000734439	0.00000248157	0.9049	0.9489
15	Gen 3, Line 2 and 3	0.0000067072	0.00000000227	0.2407	0.5232

Table 21. Reliability Index Evaluated for Case I

Reliability Index	*Analytically*	*Monte-Carlo*
EENS Without L Constraint (MW-hrs)	11.760899	11.7763
EENS With L<=0.3 Constraint (MW-hrs)	16.28370	16.6572
EENS from DC flow	0.0398	-
Down Time per Year (Hours)	63.6919	63.6161

Table 22. Reliability Index Evaluated for Case II

Reliability Index	*Analytically*	*Monte-Carlo*
EENS Without L Constraint (MW-hrs)	324.734	328.604
EENS With L<=0.3 Constraint (MW-hrs)	370.615	374.043
EENS from DC flow	3.1472	-
Down Time per Year (Hours)	1650.77	1664.80

Tables 21 and 22, tabulates the results of the composite reliability measures, EENS and Down Time, with and without voltage security feature in the OPF. Both analytical and Monte-Carlo method of analysis was done for the sample case to compare the methods. For Case I, the EENS without the voltage stability margin constraint incorporation yields 11.761 MW-hrs while it is 16.283 MW-hrs when a constraint of L_{crit} of 0.3 is introduced into the load curtailment evaluation procedure. It was further observed in our computations that by reducing the L_{crit} the EENS became still larger. This brings out the fact that a more reliable operation from the point of view of voltage stability margin would be at the cost of a larger non-served energy. The same trend was observed when a larger failure rates of component, as in Case II, is present.

The down times evaluated analytically were identical when computed with and without voltage stability margin criteria. This is because of the fact that for the test case example, the states when curtailment occurred were identical when evaluated both with and without the L index criteria. The only difference was the amount of load curtailment. However, the authors feel that for larger and practical systems this situation might not be true thus resulting in different down times.

The Monte-Carlo simulation based on the next event approach is then applied to the same test system. The EENS and the down time evaluated for the two cases and both situations of with and without voltage stability index L, agree quite closely with the analytical results. This is quite evident from the simulation results as shown in Table 21 and Table 22. A coefficient of variation of 0.03 was chosen as the stopping criteria for Monte-Carlo simulation runs.

From Tables 21 and 22 another important observation is by looking at EENS values evaluated by DC power flow method. DC power flow greatly simplifies the power flow by making a number of approximations including (i) completely ignoring the reactive power balance equations, (ii) assuming all voltage magnitudes are identically one per unit (meaning that all generators have infinite reactive injection capacity) (iii) ignoring line losses, and (iv) ignoring tap dependence in the transformer reactances. The EENS measure got from DC flow methods thus primarily gives a measure of generation

adequacy requirements. For our sample system the generation adequacy is highly sufficient. However, the existence of EENS associated with DC flow method is due to the sum of probabilities of failure states associated with no transmission lines connecting towards loads and states involving no generators available.

We can summarize the observations of this illustration as follows:

- The load curtailment evaluation is effected by the proposed incorporation of the voltage stability margin index into the OPF algorithm. The amount of curtailment evaluated is observed to increase if more voltage stability margin, from a possible collapse, is required in a system.
- The EENS increases when we tend to operate the system with a larger voltage stability margin. This is because we are demanding adequacy as well as security from the given resources.
- The down time evaluated, for the simple test case used for illustration in this paper, shows no change by incorporating the voltage stability margin. However, the authors feel that for a larger and practical system the down times would be larger if the operation demands a higher voltage.
- The Monte-Carlo simulation results match closely with the analytically computed reliability indices. Thus the proposed algorithm can be implemented, on larger systems, more time efficiently by using the numerical simulation methods.
- The EENS measure got by using only DC power flow represents the generation adequacy of the system. The EENS measure got by not including voltage security incorporates adequacy as well as limits on reactive capacity of generators, maintaining reactive power balance of system and ensuring voltage magnitude constraints. The EENS measure got by including voltage security represents adequacy, reactive capabilities and additionally security from potential disturbances.

Let us know interpret how reliability is increased by using voltage security. If voltage security was not included into reliability evaluation we would have got planned EENS to be 11.761 MW-hrs as per Case I results. This implies that during actual operation if voltage insecurities were indeed encountered then actual loss of energy could be more than the planned value. However, by including voltage security of L<=0.3 we know that the maximum possible EENS is 16.283 MW-hrs and system can sustain voltage security disturbances. Thus in a way the reliability improvement of using voltage security over not using security would be the difference in EENS i.e 4.522 MW-hrs for Case I. Obviously, if lesser security margin is used then lower would be the difference of improvement in reliability estimate.

C. Incorporating Voltage Security Into Power System Planning

Having addressed methods of evaluating composite reliability measures and using our VSCOPF procedure to include voltage security let us now assess the impacts of using it in power system planning studies.

Engineering planning studies is an iterative process which assesses the adequacy requirements of resources that satisfies both an acceptable level of reliability and acceptable investment willingness amongst participants. Obviously, maintaining 100% reliability means exorbitant cost. Average power system reliability measures like EENS gives an indication of the engineering compromise between investment and reliability. If the EENS is not acceptable then resources needs to be added and the analysis reevaluated. Traditionally, reliability studies for power system planning have relied on just generation adequacy requirements using DC flow models. The provision of MW reserves in real-time took care of the variations in system load from the planned value and also ensured security towards withstanding disturbances.

However, in the context of deregulation there is a need to compute reliability measures like EENS including both adequacy and security. This is because of the fact that economic competition results, sometime, in operating the system on the verge of

insecurity leading to blackouts. Additionally, reactive reserves which impacts voltage security is distributed throughout the system and need to be evaluated centrally. To reduce the possibilities of such real-time catastrophic events it would be effective to address security along with adequacy during the planning stages. When addressing voltage security it is known that voltage magnitude alone cannot indicate the nearness to voltage instability. Moreover, dynamic voltage stability margins are definitely less than static stability but are difficult to estimate. Thus, operating the system within some acceptable steady state voltage stability threshold ensures the system operation to withstand dynamic voltage stability events. Our VSCOPF procedure, which uses a power-flow based indicator, gives quick and flexible way to control the amount of voltage security needed at various load buses by system planners. We can use the same threshold to all buses or relax the voltage security feature at selected buses by increasing their threshold in VSCOPF.

Referring to the illustration discussed in Section B, the EENS got by including voltage security is more compared to than without using it. We have used identical systems with similar loading patterns and failure/repair rate of components to compare the difference in reliability measures. If the EENS is not tolerable then system planners need to provide for more local reactive resources or reduce the loadings. The increased EENS by incorporating voltage security is because of the fact that now we are taking care of adequacy as well as operating the system always under steady state voltage security margins.

D. Summary

This chapter discusses the impact of including voltage security into the planning studies of power system operation using our VSCOPF formulation. Composite reliability analysis measure, used as a planning tool to address adequacy and security together, is seen to be impacted by incorporating voltage security. Better planning estimates could be arrived at if voltage security was included into analysis.

CHAPTER VI

EMERGING DATA COMMUNICATION ISSUES AFFECTING VOLTAGE SECURITY EVALUATION

This chapter discusses the issues concerning power system data communications in the emerging deregulated markets. Power system data management amongst the various entities would impact monitoring and managing voltage security. The voltage security evaluation tools are a part of the Energy Management Systems. An improvement towards speeding up data exchange amongst commercial EMS systems is suggested. Additionally, an information architecture that is scalable to newer emerging technologies for disseminating data in electric market is proposed.

A. Introduction

Restructuring of the electrical power industry has changed its organizational structure significantly. The restructuring of the integrated power system operation, into decentralized competitive entities in the deregulated environment, calls for an effective integration strategy amongst the various existing and newer information management systems [28][29][65]. Additionally, newer coordinating entities like Independent System Operator (ISO) have emerged to ensure security and reliability to the power delivery as well as facilitate market transparency and competitiveness. These entities require a lot of information, both system operational specific and market based, to monitor, operate and plan electric markets.

One of the centralized data sources for monitoring, operation and analysis of power system is the EMS. Traditionally EMS has remained insular in terms of data exchange with the other vendor's EMS products and also within the utility's other information systems. This real-time data exchange has become even more critical with electricity being freely and competitively traded as a commodity in the energy market. The report

by the IEEE task force on Data Exchange for Security Assessment outlines the justification of the data exchange and suggests possible types and quantities of data exchange. From viewpoint of economics and security analysis, utilities have always needed model information from neighboring systems. For a local EMS the real time data got from other external areas helps in providing a more robust and observable state estimator solution. Moreover, getting a more real picture of the breaker status information of the external areas could help in evaluating more accurate and realistic security assessments. The failure to timely recognize the outage of transmission line is cited to be one of the major initiating causes according to the Joint Taskforce's interim report of the August 2003 blackout. Failure in some of the functionalities of Energy Management Systems (EMS), like State Estimators (SE), is cited as another significant reason. Thus, managing data is the key in monitoring, controlling and securely operating the electrical system network in the presence of market forces. This chapter addresses the issue of how power system operational and market data can be effectively exchanged and transmitted in the context of emerging deregulated electric markets [33].

Newer software and information architectures are being proposed for future electric power systems [29][66]. The path taken by power system data is still very much the same as it used to be in vertically integrated operations. Supervisory Control and Data Acquisition (SCADA) still has the same functionality i.e. to provide accurate and real-time information on an electrical power network. Newer data paths are added because of the emergence of distributed generation and Automatic Meter Reading (AMR). A number of communication media ranging from twisted pair metallic cable to satellites are currently in existence to transfer this data [67]. Attempts to migrate SCADA communication to the popular TCP/IP networking ensuring quality of standards (QoS), have been reported [68][69][70].

There are numerous publications addressing the various communication architecture alternatives, data formats and data transfer in electrical networks. However, the authors did not find any article that brings together all the relevant issues together at one place. The power system data, firstly, needs to be classified in some functional objective-

oriented way. Then the existing and emerging communication technologies need to be looked into the context of how effectively they pass on data in the restructured markets. Finally, efficient and scalable architectures must be designed to effectively exchange and transmit the relevant data within the existing and emerging communication framework seamlessly. This chapter attempts to address all these aspects.

B. Common Information Model (CIM)

Traditionally the bus / branch oriented models are used for analyzing the planning functions for system support. In these models simplified representation of equipment and connectivity are involved. However, from a system operational viewpoint the model referred as the node/breaker model, that shares more details about equipment, is more meaningful for the real-time power system operation. Within the restructured power system scenario the ISO's, RTO's, market operators all would need such operational data on a regular basis to work out a secure, reliable and competitive operation. There are topology processors available in available EMS systems that convert a typical bus breaker EMS model into a bus branch model.

The Control Center Application Program Interface (CCAPI) task force of Electric Power Research Institute (EPRI) has developed the Common Information Model (CIM) that is a comprehensive description of the types of data found in electric utility EMS systems. The CIM thus semantically describes the entities in the operational domain of an electric utility. In other words CIM is able to model the power system network in a node/breaker level. CIM filters have been developed for all the existing proprietary EMS systems. These filter help in populating the CIM database, which can then provide a standard data interface for other systems and applications. Thus, it provides a key link for aggregation of data from EMS of different vendors into a single data model for the whole system. Now let us look at how CIM representation is used, how it can be represented and how it can be transported amongst software components.

1. Power System Modeling Using CIM

To manage the extensive power system entities and their relationship, CIM has been fragmented into various packages or models like the core, wires, generation etc. CIM is defined and maintained using a set of Unified Modeling Language (UML) classes that help in specifying, visualizing and documenting in an object-oriented way. To take advantage of the property of inheritance a PowerSystemResource base class is defined to describe a generic power system component that needs to be modeled, monitored or measured. Other subclasses like Conducting Equipment subclass, as shown in Fig.22, are derived from this base class and associations are used to specify the connectivity amongst the objects of the subclass. The subclasses of the base class inherit the "measured by", "owned by" and "member of" relationship from it. Fig. 22, shows the objects and their associations for the connectivity model. The arrowhead represents the generalization type of relationship existing between the two entities. The diamond symbol represents the aggregation-type relationship that exists between classes, for example between the connectivity nodes and a topological node.

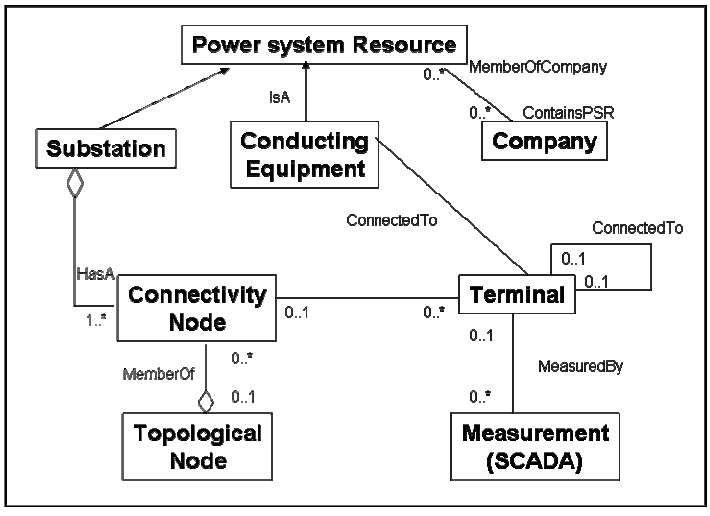

Fig.22. Portion of Connectivity Model from Wires Package

The state information of these generic power system components is stored in the MeasurementValue table, which has the relationship with the measurement class as shown in Fig.23. The Measurement class is included in the SCADA package of CIM. They contain the real-time data from telemetry systems and solutions obtained from applications like load flow or state estimation.

The CIM, being described in a UML framework, helps being in direct conformance with software technology that uses the object-oriented representation of the various system entities. The file created by such software could then be understood by any system that shares the same meaning of objects as described in CIM.

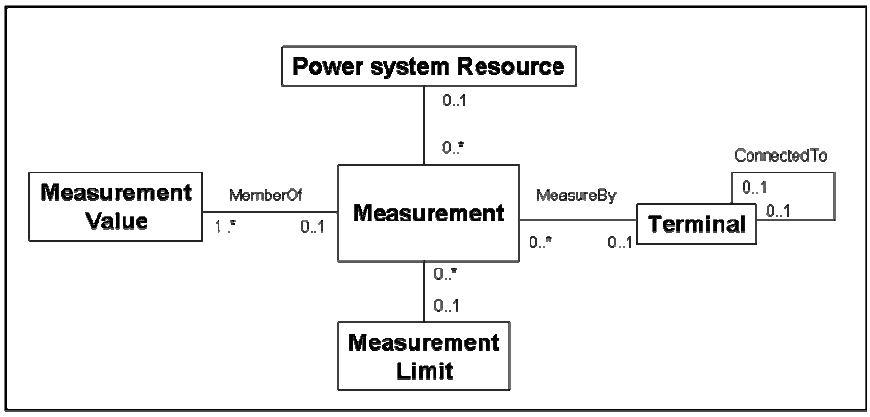

Fig.23. Portion of Measurement Pattern from SCADA Package

In deregulated power markets, distribution management system (DMS) has started growing and developing more application suites. Some of the established DMS functions are outage management, fault location, network management and Geographic Information System (GIS). Distribution system usually has a very large data model. Besides unbalanced three-phase and single phase operation also needs to be modeled. Applying CIM data models to electrical distribution are being explored. Efforts to include distribution system components to the data models have also started [71].

2. CIM-RDF Schema

The International Standards specifies a Component Interface Specification (CIS) for EMS Application Program Interfaces (EMSAPI) that describes the format and rules for producing a machine- readable form of the CIM. It describes a CIM vocabulary to support the data access facility and associated CIM semantics. Secondary objectives are to provide CIM versioning capabilities and a mechanism that is easily extensible to support site-specific needs. The solution to achieve the above objectives should also be such that it can be accessed using any tool that supports the Document Object Model (DOM) application program interface. The DOM is a platform independent and language-neutral interface defined by the World Wide Web Consortium (W3C) that allows programs and scripts to dynamically access and exchange content, structure and style of the documents.

Resource Description Framework (RDF) is a language recommended by the W3C for expressing metadata that machines can process simply. The unit of information in a RDF data model, called a statement, is comprised of the triplet namely Resource, Property and Value. A resource is anything that can have a Uniform Resource Locator (URL) that helps in its identification. A property is some special characteristic of the resource. The value as the name suggests identifies with the description of the property.

RDF Schema is a schema specification language expressed using RDF to describe resources, their properties and their relationship with other resource that is used to specify an application-specific vocabulary. The RDF schema is better suited for graph-oriented models, so this is the approach that was chosen for CIM that has an entity-relationship view of data. The CIM RDF schema allows definition of metadata in CIM's abstract model that is described using UML. This schema also supports UML properties like multiplicity, Inverse Rolename etc. that are useful in expressing CIM.

3. CIM-XML

Extensible Markup Language (XML) has been primarily evolved to make it easy to interchange structured documents over the Internet. XML is unequalled as an exchange format on the Web. Since its inception numerous applications have been built around the technology, which has led to development of a large number of supporting tools and libraries. XML has hence been preferred as the method for common model exchange of the CIM data. Something like XML is an absolutely necessary part of the solution to CIM RDF's Interchange design goal. But by itself, it doesn't provide what you need in a metadata framework. The CIM XML language thus acts as a vehicle of the RDF schema representation of CIM.

The Common Information Model (CIM) data format [31] was developed so that a common data structure for interchange of power system modeling and operational data, amongst the various existing proprietary EMS formats, could be made possible. The use of Extensible Markup Language (XML), as a vehicle for the data exchange of the CIM databases amongst EMS, has gained general acceptance [30]. This is because of a variety of data exchanging technology existing around XML today. Some of these applications like the healthcare, chemicals and financial industries have separate exchange standards built around XML technology.

C. Improvements to CIM Based EMS Data Exchange

1. Existing Architecture

Power system applications in an EMS are real-time functions intended to assist the operator in his tasks. These functions can be grouped into the following categories:

a. Production Planning

- Unit Commitment (UC)
- Interchange Transaction Scheduling

b. Production Control

- Economic Dispatch (ED) Calculation
- Automatic Generation Control (AGC)
- Generation Reserve Monitor
- NERC Performance Monitor

c. Power System Analysis

- Network Topology Processor
- State Estimator (SE)
- Network Reduction
- Dispatcher Load Flow (DLF)
- Optimal Power Flow (OPF)
- Short Circuit (SC) Calculation
- Contingency Analysis (CA)

The input data to the EMS is from the SCADA system and the power system application output data from EMS helps system operators to maintain electric system security and reliability. In vertically integrated operation each vendors EMS had its application data stored only in proprietary databases. Following standardization efforts, CIM filters have been developed for all the existing proprietary EMS systems. These filter help in populating the CIM database, which can then provide a standard data interface for other newer systems and applications. Thus, it provides a key link for aggregation of data from EMS of different vendors into a single data model for the whole system.

All the currently available EMS systems maintain both proprietary and CIM databases having the same data populated by measurements and application functions. The application functions, which are legacy software in many old systems, still populate the proprietary databases. The CIM filter then converts this data to populate the CIM database. This way the reliable legacy software still computes the processed output using proprietary databases. At the same time the CIM databases can take care of the

standardization requirement. Care is taken to maintain data consistency between both the databases.

In the restructured operation of power systems there is a need for exchanging information from neighboring EMS. This is primarily because of increasing large and long-term transactions over tie-lines. From viewpoint of potential on-line security assessment, the power system security model should be initialized with real-time data for the topology of the monitored portion. The external network for the above assessment, used to be generally populated using the sensitivity analysis obtained from larger network planning models. To make the assessment more robust, real-time information regarding the external system is essential. This can be got only by exchanging raw and processed data from neighboring systems. Getting credible information regarding the external system also helps in maintaining a more credible and robust state estimator.

Fig.24, shows the method of data exchange that could be used amongst proprietary EMS systems using the CIM XML documents. Data between proprietary databases can be exchanged through the XML document that conforms to the CIM RDF schema. Separate XML tools can be used to validate the format of the file and the conformance with XML and RDF Syntax which would ensure the integrity of the conversion wrapper. The CIM XML document can also be viewed through a browser using an XSL Style Sheet to format the contents for human readability. The communication medium could be either through corporate WAN or dedicated channels. A cheaper option of communicating using the internet (TCP/IP) could also be implemented if QoS and security requirements are addressed.

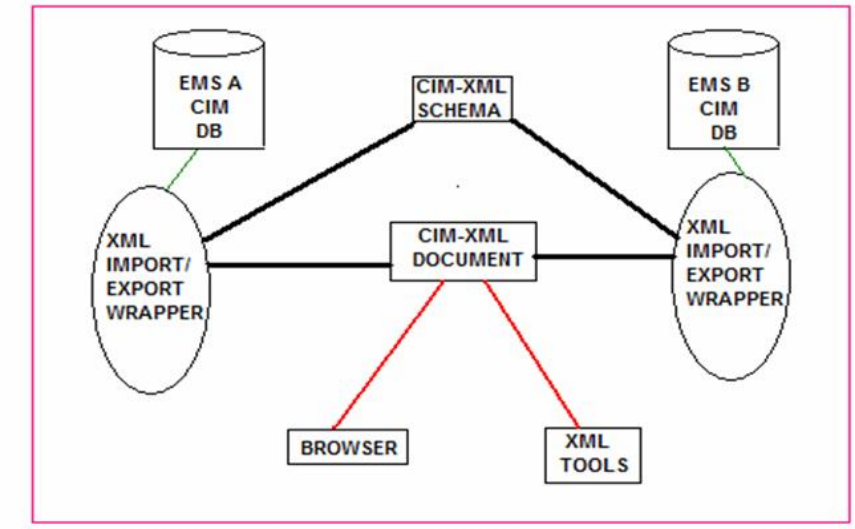

Fig.24. CIM-XML Data Exchange Model

In the future, other communication technologies like facsimile, wireless etc. that have its own XML standards can be adapted to handle CIM-XML documents in the electrical energy market. Thus, the XML based data exchange approach for CIM is scalable with the existing and newer communication technologies that are bound to be commonplace in the newer competitive electrical energy markets.

2. Proposed method to speedup exchange

In a realistic power system network handled by any EMS today, the amount of CIM data that would have to be exported/imported to transfer the complete network picture would be enormous. The overheads on communicating this document and conforming it to be a well-formed one on a smaller time frame would be very large because of the size of the CIM-XML document. Recently, a RDF difference model schema [72] has been suggested which would handle only the changes or the differences to be exchanged, thus making validation and communication within a reasonable time frame possible.

However, we propose the exchange in a slightly different manner based on the power system operation. One can broadly divide the entire system data into two broad categories, namely static and dynamic, based on the frequency of change in the value of the data. For the electrical system some of the dynamic data could be the load flow/state estimation data, the status of the switches, the transformer tap position etc. Within the framework of the CIM, these data describes the connectivity model represented in the Wires Package with the associated Measurement class from the SCADA package. The CIM-XML document corresponding to these objects can be then called as the Dynamic XML document. The rest of the information then could be aggregated into the Static XML document. The dynamic XML document would be much smaller in size compared with the whole picture and hence could be communicated and validated faster.

Based on the above approach, a data wrapper for generating a dynamic XML document containing the measurement values associated with the connectivity model, transformer and switch status could be developed in commercial EMS packages. The values associated with the objects could be populated from the Load Flow application or from the State Estimation application. To illustrate the procedure of dynamic data extraction, a 3-bus sample example is shown in Fig. 25. The CIM semantic entities based on the modeling standards, for the example, is shown in Fig. 26. The measurement values associated with the Topological Node object, the Transformer Tap Object, Breaker Switch Status represents the dynamic picture for this example.

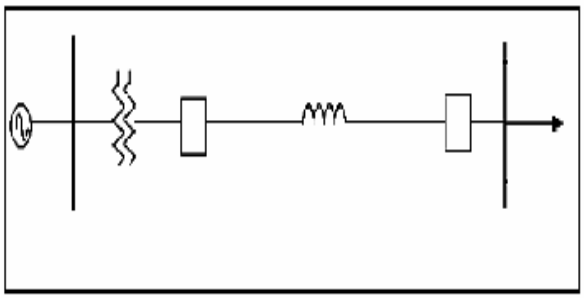

Fig.25. A Three Bus Sample System

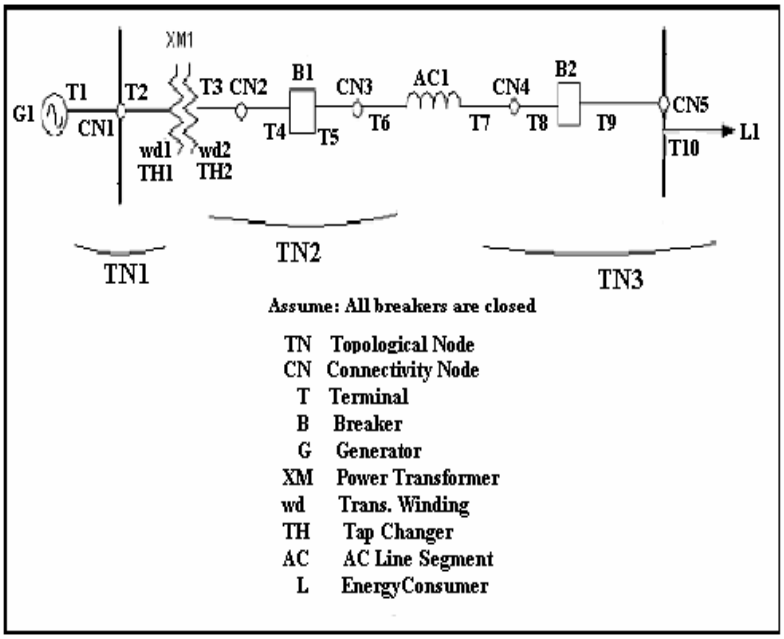

Fig.26. CIM Modeling of Three Bus Sample System

Conforming to the RDF schema the dynamic and the static CIM-XML document for this example would be as shown in Fig.27, Fig.28 and Fig.29. In these figures, objects of different types are expanded to show its child elements. However, to save space the recurring objects of the same kind are not expanded, in the figures. It can be seen from Fig.6 that the dynamic XML picture contains the information of the three Topological nodes, the two breakers and the tap changer objects. These objects could be updated by the load-flow or the state estimation application interfaces of the EMS. The static picture Fig. 28 and Fig. 29, however, shows the resources, properties and values of the system objects for this sample power system. The static picture has been represented in two figures since it is too big to be presented clearly in one figure.

```
rdf:RDF xmlns:rdf="http://w3.org/1999/02/22-rdf-syntax-ns#" xmlns:cim="http://epri.com/CCAPI/CIM-
schema-08b.xml">
!-- ThreeLoadFlowBusSystem: dynamic XML -->
cim:TopologicalNode rdf:ID="{TN1}">
cim:TopologicalNode.TopologicalNodeName>TN1X</cim:TopologicalNode.TopologicalNodeName>
cim:TopologicalNode.voltage>226.3</cim:TopologicalNode.voltage>
cim:TopologicalNode.phaseAngle>23.5</cim:TopologicalNode.phaseAngle>
cim:TopologicalNode.netInjectionMW>96</cim:TopologicalNode.netInjectionMW>
cim:TopologicalNode.netInjectionMVar>36.8</cim:TopologicalNode.netInjectionMVar>
cim:TopologicalNode.Contains rdf:resource="#{CN1}" />
/cim:TopologicalNode>
<cim:TopologicalNode rdf:ID="{TN2}">
<cim:TopologicalNode rdf:ID="{TN3}">
cim:Measurement rdf:ID="{MEAS1_BRK1}">
cim:Measurement.measurementName>Breaker1 status</cim:Measurement.measurementName>
cim:Measurement.Measures rdf:resource="#{B1}" />
cim:Measurement.Contains rdf:resource="#{MEAS1_VALUE}" />
cim:Measurement.HasUnit>open</cim:Measurement.HasUnit>
/cim:Measurement>
cim:MeasurementValue rdf:ID="{MEAS1_VALUE}">
cim:MeasurementValue.MeasurementValue>false</cim:MeasurementValue.MeasurementValue>
cim:MeasurementValue.Source>loadFlow</cim:MeasurementValue.Source>
/cim:MeasurementValue>
cim:Breaker rdf:ID="{B1}">
cim:PowerSystemResource.measurementBy rdf:resource="#{MEAS1_BRK1}" />
/cim:Breaker>
<cim:Measurement rdf:ID="{MEAS2_BRK2}">
<cim:MeasurementValue rdf:ID="{MEAS2_VALUE}">
<cim:Breaker rdf:ID="{B2}">
cim:Measurement rdf:ID="{MEAS3_TH1}">
cim:Measurement.measurementName>TapChanger1 tap
position</cim:Measurement.measurementName>
cim:Measurement.Measures rdf:resource="#{TH1}" />
cim:Measurement.Contains rdf:resource="#{MEAS3_VALUE}" />
cim:Measurement.HasUnit>TapPosition</cim:Measurement.HasUnit>
/cim:Measurement>
<cim:MeasurementValue rdf:ID="{MEAS3_VALUE}">
<cim:TapChanger rdf:ID="{TH1}">
cim:Measurement rdf:ID="{MEAS4_TH1}">
cim:Measurement.measurementName>TapChanger1 Regulation</cim:Measurement.measurementName>
cim:Measurement.Measures rdf:resource="#{TH1}" />
cim:Measurement.Contains rdf:resource="#{MEAS4_VALUE}" />
cim:Measurement.HasUnit>onLTC</cim:Measurement.HasUnit>
/cim:Measurement>
<cim:MeasurementValue rdf:ID="{MEAS4_VALUE}">
/rdf:RDF>
```

Fig.27. Dynamic CIM-XML Document for Three Bus Example

```
- <rdf:RDF xmlns:rdf="http://w3.org/1999/02/22-rdf-syntax-ns#"
          xmlns:cim="http://epri.com/CCAPI/CIM-schema-08b.xml">
  <!--  ThreeLoadFlowBusSystem: Static XML   -->
  <!--  Assumptions: To simplify the example: 1. The substation object is omitted.
                     2. RDFID does not follow the WSCC name convention.   -->
- <cim:Terminal rdf:ID="{T1}">
    <cim:Terminal.terminalName>T1X</cim:Terminal.terminalName>
    <cim:Terminal.RoleBConnectionFor rdf:resource="#{CN1}" />
    <cim:Terminal.ExternallyConnects rdf:resource="#{G1}" />
  </cim:Terminal>
+ <cim:Terminal rdf:ID="{T2}">
- <cim:ConnectivityNode rdf:ID="{CN1}">
    <cim:ConnectivityNode.connectivityNodeName>CN1X
    </cim:ConnectivityNode.connectivityNodeName>
    <cim:ConnectivityNode.RoleAConnectedTo rdf:resource="#{T1}" />
    <cim:ConnectivityNode.RoleAConnectedTo rdf:resource="#{T2}" />
  </cim:ConnectivityNode>
- <cim:SynchronousMachine rdf:ID="{G1}">
    <cim:PowerSystemResource.powerSystemResourceName>G1X·
    </cim:PowerSystemResource.powerSystemResourceName>
    <cim:PowerSystemResource.powerSystemResourceDescription>G1A
    </cim:PowerSystemResource.powerSystemResourceDescription>
    <cim:ConductingEquipment.phases>ABC</cim:ConductingEquipment.phases>
    <cim:SynchronousMachine.minimumKV>218.5</cim:SynchronousMachine.minimumKV>
    <cim:SynchronousMachine.inertia>6</cim:SynchronousMachine.inertia>
    <cim:SynchronousMachine.maximumKV>241.5</cim:SynchronousMachine.maximumKV>
    <cim:ConductingEquipment.ExternalConnectionFor rdf:resource="#{T1}" />
  </cim:SynchronousMachine>
- <cim:PowerTransformer rdf:ID="{XM1}">
    <cim:PowerSystemResource.powerSystemResourceName>XM1X
    </cim:PowerSystemResource.powerSystemResourceName>
    <cim:PowerSystemResource.powerSystemResourceDescription>X1
    </cim:PowerSystemResource.powerSystemResourceDescription>
    <cim:PowerTransformer.HasWinding rdf:resource="#{wd1}" />
    <cim:PowerTransformer.HasWinding rdf:resource="#{wd2}" />
  </cim:PowerTransformer>
+ <cim:TransformerWinding rdf:ID="{wd1}">
- <cim:TapChanger rdf:ID="{TH1}">
    <cim:PowerSystemResource.powerSystemResourceName>High Tap
    </cim:PowerSystemResource.powerSystemResourceName>
    <cim:TapChanger.stepVoltageIncrement>0.375</cim:TapChanger.stepVoltageIncrement>
    <cim:TapChanger.highStep>16</cim:TapChanger.highStep>
    <cim:TapChanger.normalStep>8</cim:TapChanger.normalStep>
    <cim:TapChanger.lowStep>0</cim:TapChanger.lowStep>
    <cim:TapChanger.neutralStep>8</cim:TapChanger.neutralStep>
    <cim:TapChanger.neutralKV>226.60001</cim:TapChanger.neutralKV>
    <cim:TapChanger.Contains rdf:resource="#{wd1}" />
  </cim:TapChanger>
+ <cim:TransformerWinding rdf:ID="{wd2}">
```

Fig.28. Static CIM-XML Document for Three Bus example

Fig.28. Continued

For a typical power system network, the size of the dynamic XML document generated is smaller in comparison with the static XML document that contains all the entities from the network's CIM database. Hence, for exchange of data with other EMS systems the dynamic XML document can be transferred and validated in shorter time intervals. The static picture, representing the whole power system network, could be transferred at longer intervals of time.

This dynamic CIM-XML data wrapper could be scheduled by the Energy Management Systems Application Program Interface (EMSAPI) to run along with the other network application modules. Some of these applications are Load-Flow, State-Estimation, Contingency Analysis etc.

D. New Proposed Scalable Information Architecture

1. Existing Communication Standards

Fig. 30 describes an example reference architecture, which identifies the relationship of Intelligent Electronic Devices (IEDs) to power system components, and the relationship of IEDs to communication networks (WAN, LAN, process bus, radio, microwave, and satellite). Communications between substations, between a substation and a control center, and between pole-top IEDs and a substation may use dedicated communication channels or the utility enterprise Wide Area Network (WAN). It can be seen that a variety of communication formats exist in substations and control centers.

A lot of standardization effort in the communication networks used in Fig. 29 has been going on, worldwide. Fig. 30 shows those standards that are applicable between a substation and IEDs external to the substation, again with different options on the standards that may be used.

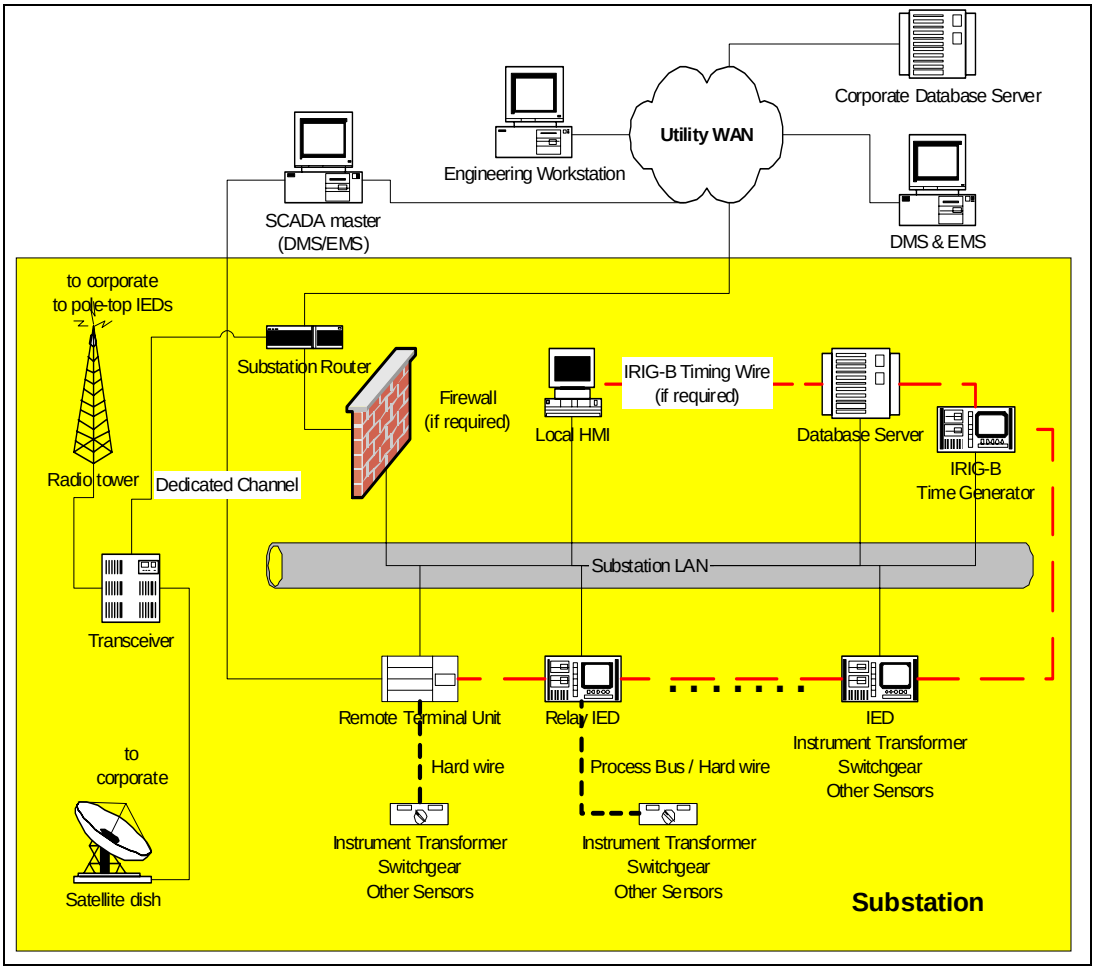

Fig.29. A Reference Communication Architecture

Both these models are referred to from IEEE/PES Substation Committee's tutorial on Automation Substation [73]. Interested readers may refer to the public-access tutorial to know more about the specific communication standards. The author's believe that as electrical market operations increases the need for compatibility amongst the various standards would increase.

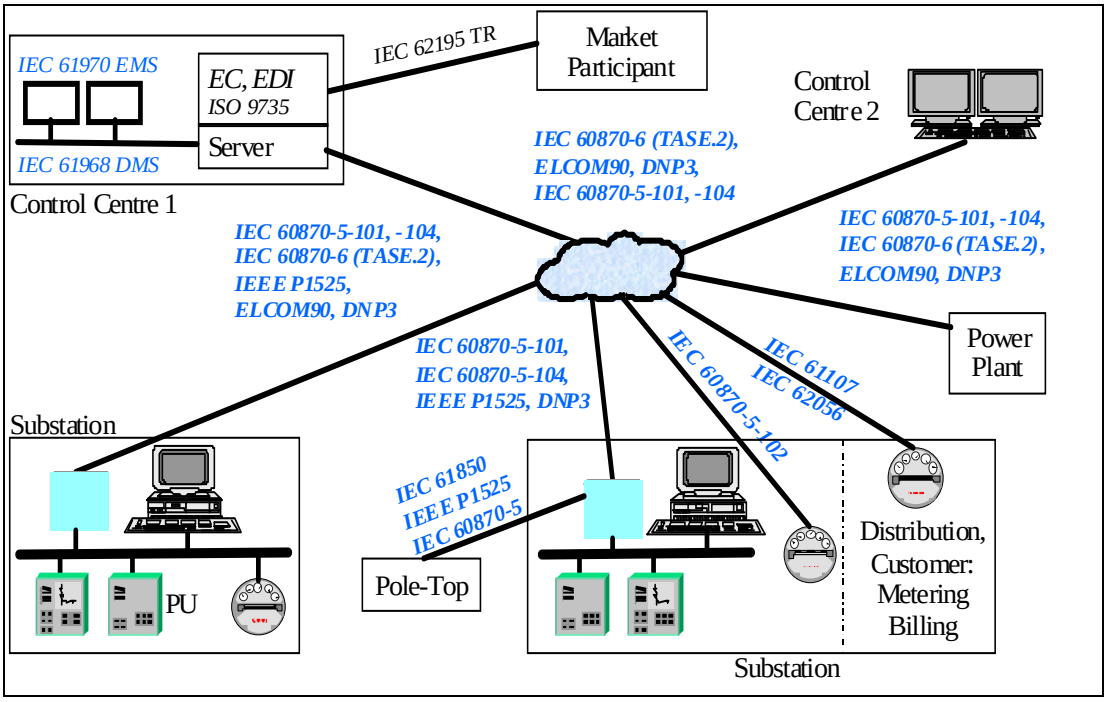

Fig.30. Communication Standards

2. Proposed Classification of Data

To address the dual objectives of operational reliability and market competitiveness, we can broadly classify the deregulated power system data into three groups.

- Raw Data: SCADA co-ordinates the collection of the power system information like power, voltage, line status information etc. collected from generating stations, substations and Remote Terminal Units (RTUs). SCADA information along with data from protective relays and other Intelligent Electronic Devices (IEDs) is classified in this group. Emerging technologies like Automatic Meter Reading (AMR) data from load, which aids in making load as a responsive and controllable resource, would also fall under this category.
- Processed Data: Energy Management Systems (EMS) and Distribution Management System (DMS) data follow under this category. These data

are used by network operators to manage system operation in real-time. Raw data from neighboring and far-off control areas are inputs to these management systems.

- Market Data: This type of data group came into existence because of the market operations in electrical energy. Any data that influences and supports market behavior falls under this category. Bidding data of generators, bilateral / long term transaction data, spot-price of electricity are some examples of this type. Processed data like Available Transmission Capacity (ATC), status information of flowgate lines, voltage security margins, load patterns could also qualify as market data. It is possible that some of the raw data from SCADA can directly find its use in the market. As market operation consolidates, this group is sure to include more data items.

The data items under the first two group influences the reliable and secure operation of the power system. While data items under the third group would qualify for impacting the transparency and competitiveness of the market operations

3. Information Architecture for Emerging Electric Markets

One of the primary goals of deregulation is to induce market competition and thereby efficiency in the electrical industry. The timely dissemination of market relevant data to all the market players is crucial in achieving this objective. Currently one such information namely the ATC is published in Open Access Same-Time Information System (OASIS) which is open to all transmission owners. The OASIS is used by electric system transmission grid operators to publish the availability of transmission line capacity for usage by power generators to deliver energy to consumers. The internet is used for dissemination of this data. In future, this basic functionality is envisaged to expand to include other sophisticated tools to establish a robust secondary market for transmission capacity, like an energy product bulletin board to facilitate energy

transaction and a mechanism to obtain multiple OASIS reservations simultaneously to provide efficiency to the reservation process.

As the market operations evolves more into deregulation the need for EMS/DMS processed data, raw data from SCADA and other economic data would find tremendous applications to market operators. Power system data would then be traded as a priced commodity. The communication infrastructure to transfer these data using different configurations exists today. This is because of the tremendous innovations occurring in the telecommunication industry. The need would then be to define architecture for deregulated electrical industry to integrate the various components as discussed in the earlier sections. One such scalable architecture proposed through our work, is shown in Fig. 31.

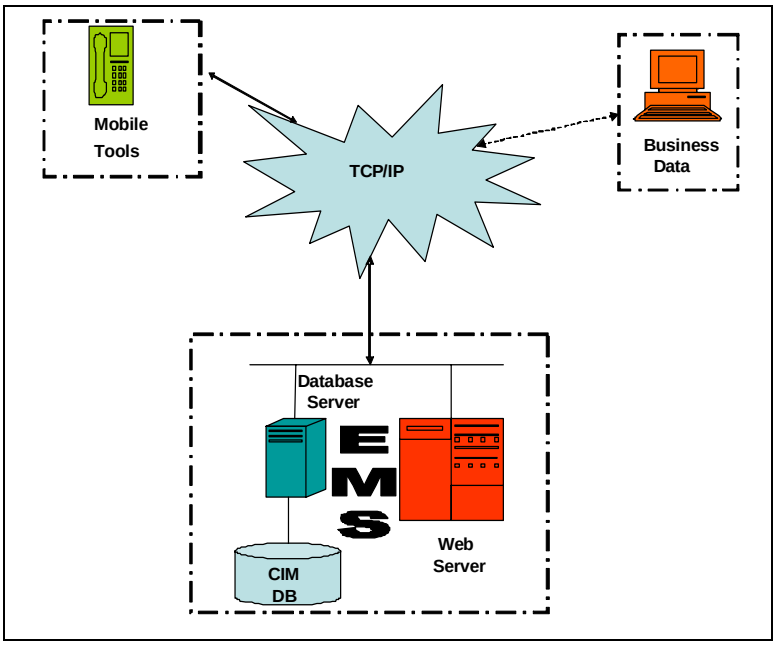

Fig.31. Information Architecture for Electric Market Data

The web server component interfaces with the request from other objects like user interface, a business data server or from mobile tools through the internet. Secure transactions can be then be made possible using the TCP/IP protocols, internet being one which uses this standard. The mobile hand-held tools shown in the figure could be

wireless or cellular based. Incidentally, newer communication technologies are also having their own XML definition standards. Wireless Markup Language (WML) is an XML-defined markup language for creating and serving up wireless-friendly information and applications for WAP (Wireless Application Protocol) enabled devices and browsers. In the future, these communication technologies that have its own XML standards can be adapted to handle CIM-XML documents in the electrical energy market. Thus, the CIM-XML based data transmission architecture is scalable with the existing and newer communication technologies that are bound to be commonplace in the newer competitive electrical energy markets.

E. Summary

In this chapter we focus on importance of power system data representation, their communication and information architecture in the context of deregulation. This is an important component in this thesis since voltage security evaluation tools proposed in this research, as well as existing computational engines, require power system data as inputs. The detail of the speed-up mechanism for exchanging CIM based data files amongst proprietary EMS databases was discussed. The concerns related to data exchange and dissemination, primarily aimed at maintaining operational security and transparency in electric markets, is addressed by classifying data into groups. Finally, the emerging scalable architecture for disseminating data items in the electric market is proposed.

CHAPTER VII

CONCLUSION

A. Summary of the Research Contributions

This dissertation addresses several important technical objectives associated with incorporating voltage security in the monitoring, operation, control and planning horizons of emerging electricity markets.

First of all, this dissertation has presented a new procedure that can estimate the transaction usages of steady state voltage stability margin in the deregulated electric markets. This falls under the monitoring and operational horizon of deregulated markets. The procedure is developed on the basis of physical laws and the economic contexts associated with market transactions. For actual system this tool, if developed, would aid in giving an overall picture of voltage security to operators. Other existing tools, that are computation intensive and time intensive, can be used for detailed investigation. To summarize, main features of this decomposition method are:

- Using current state of the system, topology and market transaction information voltage security indices can be quickly estimated to visualize the impacts of transactions throughout the system.
- The index variations is seen to concur with the singularity of power flow jacobian associated with voltage collapse which happens to be the general basis for all steady state voltage stability tools.
- The estimation correctly gives indication to the voltage insecure load bus. Further, since all values are normalized to a maximum of unity the results can be easily visualized by security operators, who typically have to deal with a large amount of processed data.

- The decomposition resulting from the procedure is voltage security utilization-reflective, i.e., it accounts for impacts of load bus voltage insecurities to power exchange amounts and locations of the traders. Thus, these estimates can be used to equitably assign curtailment amounts amongst participating transaction if load curtailment is used as a corrective strategy during voltage insecurity.
- However, it is to be noted that correct state and topology information is needed by the procedure to give a robust estimate. Errors in these quantities can potentially give false and misleading estimates.
- It can be easily incorporated along with analytical engines of modern EMS like State Estimators, Dispatcher Load Flow, Contingency Analysis .

Second, this dissertation formulated a VSCOPF procedure by including voltage stability constraints to an OPF problem. Its application has been demonstrated on a sample system. This procedure has also been used in addressing third and fourth objective of our work.

Third, this dissertation discussed the different application of voltage security index. FACT devices are being increasingly used in restructured markets to mitigate a variety of operational problems. We have illustrated the methodology to decompose loop flow impacts of TCSC on a transaction basis. We have incorporated its steady state characteristic to our VSCOPF procedure and demonstrated the impacts. Thus, this discussion addresses our objective of incorporating voltage security into control horizons emerging in deregulated markets. Additionally, it investigates application of steady state voltage stability index to detect dynamic voltage stability. The time-domain simulations, of certain dynamic events, and evaluation of indices suggest that some level of potential instability information can be obtained. The simplicity of the indicator is its advantage but it definitely cannot detect all types of dynamic instability. Our experiences suggest that more work needs to be done to come up with indicators that can spot all potentially voltage insecure dynamic events.

Fourth, this dissertation proposed the use of our VSCOPF formulation to incorporate voltage security into composite reliability analysis. The impact of using VSCOPF on

composite reliability measures has been demonstrated on an illustrative system. Incorporating this technique in simulation methods for larger systems has also been discussed. Thus, this part addresses the issue of incorporating voltage security to the planning horizon of electricity markets.

Finally, this dissertation reviewed the emerging power system data communication issues that would impact voltage security evaluation. It proposes a new EMS data exchange method and also discusses the issues concerning disseminating of data in electric market. Importance of information security, which would impact all operational security evaluations including voltage security, is the thrust of this part of our research.

B. Suggestions for Future Research

We feel that the work reported in this dissertation can be an important basis for future research activities related to voltage security in electric markets. In general, future research directions that emerge from this dissertation are summarized below.

1. Incorporating Reactive Power to Voltage Security Assessment

The voltage security estimation procedure, outline in Chapter II, would be further enhanced if some of these additional insights are researched.

- The indices currently give only numerical values corresponding to the voltage security. If we can map this index to a MW value, like in CPF analysis, it would be an useful addition.
- Voltage security is usually linked with reactive power. In fact, reactive power injections give a better picture of reactive adequacy requirements and their placement for various components like generators, lines and loads. However, in this dissertation our objective was to quickly estimate the security situation considering all components acting together. Hence, choosing an indicator based on state value and topology information was justifiable. But in the context of

electricity markets there is a need to decompose the reactive injection, flow and contribution impacts of all physical components on a real-time basis. This would help in equitable responsibility evaluation during security threats and also for applying pricing rules to reactive power and voltage security. Our general discussion on AC flow based decomposition, discussed in Chapter II, has the potential to address this requirement.

And so on.

2. Quantifying Impacts of Devices on Voltage Security

In this dissertation we have attempted to address steady state voltage security on all analysis horizons of electricity market operation i.e., monitoring & operation, control and planning. The methods and procedures proposed in this dissertation could be qualitatively enhanced by further research. Such as

- Quantifying control impacts of AVR, Exciters, FACT devices, Transformer-taps, Reactive compensation devices, Responsive Load Dynamics etc.
- Quick algorithms to coordinate the various reactive control devices, especially during potential security threats.
- Procedures to estimate the lost MW opportunity costs that are usually associated during voltage insecurity preventive and corrective controls.

3. Information Exchange and Dissemination

In this dissertation we addressed the importance of exchange and dissemination of power system data. Since all adequacy and security based power system analysis require data, issues related with information security would emerge as an important issue in electricity markets. Such as

- Completing CIM standardization for all distribution components avoiding seams issues with existing data standards for EMS.

- Once power system data becomes transparent to all entities of electric market then security impacts, especially on SCADA, would rise. Research would be needed to identify the harmful effects of false data and ways to prevent them.

4. Monitoring/Controlling Dynamic and Transient Voltage Stability

An attempt was made to map an index to some dynamic voltage insecurity situations for a small system in this dissertation. However, further work needs to be carried out to come up with indices, maybe approximate, to quickly addresses the voltage security impacts of dynamic disturbances like fault, surges, line loss etc. This would involve realistic modeling of practically all devices in power systems.

REFERENCES

[1] W. W. Hogan, “Electricity Transmission and Emerging Competition”, *PURC Annual Conference, Market and Technological Convergence: Implications for Regulation*, Gainesville, Florida, pp. 70-80, Apr. 1995.

[2] H. Rudnick, R. Varela and W.W. Hogan, "Evaluation of Alternatives for Power System Coordination and Pooling in a Competitive Environment," *IEEE Trans. on Power Systems*, vol. 12, no. 2, pp. 605-613, May 1997.

[3] H. Rudnick, R. Palmar and J. E. Fernandez, “Marginal Pricing and Supplement Cost in Transmission Open Access,” *IEEE Trans. on Power Systems*, vol. 10, no. 2, pp. 1125-1142, May 1995.

[4] F. Albuyeh and Z. Alaywan, "California ISO Formation and Implementation," *IEEE Computation Application in Power*, vol. 12, no. 4, pp. 30-34, Oct. 1999.

[5] F. A. Rahimi and A. Vojdani, "Meet the Emerging Transmission Market Segments," *IEEE Computer Application in Power*, vol. 12, no. 1, pp. 26-32, Jan. 1999.

[6] F. F. Wu and P. Varaiya, “Coordinated Multilateral Trade for Electric Power Networks: Theory and Implementation,” University of California Energy Inst., Power Rep. PWP-031, Dept. of ECE, Berkeley, Jun. 1995.

[7] H. M. Merrill, “Regional Transmission Organizations: FERC Order 2000,” *IEEE Power Engineering Review*, vol. 20, no.7, pp. 3-5, Jul. 2000.

[8] S. S. Oren, P. T. Spiller, P. Varaiya and F. F. Wu, “Nodal Prices and Transmission Rights: a Critical Appraisal,” University of California Energy Inst., Power Rep. PWP-025, Berkeley, Dec. 1994.

[9] D. Kirschen, R. Allan and G. Strbac, "Contributions of Individual Generators to Loads and Flows," *IEEE Trans. on Power Systems*, vol. 12, no.1, pp. 52-60, Feb. 1997.

[10] A. Zobian and M. D. Ilic, “Unbundling of Transmission and Ancillary Services: Part I: Technical Issues,” *IEEE Trans. on Power Systems*, vol.12, no.2, pp. 539-

548, May 1997.

[11] G. Huang and H. Zhang, “Transmission Loss Allocations and Pricing Via Bilateral Energy Transactions,” in *Proc. IEEE/PES Summer Meeting*, Edmonton, Alberta, Canada, Jul. 1999, pp. 720-725.

[12] G. Huang and H. Zhang, “Dynamic Voltage Stability Reserve Studies For Deregulated Environment,” *Proc. IEEE/PES Summer Meeting*, Vancouver, Canada, Jul. 2001, pp. 301-306.

[13] G. Huang and A. Abur, “Voltage Security Margin Assessment”, [online] Available: *PSERC Publication 02-49*, http://www.pserc.wisc.edu, April 2003.

[14] C. W. Taylor, *Power System Voltage Stability*, Singapore: McGraw-Hill, Inc., 1994.

[15] V. Ajjarapu and C. Christy, “The Continuation Power Flow: A Tool for Steady State Voltage Stability Analysis,” *IEEE Trans. on Power Systems*, vol. 7, no. 1, pp. 416-423, Feb. 1992.

[16] C. A. Canizares and F. L. Alvarado, “Point of Collapse and Continuation Method for Large AC/DC Systems,” *IEEE Trans. on Power Systems*, vol. 8, no.1, pp. 1-8, Feb. 1993.

[17] M. K. Pai, “Voltage Stability Conditions Considering Load Characteristics,” *IEEE Trans. on Power Systems*, vol. 7, no.1, pp. 243-249, Feb. 1992.

[18] G.K. Morison, B. Gao and P. Kundar, “Voltage Stability Analysis Using Static and Dynamic Approaches,” *IEEE Trans. on Power Systems*, vol. 8, no.3, pp. 1159-1171, Aug. 1993.

[19] G. Huang and N. C. Nair, “Allocating Usages of Voltage Security Margin in Deregulated Electric Markets,” in *Proc. IEEE ISCAS Conference*, Bangkok, Thailand, vol. 3, pp. 363-366, May 2003.

[20] R. Billinton and S. Aboreshaid, "Voltage Stability Considerations in Composite Power System Reliability Evaluation,” *IEEE Trans. on Power Systems*, vol. 13, No.2, pp.665-660, May 1998.

[21] S. Aboreshaid and R. Billinton, "Probabilistic Evaluation of Voltage Stability," *IEEE Trans. on Power Systems*, vol. 14, No. 1, pp. 342-348, Feb 1999.

[22] G. Huang and N. C. Nair, "Voltage Stability Constrained Load Curtailment Procedure to Evaluate Power System Reliability Measures," in *Proc. IEEE/PES Winter Meeting*, New York, Jan 2002, pp. 761-765.

[23] L. A. S. Pilotto, W. W. Ping, A. R. Carvalho, A. Wey, W. F. Long, F. L. Alvarado and A. L. Edris, "Determination of needed FACTS Controllers that Increase Asset Utilization of Power Systems," *IEEE Trans. Power Delivery*, vol. 12, no. 1, pp.364-371, Jan. 1997.

[24] E. V. Larsen, J. J. Sanchez-Gasca and J. H. Chow, "Concepts for Design of FACTS Controllers to Damp Power Swings," *IEEE Trans. Power System*, vol. 10, no. 2, pp.948-956, May 1995.

[25] G. Huang and P. Yan "The Impacts of TCSC and SVC on Power System Load Curtailments," in *Proc. IEEE/PES Summer Meeting*, Toronto, July 2001, pp. 33-37.

[26] N. C. Nair and G. Huang, "Impacts of TCSC Control on Parallel Flow in Deregulated Electrical Markets," in *Proc. of NAPS 2003*, Rolla, Missouri, Oct. 2003, pp. 383-389.

[27] G. Huang and N. C. Nair, "Incorporating TCSC into the Voltage Stability Constrained OPF Formulation," in *Proc. IEEE/PES Summer Meeting*, Chicago, Jul. 2002, pp. 1547-1552.

[28] P. Hirsch and S. Lee, "Security Applications and Architecture for an Open Market," *IEEE Computer Applications in Power*, vol. 12, no. 3, pp.26–31, Jul. 1999.

[29] Q. Zhao, G. Huang, X. Luo and X. Wu,"A Software Architectural Style for Deregulated Power Markets," in *IEEE/PES Winter Meeting*, New York, Jan. 2001, pp. 1497 –1502.

[30] A. deVos, S. E. Wildergren and J. Zhu, "XML for CIM Model Exchange," *PICA-2001 Conference*, Sydney, Australia, May 2001, pp. 31-37.

[31] Report on "Common Information Model (CIM) for the Control Center Application Program Interface," Electrical Power Research Institute, EPRI Rep. TR-106324, Palo Alto, California, Sept 1998.

[32] N. C. Nair and G. Huang, "Static and Dynamic CIM-XML Documents for Proprietary EMS," in *Proc. IEEE/PES General Meeting*, Toronto, July 2003, pp. 1081-1086.

[33] N. C. Nair and G. Huang, "Exchange and Dissemination of CIM Compliant Data in Restructured Power Markets," in *Proc. IEEE/PES General Meeting*, Denver, Colorado, Jun 2004, PESGM2004-0083 [on CD].

[34] G. Huang and S. C. Hsieh, "Fast Textured Algorithms for Optimal Power Delivery Problems in Deregulated Environments," *IEEE Trans. on Power Systems*, vol. 13, No. 2, pp. 493-500, May 1998.

[35] A. K. David and X. Lin, "Dynamic Security Enhancement in Power Market Systems," *IEEE Trans. on Power Systems*, vol. 17, No. 2, pp. 431-438, May 2002.

[36] I. Kockar and F. D. Galiana, "Combined Pool/bilateral Dispatch: Part II – Curtailment of Firm and Nonfirm Contracts," *IEEE Trans. on Power Systems*, vol. 17, No. 4, pp. 1184-1190, Nov 2002.

[37] D. Chattopadhyay, B. B. Chakrabarti and E. G. Read, "Pricing for Voltage Stability," in *Proc. IEEE /PICA Conference*, Sydney, May 2001, pp. 235-240.

[38] K. Bhattacharya and J. Zhong, "Reactive Power as an Ancillary Service,", *IEEE Trans. on Power Systems*, vol. 16, No. 2, pp. 294-300, May 2001.

[39] P. Kessel and H. Glavitsch, "Estimating the Voltage Stability of a Power System," *IEEE Trans on Power Delivery*, vol. PWRD-1, No.3, pp. 346-354, July 1986.

[40] G. Huang and N. C. Nair, "An OPF Based Algorithm to Evaluate Load Curtailment Incorporating Voltage Stability Margin Criterion," in Proc. of NAPS 2001, College Station, Texas, Oct. 2001, pp. 164-167.

[41] F. D. Galinana and M. Phelan, "Allocation of Transmission Losses to Bilateral Contracts in a Competitive Environment," *IEEE Trans. on Power Systems*, vol. 15, no. 1, pp. 143-150, Feb. 2000.

[42] H. Chao, S. Peck, S. Oren and R. Wilson, "Flow-Based Transmission Rights and Congestion Management," in *The Electricity Journal*, vol. 13, no. 8, pp. 38-58, October 2000.

[43] C. W. Taylor, "Concepts of Undervoltage Load Shedding for Voltage Stability,", *IEEE Trans. On Power Systems*, vol. 7, No. 2, pp 480-488, April 1992.

[44] T. Q. Tuan, J. Fandino, N. Hadjsaid, J. C. Sabonnadiere and H. Vu, "Emergency Load Shedding to Avoid Risks of Voltage Instability Using Indicators,", *IEEE Trans. On Power Systems*, vol. 9, No. 1, pp. 341-351, Feb. 1994.

[45] H. W. Dommel and W. F. Tinney, "Optimal Power Flow Solutions,", *IEEE PAS*, vol. 87, pp. 1866-1876, Oct 1968.

[46] D. I. Sun, B. Ashley, A. Hughes and W. F. Tinney, "Optimal Power Flow by Newton Approach," *IEEE Trans. Power System*, vol. 103, pp. 2684-2880, 1984.

[47] O. Alsac and B. Stott, "Optimal Power Flow with Steady State Security," *IEEE PAS*, vol. 93, pp. 745-751, May 1974.

[48] O. Alsac, J. Bright, M. Prais and B. Stott, "Further Developments in LP-based OPF," *IEEE Trans. on Power Systems*, vol. 5, no. 3, pp. 697-711, Aug 1990.

[49] A. J. Wood and B. F. Wollenberg, *Power Generation, Operation, and Control*, New York: Wiley, 1984.

[50] Q. Zhao, "Development of Multi-Objective Solutions and an Electronic Commerce Software Architecture for Commodity Trading in Deregulated Power Markets," Ph.D. Dissertation, Texas A&M University, College Station, Dec. 2000.

[51] D. Gan, R. J Thomas and R. D. Zimmerman, "Stability constrained OPF," *IEEE Trans. on Power Systems*, vol. 15, no.2, pp. 535-540, May 2000.

[52] MATLAB, "FAQ on Optimization Tool box," [online]. Available: http://www. mathworks.com/ access/ helpdesk/help/toolbox/optim/, accessed on Aug. 2004.

[53] S. G. Jalali, R. A. Hedin, M. Pereira and K. Sadek, "A Stability Model for the Advanced Series Compensator," *IEEE Trans. Power Delivery*, vol. 11, no. 2, pp.1128-1137, Apr. 1996.

[54] C. R. Fuerte-Esquivel, E. Acha and H. Ambriz-Perez, “A Thyristor Controller Series Compensator Model for the Power Flow Solution of Practical Power Networks,” *IEEE Trans. Power Systems*, vol. 15, no. 1, pp.58-64, Feb. 2000.

[55] B. K. Perkins and M. R. Iravani, “Dynamic Modeling of a TCSC with Application to SSR Analysis,” *IEEE Trans. Power System*, vol. 12, no. 4, pp.1619-1625, Nov. 1997.

[56] J. J. Paserba, N. W. Miller, E. V. Larsen and R J. Piwko, “A Thyristor Controlled Series Compensation Model for Power System Stability Analysis,” *IEEE Tran. Power Delivery*, vol. 10, no. 3, pp.1471-1478, July 1995.

[57] P. Preedavichit and S. C. Srivastava, “Optimal Reactive Power Dispatch Considering FACTS Devices,” in *APSCOM-97, Fourth International Conference*, Hong Kong, Nov. 1997, pp. 620 –625.

[58] Y. Tamura, H. Mori and S. Iwamoto, “ Relationship Between Voltage Instability and Multiple Load Flow Solutions in Electric Power Systems,” *IEEE Trans. on Power Apparatus and Systems*, vol. PAS-102, no. 5, pp. 1115-1125, May 1983.

[59] B. Gao, G. K. Morison and P. Kundur, “Voltage Stability Evaluation Using Modal Analysis,” *IEEE Trans. on Power Systems*, vol. 7, no. 4, pp. 1529-1542, Nov. 1992.

[60] G. Huang and N. C. Nair, “Detection of Dynamic Voltage Collapse,” in *Proc. IEEE/PES Summer Meeting*, Chicago, Jun. 2002, pp. 1284-1289.

[61] G. Huang and K. Men, “Contribution Allocation for Voltage Stability In Deregulated Power Systems,” in *Proc. IEEE/PES Summer Meeting*, Chicago, Jun. 2002, pp. 1290-1295.

[62] R. Allan and R. Billinton, "Probabilistic Assessment of Power Systems," *Proceedings of IEEE*, vol. 88, No.2, Feb. 2000

[63] S. Aboreshaid and R. Billinton, "A Framework for Incorporating Voltage and Transient Stability Considerations in Well-being Evaluation of Composite Power Systems," in *Proc. IEEE/PES Summer Meeting*, Edmonton, Canada, Jul. 1999, pp. 219-224.

[64] N. Amjady, "A Framework of Reliability Assessment with Consideration Effect of Transient and Voltage Stabilities," *IEEE Trans. on Power Systems*, vol. 19, No. 2, pp. 1005-1014, May 2004.

[65] D. Becker, H. Falk, J. Gillerman, S. Mauser, R. Podmore and L. Schneberger, "Standards-Based Approach Integrates Utility Applications," *IEEE Computer Applications in Power*, vol. 13, no. 4, pp.14–20, Oct. 2000.

[66] Z. Xie, G. Manimaran, V. Vittal, A. G. Phadke and V. Centeno, "An Information Architecture for Future Power Systems and Its Reliability Analysis," *IEEE Trans. Power Systems*, vol. 17, no.3, pp. 857–863. Aug. 2002.

[67] D. Marihart, "Communications Technology Guidelines for EMS/SCADA Systems," *IEEE Trans. on Power Delivery*, vol. 16, no. 2, pp.181–188, Apr. 2001.

[68] K. Mak and B. Holland, "Migrating Electrical Power Network SCADA Systems to TCP/IP and Ethernet Networking," *IEE Power Engineering Journal*, vol. 16, no. 6, pp.305–311, Dec. 2002 .

[69] C. Su, C. Lu and T. Hsiao, "Simulation Study of Internet Based Inter Control Center Data Exchange for Complete Network Modeling," *IEEE Trans. Power Systems*, vol. 17, no. 4, pp.1177–1183, Nov. 2002.

[70] W. Dieterle, H. Kochs and E. Dittmar, "LAN Based Data Communication in Modern EMS," *IEEE Trans. Power Systems*, vol. 11, no. 1, pp.469–474, Feb. 1996.

[71] X. Wang, N. Shulz and S. Neumann, "CIM Extension to Electrical Distribution and CIM XML for the IEEE Radial Test Feeders," *IEEE Tran. Power Systems*, vol. 18, no. 3, pp.1021–1027, Aug. 2003.

[72] A. Voss, "RDF Difference Models," [online]. Available: http://www. langdale.com.au/CIMXML/DifferenceModelsR05.pdf, accessed on Aug. 2004.

[73] IEEE/PES Substation Committee "Tutorial on Automation Substation," [online]. Available: http://www.ewh.ieee.org/cmte/pes-sub/tutorial.html, accessed on Aug. 2004

APPENDIX A

ELECTRICAL PARAMETERS OF THE WSCC9-BUSES SYSTEM

Table 23. Branch Electrical Parameters of WSCC9-Buses System

Branch#	*From*	*To*	*R (P.U.)*	*X (P.U.)*	*B (P.U.)*	*Ratio* T_{ij}
1	1	4	0	0.0576	0	1.00
2	4	5	0.0170	0.0920	0.1580	1.00
3	6	5	0.0390	0.1700	0.3580	1.00
4	3	6	0	0.0586	0	1.00
5	6	7	0.0119	0.1008	0.2090	1.00
6	8	7	0.0085	0.0720	0.1490	1.00
7	2	8	0	0.0625	0	1.00
8	8	9	0.032	0.1610	0.3060	1.00
9	4	9	0.0100	0.0850	0.1760	1.00

APPENDIX B

TRANSACTION BASED POWER FLOW ANALYSIS

We shall formulate the decomposition formulae on a general power system with N-buses and L-branches. To simplify the representation, we assume only two market players in the system: PX being a central power exchange market; TX is a bilateral transaction. A system-wide reactive power market Q conducted by ISO is responsible for overall reactive support services.

Step1: Select an appropriate angle for the slack bus from the given power flow solution,

Step 2: Decompose the nodal current vector based on TXs.

From a known operating point (V,θ), the (n×1) nodal current vector I_{bus} is determined by

$$I_{bus} = [Y_{bus}] \times E_{bus} \text{ , where } \quad E_{bus} = \begin{bmatrix} V_1 e^{j\theta_i} \\ . \\ V_n e^{j\theta_i} \end{bmatrix} \tag{A1}$$

$$I_{PX} = \begin{bmatrix} . \\ \dfrac{P_{G,i}^{PX} - P_{D,i}^{PX}}{V_i \cos\theta_i} \\ . \\ . \\ \dfrac{P_{G,n}^{PX} - P_{D,n}^{PX}}{V_n \cos\theta_n} \end{bmatrix} \qquad I_{TX} = \begin{bmatrix} 0 \\ \dfrac{P_{G,k}^{TX}}{V_k \cos\theta_k} \\ 0 \\ \dfrac{-P_{D,m}^{TX}}{V_m \cos\theta_m} \\ 0 \end{bmatrix} \quad I_Q = I_{bus} - I_{PX} - I_{TX} \tag{A2}$$

where

$P_{G,*}^{SC_k}, P_{D,*}^{SC_k}$ are the active power generation and load at bus i, in association with PX or TX. TX is with the source and sink buses at k and m respectively.

Step 3: Decomposed nodal voltage components

$$E_* = [Y_{bus}]^{-1} \times (I_*)^* \tag{A3}$$

where the subscript symbol $*$ means PX, TX or Q individually.

Normally it is satisfied that

$$|E_Q| \approx |E_{bus}| \approx 1 \qquad |E_{PX}| \approx 0 \quad |E_{TX}| \approx 0 \tag{A4}$$

Step 4: Compute branch current components between buses i and j

$$I_{*,i-j} = E_{*,i} b_{0,l} + (E_{*,i} - E_{*,j}) \times (g_{ij} + jb_{ij}) \tag{A5}$$

$$I_{*,j-i} = E_{*,j} b_{0,l} + (E_{*,j} - E_{*,i}) \times (g_{ij} + jb_{ij}) \tag{A6}$$

where

b_l is the half line shunt susceptance, the symbol $*$ means PX, TX or Q individually.

Step 5: Decompose complex power flows over each branch.

$$S_{i-j} = E_{bus,i} \times I_{i-j}^* \tag{A7}$$

Further, it can be rewritten as

$$\begin{aligned} S_{i-j} &= (E_{Q,i} + E_{PX,i} + E_{TX,i}) \times (I_{Q,i-j} + I_{PX,i-j} + I_{TX,i-j})^* \\ &= \underbrace{(E_{Q,i} + E_{PX,i}) I_{PX,i-j}^*}_{1st\ \text{term}} + \underbrace{(E_{Q,i} + E_{TX,i}) I_{TX,i-j}^*}_{2nd\ \text{term}} \\ &+ \underbrace{E_{Q,i} I_{Q,i-j}^*}_{3rd\ \text{term}} + \underbrace{(E_{PX,i-j} I_{TX,i-j}^* + E_{TX,i} I_{PX,i-j}^*)}_{4th\ \text{term}} \\ &+ \underbrace{E_{PX,i} I_{Q,i-j}^*}_{5th\ \text{term}} + \underbrace{E_{TX,i} I_{Q,i-j}^*}_{6th\ \text{term}} \end{aligned} \tag{A8}$$

where $E_{bus,i}, E_{PX,i}, E_{TX,i}, E_{Q,i}$ is the ith element of the voltage vectors $E_{bus}, E_{PX}, E_{TX}, E_Q$ individually.

We categorize terms of (A8) as follows:

$$S_{i-j} = S_{PX,i-j} + S_{TX,i-j} + S_{Q,i-j} \tag{A9}$$

where

$$S_{PX,i-j} = (E_{Q,i} + E_{PX,i}) \times I_{PX,i-j}^* + E_{PX,i} I_{Q,i-j}^* + f_{PX\omega TX} \times (E_{PX,i} I_{TX,i-j}^* + E_{TX,i} I_{PX,i-j}^*)$$

$$S_{TX,i-j} = (E_{Q,i} + E_{TX,i}) \times I_{TX,i-j}^* + E_{TX,i} I_{Q,i-j}^* + f_{TX\omega TX} \times (E_{TX,i} I_{PX,i-j}^* + E_{TX,i} I_{PX,i-j}^*)$$

$$S_{Q,i-j} = E_{Q,i} I_{Q,i-j}^*$$

$f_{PX\omega TX}, f_{TX\omega PX}$ are sharing factors imposed upon PX and TX for their interactive component. $f_{PX\omega TX} + f_{TX\omega PX} \equiv 1$.

Similarly,

$$S_{j-i} = S_{PX,j-i} + S_{TX,j-i} + S_{Q,j-i} \tag{A10}$$

where

$$S_{PX,i-j} = (E_{Q,i} + E_{PX,i}) \times I^*_{PX,i-j} + E_{PX,i} I^*_{Q,i-j} + f_{PX \varpi TX} \times (E_{PX,i} I^*_{TX,i-j} + E_{TX,i} I^*_{PX,i-j})$$
$$S_{TX,i-j} = (E_{Q,i} + E_{TX,i}) \times I^*_{TX,i-j} + E_{TX,i} I^*_{Q,i-j} + f_{TX \varpi PX} \times (E_{PX,i} I^*_{TX,i-j} + E_{TX,i} I^*_{PX,i-j})$$

$$S_{Q,j-i} = E_{Q,j} I^*_{Q,i-j}$$

Further, the decomposed real flow, real loss, reactive flow and reactive loss components on the branch

$$P_{flow(*),i-j} = \frac{1}{2} \mathrm{Re}(S_{*,i-j} - S_{*,j-i}) \tag{A11}$$

$$P_{loss(*),i-j} = \mathrm{Re}(S_{*,i-j} + S_{*,j-i}) \tag{A12}$$

$$Q_{flow_{(*),i-j}} = \frac{1}{2} \mathrm{Im}(S_{*,i-j} - S_{*,j-i}) \tag{A13}$$

$$Q_{loss(*),i-j} = \mathrm{Im}(S_{*,i-j} - S_{*,j-i}) \tag{A14}$$

where * means PX, TX or Q individually.

Step 6: Distribute the portion of transmission loss arising from reactive power delivery to the energy customers, in proportion to their reactive power usage.

$$\Delta P_{L(*,Q)} = \frac{\sum_{i \in N} Q_{D*,i} + \sum_{L} Q_{loss\,(*),i-j}}{\sum_{k=PX,TX} \left(\sum_{i \in N} Q_{Dk,i} + \sum_{L} Q_{loss\,(k),i-j} \right)} \times \sum_{L} P_{loss\,(Q),i-j} \tag{A15}$$

where * denotes energy interchange schedules PX or TX.

Eventually, the transmission loss charges to PX and TX are

$$P_{L(PX)} = \sum_{L} P_{loss(PX),i-j} + \Delta P_{L(PX,Q)} \tag{A16}$$

$$P_{L(TX)} = \sum_{L} P_{loss(TX),i-j} + \Delta P_{L(TX,Q)} \tag{A17}$$

Step 7: Adjust loss shares among the market players by an iteration scheme.

It is straightforward to generalize to cases with a large number of the TXs. For any SC_k, the complex power flow contributions to one branch between the buses i and j are

$$S_{SC_k,i-j} = (E_{Q,i} + E_{SC_k,i}) \times I_{SC_k,i-j} + E_{SC_k,i} I_{Q,i-j} + \sum_{h \in T-k} f_{SC_k \varpi SC_h} \times (E_{SC_k,i} I_{SC_h,i-j} + E_{SC_h,i} I_{SC_k,i-j}) \tag{A18}$$

and

$$S_{SC_k,j-i} = (E_{Q,j} + E_{SC_k,j}) \times I_{SC_k,j-i} + E_{SC_k,j} I_{Q,j-i} + \sum_{h \in T-k} f_{SC_k \omega SC_h} \times (E_{SC_k,j} I_{SC_h,j-i} + E_{SC_h,j} I_{SC_k,j-i}) \quad \text{(A19)}$$

where

T is the number of all energy scheduling coordinators including all the TXs and PXs.

VITA

Nirmal-Kumar Nair was born in Palghat, India. He received his B.E. in electrical engineering from Maharaja Sayajirao University, Baroda, India, in January 1990 and M.E. in electrical engineering from the Indian Institute of Science (IISc.), Bangalore, India in January 1998. From January 1990 to July 1990, he worked as an R&D Electrical Engineer at Jyoti Electricals, Baroda. From August 1990 to July 1991 he was with the L.E Engineering College, Morbi as a Lecturer in Electrical Engineering. From August 1991 through June 2000 he served as a Lecturer in Electrical Engineering with the BVM Engineering College, Gujarat, India.

He started his Ph.D. program in Summer 2000 at Texas A&M University, and began working as Graduate Research Assistant with Dr. Garng Huang. During the summers of 2001 and 2002, he interned with M/s ABB Network Management, Houston. During Fall 2002 to Summer 2004, he worked part-time initially as a Graduate Teaching Assistant and later as Graduate Assistant Lecturer with the Department of Electrical Engineering at Texas A&M University. He received his Ph.D. degree in December 2004, in electrical engineering at Texas A&M University. His current research interests are in issues related to voltage security and data communication for electric energy markets. In this area, he has published eight technical papers to date. He joins the Department of Electrical and Computer Engineering at the University of Auckland, New Zealand as a faculty beginning the second semester of 2004.

His permanent mailing address is:

Mr. Nirmal-Kumar C Nair
7, Avdhoot Society, Nana Bazar
V.V.Nagar, Gujrat, 388120, INDIA